

**Age and setting of Permian Slide Mountain terrane ophiolitic  
ultramafic-mafic complexes in the Yukon: Implications for late Paleozoic-  
early Mesozoic tectonic models in the northern Canadian Cordillera,**

**Cees R. van Staal<sup>1,2\*</sup>, Alexandre Zagorevski<sup>3</sup>, William C. McClelland<sup>4</sup>, Monica P.  
Escayola<sup>5</sup>, James J. Ryan<sup>1</sup>, Andrew J. Parsons<sup>1,6</sup> and Joaquin Proenza<sup>7</sup>**

[\\*cees.vanstaal@canada.ca](mailto:cees.vanstaal@canada.ca)

<sup>1</sup> *Geological Survey of Canada, 1500-605 Robson Street, Vancouver, BC, V6B 5J3, Canada*

<sup>2</sup> *Dept. Earth and Environmental Sciences, University of Waterloo, ON, N2L 3G1, Canada*

<sup>3</sup> *Geological Survey of Canada, 601 Booth St., Ottawa, ON, K1A 0E8, Canada*

<sup>4</sup> *Dept. Earth and Environmental Sciences, 115 Trowbridge Hall, University of Iowa, Iowa City,  
IA, 52242, USA*

<sup>5</sup> *Fueguia Basket 251, (9410) Ushuaia, Tierra del Fuego, Argentina.*

<sup>6</sup> *Department of Earth Sciences, Oxford University, Parks Road, Oxford OX1 3PR, UK*

<sup>7</sup> *Departament de Cristallografia, Mineralogia i Dipòsits Minerals. Universitat de Barcelona.*

*C/ Martí i Franquès, s/n - 08028 Barcelona España*

**Abstract**

The Yukon Tanana (YTT) and Slide Mountain terranes (SMT) of the Cordillera in Canada and Alaska are commonly interpreted in terms of opening and closing of a Late Devonian-Permian Japan Sea-style backarc basin behind a continental arc built upon YTT, which rifted from Laurentia during the Famennian-early Mississippian. Upper Devonian mafic-ultramafic complexes in YTT may represent remnants of transitional oceanic lithosphere exhumed onto the seafloor during rifting.

The studied Clinton Creek and Midnight Dome complexes represent suprasubduction zone ophiolites formed at ca. 265 Ma, consistent with analyses of other SMT ophiolites. Most SMT ophiolites are dominated by ultramafic rocks, lack sheeted dikes and contain relatively minor volumes of mafic plutonic and volcanic rocks, suggesting they formed in oceanic core complexes characterised by slow spreading and low magma productivity. The Permian ophiolites formed during or immediately after eclogite formation in YTT, coeval with or immediately preceding emplacement of orogenic peridotites into YTT due to hyperextension. Several tectonic scenarios are discussed to explain these events. We propose that YTT is a composite terrane comprising a continental block and an oceanic arc-backarc complex with the latter obducted onto the former during the middle Permian-early Triassic Klondike orogeny. Obduction may have come from the west or east, but east-directed obduction is most consistent with geological constraints. Obduction was followed by initiation of west-dipping subduction east of the composite YTT; slab roll back causing extension in the composite upper plate, leading to exhumation of orogenic peridotites. Tectonic relationships show many analogies to the collision between Australia and the New Britain-Solomon arc, in which on-going collision in the Huon Peninsula of New Guinea is contemporaneous with extension in Australian crust in the adjacent

Woodlark basin. Syn-orogenic Permian Klondike-cycle calc-alkaline magmatism is attributed to extension in a Woodlark basin-like setting rather than a representing a continental arc.

## Introduction

The Northern Cordillera in Canada and Alaska is thought to preserve evidence of opening and closing of the Late Devonian-Permian Slide Mountain Ocean (SMO). Late Permian closure of this oceanic basin is generally interpreted to have resulted in collision of the western Laurentian passive margin with the Yukon-Tanana terrane (YTT; Colpron et al., 2006b) following the Permian Klondike arc cycle. This model of arc-continent collision, which returned the YTT to its ancestral place of origin along northwestern Laurentia, is generally referred as the Klondike orogeny in Canada (Mortensen, 1992; Beranek and Mortensen, 2011). However, evidence for this collision is enigmatic and is opposite to what is expected in an arc-continent collision (e.g. Brown et al., 2011). That is the passive margin of western Laurentia (downgoing plate) preserves little structural and sedimentological evidence for the Klondike orogeny (Gordey et al., 1992; Gordey, 2002), whereas Permian orogenesis and metamorphism is widespread in the YTT, the upper plate in this scenario (Berman et al., 2007; Beranek and Mortensen, 2011; Petrie et al., 2015). Numerous ultramafic-mafic massifs and associated marine sedimentary rocks are exposed *along* the suture zone and as structural outliers above the YTT. Most of these rocks were previously grouped into the Slide Mountain terrane (SMT) and are generally considered to represent vestiges of the SMO, which is considered to represent an extension of the Anvil (Tempelman-Kluit, 1979) or Angayucham oceans further to the north (e.g., Nelson, 1993; Nelson et al., 2006; Plint and Gordon, 1997). Many workers have interpreted these ultramafic-mafic massifs as components of structurally dismembered ophiolites (e.g., Foster and Keith, 1974; Nelson, 1993; Roback et al., 1994; Dusel-Bacon et al., 2006; Dusel-Bacon et al., 2013;

Parsons et al., in pressa) that formed during separation of the YTT from North America and opening of the SMO backarc basin (e.g., Mortensen et al., 1992; Creaser et al., 1997a; Colpron et al., 2006; Nelson et al., 2013). These ophiolites represent a crucial, yet enigmatic tectonic element of the SMO in Alaska, Yukon and British Columbia because they are interpreted to have formed part of the upper plate during departure of the YTT from Laurentia and protracted opening of the SMO, subsequently becoming part of the subducting plate during closure of the SMO and yet were obducted onto YTT and Laurentia during the terminal Permian collision.

Understanding the origin and tectonic setting of the ultramafic-mafic complexes currently assigned to SMT and YTT is of fundamental importance to understanding the Paleozoic-Mesozoic tectonic evolution of the northern Cordillera; yet their ages and chemical characteristics are generally poorly known. Hence, the timing and tectonic setting of ophiolite formation, which has a profound influence on interpretation of the mafic-ultramafic complexes and their ultimate emplacement mechanisms, are unclear. In this paper, we examine the relatively well preserved mafic-ultramafic complexes at Clinton Creek, Midnight Dome and the St. Cyr klippe in western Yukon, which are generally interpreted as correlatives of the SMT (Colpron et al., 2016). We present new geochemical and geochronological data, discuss their tectonic setting and compare these mafic-ultramafic complexes to broadly coeval rocks elsewhere in the northern Cordillera. We demonstrate that extant and herein presented data indicate that the current terrane concept and tectonic models require revision and propose that the suprasubduction zone (SSZ) ophiolitic rocks of the SMT formed in the Panthalassa Ocean, outboard of YTT, rather than in the marginal basin referred to as the SMO. We discuss several tectonic scenarios that are based on modern and ancient analogues to explain the observed characteristics and propose that the term SMO should be abandoned.



## **Geological setting and existing tectonic models**

Paleozoic tectonic evolution of the Intermontane belt of the Canadian Cordillera (Fig. 1) is commonly interpreted in terms of development, departure and re-accretion of an episodic Late Devonian-late Permian continental arc, remnants of which are now preserved in the YTT (e.g., Mortensen, 1992; Creaser et al., 1997a, b; Colpron et al., 2006a, b; Colpron et al., 2007; Pecha et al., 2015 and references therein). This Paleozoic arc is inferred to have been built upon the leading Panthalassan (proto-Pacific) edge of Laurentia and developed above an east-dipping subduction zone. Most of the YTT is complexly deformed and metamorphosed (e.g. Tempelman-Kluit, 1979; Berman et al., 2007; Staples et al., 2016) making primary tectono-stratigraphic relationships difficult to establish. Correlative rocks in the YTT of southeast Alaska have a similar Laurentian provenance. However, arc magmatism may have initiated there much earlier in the Late Ordovician (e.g. Endicott Arm assemblage, Fig. 1) (Gehrels et al., 1992; Pecha et al., 2016).

The YTT is underlain by Devonian, and older predominantly siliciclastic sedimentary basement, which is generally referred to as the Snowcap assemblage in the Yukon (Colpron et al., 2006a, 2007). Detrital zircon and isotopic provenance studies indicate that the Snowcap assemblage has a continental, Laurentian detrital source (Piercey and Colpron, 2009 and references therein), however the basement to the siliciclastic rocks is not exposed. Isotopic, geochemical and inheritance data from middle Paleozoic felsic intrusive rocks also support presence of Laurentian continental crust below most (but not necessarily all – see below) of the Snowcap assemblage (Piercey et al., 2003; Murphy et al., 2006; Piercey et al., 2006; Ruks et al., 2006 and references therein).

Late Devonian magmatism in the Laurentian margin and YTT is generally interpreted to indicate east-directed subduction beneath the Panthalassan margin of Laurentia, which resulted in Famennian-Mississippian rifting of the YTT from Laurentia and opening of the SMO in a backarc setting. The remnants of the SMO are thought to be preserved in the SMT (Colpron et al., 2006b, 2007), which is mainly situated in a belt and isolated allochthons near the eastern edge of the YTT and on Laurentia.

Backarc spreading progressively moved and isolated the YTT arc terrane(s) from the ancestral Panthalassan margin of Laurentia (Harms and Murchey, 1992; Nelson, 1993; Stevens et al., 1996; Piercey et al., 2004). YTT in these models thus differs from its Laurentian parent by principally displaying post-Famennian magmatism, whereas the remaining autochthonous edge of Laurentia was situated farthest inboard and became the passive margin to the SMO. These models propose that subsequent subduction initiation in the SMO led to its middle-late Permian closure and re-assembly of the YTT, SMT and Laurentia (Mortensen, 1992; Nelson et al., 2006; Murphy et al., 2006; Colpron et al., 2006; 2007). The resultant deformation, metamorphism and concomitant magmatism resulted in the Klondike orogeny in Yukon (Beranek and Mortensen, 2011).

The width of the SMO during the Permian is largely unconstrained. Some workers proposed a width of several thousand kilometers (Belasky et al., 2002, 2006; Nelson et al., 2006, 2013), whereas others suggested a narrow marginal oceanic seaway (Nelson, 1993; Creaser et al., 1999; Piercey et al., 2012). Since the YTT is generally inferred to have returned to approximately its place of origin (Nelson et al., 2006; Pecha et al., 2016), this requires that either the divergence and convergence vectors during its opening and closing to have been broadly coincident or that Mesozoic rearrangement of terranes resulted in virtually no net displacements

parallel to the Panthalassan Laurentian margin. If correct, this would support a narrow seaway rather than a wide ocean. On the other hand, faunal data such as the Permian McCloud fusulinid fauna in the SMT and YTT and paleomagnetism recorded in red chert units of SMT suggest that these terranes were possibly as far south as Texas during the Permian (Ross, 1969; Richards et al., 1993), hence requiring large successive southward and northward margin-parallel translations of surprisingly similar magnitude (Nelson et al., 2006).

This model of YTT-SMT-North America evolution is widely accepted, yet, existing geological data and tectonic considerations raise questions or require special conditions with respect to its underlying assumptions. These include (i) a causative mechanism for initiation of subduction in the SMO, (ii) development of eclogite within the upper plate YTT (Gilotti et al., 2017), (iii) detachment and obduction of the SMT ophiolites while forming part of the downgoing plate. We will examine each of these issues in greater detail below.

(i) Established tectonic models do not adequately explain the cause of subduction flip from east-dipping subduction in Panthalassa to initiation of west-dipping subduction in the SMO backarc following as much as 70 my of continuous or discontinuous backarc spreading. Berman et al. (2007) suggested that the west-facing YTT arc “overtook rollback” such that the upper plate YTT velocity was greater than trench retreat, resulting in intra-arc shortening, subduction flip and initiation of west-dipping subduction in the SMO (Fig. 2). This scenario does not appear to have modern analogues, because modern subduction zones that are not proximal to a collision zone and have higher upper plate velocities than trench retreat are not associated with subduction flips (e.g., Aleutians: Lallemand et al., 2005). Recent examples of subduction flip or step-back in the southwest Pacific have generally resulted from a collision (e.g., Hall, 2002). For example, the subduction initiation along the southern Philippine and Cotabato trenches can be, in-part,

attributed to the closure of the Molucca Sea and collision of Halmahera and Sangihe arcs (see Fig. 2 in Sajona et al., 2000), whereas subduction initiation along the San Cristobal trench was caused by Solomon arc – Ontong Java plateau collision (e.g., Taira et al., 2004). As such, termination and reversal of Panthalassan subduction and initiation of SMO subduction seem to require a collider that has not been identified in the established models, although potential candidates may be hidden in the composite YTT.

(ii) Established tectono-stratigraphic relationships between various components of the YTT indicate that they have undergone episodic magmatism, crustal shortening, deformation and metamorphism (e.g., Gabrielse et al., 1993b; Colpron et al., 2006b; Murphy et al., 2006; Berman et al., 2007). Metamorphism is particularly intriguing because parts of the YTT were metamorphosed to eclogite and blueschist and along the YTT-SMT boundary (Fig. 1) during both the Early Mississippian and Permian (Erdmer and Helmstaedt, 1983; Erdmer et al., 1998; Devine et al., 2006; Petrie et al., 2015; Gilotti et al., 2017; Colpron et al., 2017). Development of high-pressure rocks such as eclogite within the YTT while it occupied an upper plate arc setting can occur when rocks of the arc-trench gap are partially subducted (e.g., Abbott et al., 1994; McIntosh et al., 2005) or dragged down by subduction erosion (Gilotti et al., 2017). The presence of Mississippian eclogite in the upper plate was also explained by east-directed translation of a nappe containing Mississippian eclogite derived from a pre-Permian west-facing forearc/accretionary prism over its associated west-facing arc (Devine et al., 2006). Once the nappe had moved into the retro arc region, it was finally incorporated into an imbricate stack with elements derived from the closing SMO backarc, along the future YTT-SMT boundary (Fig. 2b). However, we are not aware of any recent analogues for such a tectonic scenario, neither do we understand the driving mechanism for such a process.

(iii) Established models infer that the SMO ocean floor, represented by the SMT, was obducted both onto the YTT and Laurentian margin from a lower plate position rather than entering the subduction channel with its parent subducting plate. Normal oceanic crust (formed in a mature backarc or mid-ocean ridge) lacks crustal thickness and buoyancy for collisional orogenesis (e.g., Cloos, 1993) and is almost universally subducted with many of its topographic anomalies, commonly accompanied by subduction erosion of the upper plate (e.g., von Huene and Scholl, 1991; Stern, 2011). Accreting margins only comprise 26% of present day global subduction systems and commonly occur where there is abundant sediment supply to the trench (e.g. Scholl and von Huene, 2007). Some of these accretionary complexes do preserve minor subducting ophiolitic oceanic crust as off-scraped or underplated thrust sheets (e.g., Kimura and Ludden, 1995; Calvert, 1996), but these generally lack mantle sections and are uncommon. Locally, ophiolitic rocks along suture zones do originate from the subducting plate but these are underplated and generally metamorphosed to relatively high grade conditions (e.g., Manatschal et al., 2011; van Staal et al., 2013). Obduction of downgoing plate-derived SMT ophiolitic rocks characterised by low metamorphic-grade, thus does not seem very likely and needs to be re-evaluated along with its relationship to YTT (c.f. Parsons et al., in pressa).

These underlying assumptions and issues relating to SMT-YTT interactions can be tested by establishing constraints on the timing and nature of the mafic-ultramafic complexes along the suture between Slide Mountain and Yukon-Tanana terranes. Consequently, this study is focused on the Clinton Creek and Midnight Dome and ultramafic-mafic complexes west of the Tintina Fault near the town of Dawson (Fig. 1, localities i and k) and a large ultramafic-mafic body of the St. Cyr klippe near Quiet Lake area (Fig. 1, locality d)

## **Existing constraints on the time of opening of the Slide Mountain Ocean**

The exact time of SMO opening in the models of Nelson (1993), Nelson et al. (2006) and Colpron et al., (2006, 2007) is difficult to establish with the existing database, because autochthonous Laurentia does not preserve a rift-drift transition of an appropriate age. As such, timing is largely based on circumstantial evidence. Opening is generally inferred to be Famennian-Early Mississippian, largely based on the presence of Famennian-Mississippian rift-related magmatism in both YTT and the Laurentian margin, and an absence of younger magmatism in the Laurentian margin (e.g., Piercey et al., 2003, 2004, 2006). However, the departure of the YTT may have occurred earlier. Late Famennian folding and metamorphism in parts of YTT (e.g. Murphy et al., 2006), but not in the Laurentian margin suggests that YTT was already separated from Laurentia by the late Devonian. This is consistent with the presence of ca. 379 and 364 Ma N-MORB-like intrusive rocks in rocks assigned to the Snowcap assemblage (Petrie et al., 2016), suggesting rifting was in an advanced stage at this time. Similar relationships may be present in the Klatsa metamorphic complex (Fig. 1, Devine et al., 2006), where leucogabbro in Klatsa serpentinite yielded a U-Pb zircon age of ca 368 Ma (Devine et al., 2006). Although the primary relationships are difficult to establish, these Upper Devonian rocks may represent parts of transitional oceanic lithosphere that is overlapped by Upper Devonian Snowcap assemblage sediments throughout the nascent SMO (see Manaschtal, 2004; Manaschtal et al., 2006). Isolated extensional allochthons of thin continental crust and overlapping continentally-derived sediments could be the source of crustal contamination in Carboniferous-Permian oceanic arc sequences (Parsons et al., in pressa, see below).

## **Constraints on the setting and age of the SMT ophiolitic rocks**

Mafic-ultramafic complexes in the SMT were previously mainly interpreted as  
 dismembered ophiolitic slivers that were tectonically imbricated with the enclosing rocks (e.g.  
 Nelson, 1993; Colpron et al., 2005; Piercey et al., 2012). These ultramafic-mafic complexes are  
 typically dominated by voluminous ultramafic rocks, subordinate gabbroic rocks, and variably  
 abundant mafic volcanic rocks (Nelson, 1993; Colpron et al., 2005; Murphy et al., 2006; Piercey  
 et al., 2012; Ryan et al., 2015; Parsons et al., 2017, in pressa). The ultramafic-mafic complexes  
 in the part of the Finlayson district underlain by YTT rocks (Fig. 1) of southwest Yukon,  
 however, generally were considered to represent layered intrusions (Murphy et al., 2006). In  
 contrast, we interpret the Finlayson district ultramafic-mafic complexes as allochthonous slices  
 of mantle and lower crust. These bodies are locally well exposed in three dimensions, are not  
 obviously layered, but are variably serpentinized, foliated chromite-bearing peridotite, locally  
 preserving a shape fabric defined by chromite and/or bastite pseudomorphs after orthopyroxene.  
 These peridotites are also locally overlain by basalts, which is inconsistent with intrusion in the  
 lower or middle crust. Pegmatitic pyroxenite bodies within the peridotite do not extend into the  
 highly transposed enveloping country rocks and neither do the latter contain mafic-ultramafic  
 feeder dikes and/or satellite sills. In addition, there is no evidence of high temperature contact  
 metamorphism in the country rocks along the base of the thick peridotite bodies (50-500m).  
 These observations have implications for the tectono-stratigraphy of the YTT, which was  
 established in the Finlayson district in part using these ultramafic rocks as stitching plutons  
 (Murphy et al., 2006) and correlation of distinct basalt-dominated units across faults (cf. Piercey  
 et al., 2012).

Direct age constraints on the ophiolitic mafic-ultramafic complexes in the SMT are  
 sparse (Fig. 1), but come from the Sylvester allochthon in British Columbia (Nelson, 1993;

Nelson and Bradford, 1993) and in the Yukon mainly from the Finlayson district (Murphy et al., 2006), the Dunite Peak area (de Keijzer et al., 2000; Parsons et al., in pressa) and the Tummel fault zone and Ragged Lake klippe (Colpron et al., 2005, 2006). Carboniferous or older members of the SMT are preserved in the St. Cyr klippe (see below) and potentially in the Klatsa metamorphic complex in the Finlayson district (Fig. 1), where leucogabbro in serpentinized ultramafic rocks yielded a U-Pb zircon age of  $368 \pm 10$  Ma (Devine et al., 2006). Chert associated with basalt of the Campbell Range Formation, part of the SMT in the Finlayson district, contains mid-Pennsylvanian to Early Permian radiolaria, whereas gabbroic intrusive rocks that cut the basalt yielded ca. 273 Ma U-Pb zircon crystallization ages (Mortensen, 1992b; Murphy et al., 2006). The Campbell Range Formation is dominated by enriched and normal mid-ocean ridge (E-MORB, N-MORB and OIB) basalt, but also contains minor greenstone, gabbro and leucogabbro, island arc tholeiitic to calc-alkaline (IAT/CA) basalt and backarc basin basalt (BABB) (Plint & Gordon, 1997; Murphy et al., 2006; Piercey et al., 2006), which have been interpreted to have formed as a result of highly oblique spreading, juxtaposing different backarc settings along giant transform faults in the SMO (Piercey et al., 2012). However these interpretations were in part based on using the ophiolitic ultramafic rocks as stitching intrusions.

The Dunite Peak area preserves structurally dismembered SSZ juvenile ophiolitic rocks with IAT and BABB compositions, structurally emplaced on top of marble and siliciclastic rocks of the Snowcap assemblage (Parsons et al., 2017; in pressa). Associated IAT gabbroic rocks yielded ca. 265 Ma ages (de Keijzer et al., 2000; Parsons et al., in pressa) corresponding to SSZ ophiolite generation in an extensional intra-oceanic arc setting. In the Glenlyon region, mafic rocks with similar IAT to CA geochemical compositions indicative of an SSZ setting were recorded from SMT andesitic greenstones and gabbro in the Tummel fault zone and Ragged



Lake klippe, which yielded U-Pb igneous ages of ca. 268 and 260 Ma respectively (Colpron et al., 2005; 2006).

The Sylvester Allochthon in British Columbia (Nelson, 1993; Nelson & Bradford, 1993) preserves several distinct tectono-stratigraphic slices including equivalents of the YTT (Harper Ranch, Division 3 of Nelson, 1993) and SMT (Division 2 of Nelson, 1993). Division 2 SMT comprises basinal sediments and basalt. The basalts are predominantly N-MORB and E-MORB, but a minority have IAT to CA signatures, indicating an SSZ setting (Nelson, 1993). Associated sediments yield Mississippian to middle Permian fossils (Harms and Murchey, 1992; Nelson, 1993). A SMT gabbro-trondhjemite complex at Zus Mountain yielded a ca. 269 Ma U-Pb zircon crystallization age suggesting that the ophiolitic rocks are middle Permian (Gabrielse et al., 1993b). Other plutonic rocks in the area, ranging from granite to gabbro, yield similar middle Permian ages (270-262 Ma: Gabrielse et al., 1993b; Roback et al., 1994). The existing age data summarized above provide direct constraints on the ophiolitic rocks included in the SMT and YTT in Yukon and British Columbia that suggest an age range from ca. 368 to 260 Ma. Middle Permian ages are typical of the ophiolitic rocks that are exposed near the suture between the oceanic SMT and the Laurentian margin and are broadly coeval with the eclogite facies metamorphism and Klondike orogeny in the YTT. The broadly coeval timing of these events raises the questions as to why the preserved parts of the SMT were formed by spreading in a SSZ setting while the overriding YTT was undergoing collisional orogenesis and eclogite facies metamorphism.

**Geochronology, geochemistry and setting of the Clinton Creek, Midnight Dome and St. Cyr ultramafic-mafic complexes of the Yukon SMT.**

*Analytical Methods*

## Zircon U-Pb geochronology

U–Th–Pb isotopic data of zircon crystals from mafic and intermediate igneous rocks closely associated with the ultramafic rocks were analyzed using the sensitive high-resolution ion microprobe-reverse geometry (SHRIMP-RG) mass spectrometer at the U.S. Geological Survey – Stanford Micro-Analysis Center at Stanford University. Zircon grains were separated from 1-3 kg samples by standard physical separation techniques and mounted in 2.54 cm epoxy rounds, which were polished to expose grain interiors. Cathodoluminescence (CL), transmitted light, and reflected light images were used to characterize zircon domains, including homogeneous regions of the zircons and to avoid complex internal structures, cracks, and zones of potential Pb loss. Calibration of U was based on zircon standard Madagascar Green (MAD; 4196 ppm U; Barth and Wooden, 2010). Isotopic ratios were calibrated by replicate analyses of zircon standard R33 (421 Ma, Black et al., 2004; Mattinson, 2010), which were rerun after every fourth analysis (Table 1). The analytical routine followed Barth and Wooden (2006, 2010) using a 20  $\mu\text{m}$  spot diameter. Data reduction used Squid 2.51 program of Ludwig (2009). Crystallization ages were calculated as weighted mean 207-corrected  $^{206}\text{Pb}/^{238}\text{U}$  ages and Tera-Wasserburg diagrams were generated using the Isoplot/Ex program of Ludwig (2003). Reported age errors are at the 95% confidence level and incorporate the  $2\sigma$  external spot-to-spot error of the R33 standard, which was 0.56% and 0.66% for the two mounts analyzed.

Trace-element data for Y, REE, and Hf were collected simultaneously with the U, Th and Pb analyses (Table 1). Data reduction of elemental concentrations used zircon standards MAD (Barth and Wooden, 2010). Chondrite-normalised REE plots (Fig. 3) use the chondrite REE abundances of Anders and Grevesse (1989) multiplied by a factor of 1.36 (Korotev, 1996). Chondrite-normalized values for Pr were calculated by interpolation ( $\text{Pr}_{(\text{N})} = \text{La}_{(\text{N})}^{0.33} \times \text{Nd}_{(\text{N})}^{0.67}$ ).

Eu and Ce anomalies are based on  $\text{Eu}_{(N)}/\text{Eu}^*$  and  $\text{Ce}_{(N)}/\text{Ce}^*$  with  $\text{Eu}^*$  and  $\text{Ce}^*$  calculated as geometric means (e.g.,  $\text{Eu}^* = (\text{Sm}_{(N)} \times \text{Gd}_{(N)})^{0.5}$ ).

### Lithogeochemistry

Whole-rock major and trace element concentrations of the studied mafic and ultramafic rocks were determined by inductively coupled plasma-mass spectrometry (ICP-MS) at Activation Laboratories in Ancaster, Ontario (Table 2). Because rocks in the study area were subjected to greenschist to amphibolite facies metamorphic conditions and major and low field strength elements are likely to have been mobile (e.g., Na, K, Ca, Si, Cs, Ba, Rb). As such, geochemical discriminations utilized herein are based mainly on high field-strength elements (HFSE: Hf, Nb, Ta, Ti, Sc, Y, Zr), rare earth elements (REE), and Th which are considered to be immobile under typical greenschist to amphibolite facies conditions (e.g., Pearce, 1996).

### Microprobe

Electron microprobe analyses of chromian spinel were carried out on polished sections of serpentinites. Analyses were conducted with a four-channel CAMECA SX50 electron microprobe at the Serveis Científicotècnics of the Universitat de Barcelona (Barcelona, Spain). Mineral compositions were obtained by analyzing several grains in each section (Table 3). The analytical conditions were 20 kV accelerating voltage, 20 nA beam current, 2  $\mu\text{m}$  beam diameter, and counting time of 10 seconds per element. Calibrations were performed using natural and synthetic reference materials: chromite (Cr, Al, Fe), periclase (Mg), rhodonite (Mn), rutile (Ti), NiO (Ni) and metallic V. The proportion of trivalent iron in chromian spinel was calculated assuming stoichiometry.

### 339 *Clinton Creek complex*

340       The Clinton Creek complex (Abbott, 1983) occurs close to the Alaska-Yukon border  
 341 (Fig. 1) and was previously correlated with ultramafic-mafic rocks of the Seventymile terrane, a  
 342 correlative of the SMT in Alaska, which are associated with Permian and Triassic volcanic and  
 343 sedimentary rocks (Foster & Keith, 1974; Foster *et al.*, 1994; Dusel-Bacon *et al.*, 2006 and  
 344 references therein). The Clinton Creek complex mainly comprises a sheared assemblage of  
 345 strongly altered ultramafic rocks with minor mafic intrusive rocks and is associated with  
 346 greenschist facies tectonites of uncertain origin (Abbott, 1983). These rocks occur as generally  
 347 shallowly dipping, sheared lenses within weakly metamorphosed sedimentary rocks.  
 348 Sedimentary rocks yielded one conodont suggestive of a Norian age (Orchard *et al.*, 2006). The  
 349 ultramafic rocks were subjected to pervasive low-grade metamorphism and/or hydrothermal  
 350 alteration, which produced abundant serpentinite and listwaenite (Fig. 4a) and destroyed most  
 351 primary features. K-Ar and Rb-Sr age determinations of the intimately associated mafic rocks  
 352 and schist yielded Permian ages (Htoon, 1981). The serpentinite is intruded by leucogabbro  
 353 (diorite of Abbott, 1983), which locally has coarse pegmatitic patches (Fig. 4b) which were  
 354 sampled for geochronology.

### 355 Geochronology

356       The sampled pegmatitic leucogabbro gabbro (VL10-12) cuts serpentinitized and altered  
 357 ultramafic rocks, but is itself also cut by fractures, carbonate veins and is locally altered to  
 358 chlorite, serpentinite and carbonate-bearing assemblages (Fig. 4b). Plagioclase is saussuritised.  
 359 The gabbro thus postdates at least some of the alteration and serpentinitization of the ultramafic  
 360 rocks, but is itself also affected by it, suggesting the gabbro intruded while hydrothermal  
 361 alteration was active in the host. The sample yielded a small population of elongate subhedral

zircon with oscillatory zoned to unzoned cores overgrown by unzoned, CL-bright, 2- to 25- $\mu\text{m}$ -thick rims (Fig. 3a). Core analyses lack a well developed Eu anomaly ( $\text{Eu}/\text{Eu}^* = 0.8\text{-}0.9$ ) but have steep HREE patterns ( $\text{Yb}/\text{Gd} = 12\text{-}36$ ). The rim analyses show steeper HREE patterns ( $\text{Yb}/\text{Gd} = 165\text{-}1192$ ) and lower middle REE concentrations, demonstrating that they are chemically distinct from the core domain (Fig. 3a). Eight of nine core analyses give a  $^{206}\text{Pb}/^{238}\text{U}$  age of  $265 \pm 3$  Ma (MSWD = 1.5; Fig. 3). This age is interpreted as the crystallization age of the leucogabbro and the age of mafic magmatism in the Clinton Creek complex. This age is also interpreted to provide a minimum age constraint on the exhumation and serpentinization of the host harzburgite. The latter indicated by gabbro intrusion during high-level hydrothermal alteration of the ultramafic host rocks. The two youngest rim analyses suggest the timing of rim growth is ca 125 Ma.

### Geochemical characteristics

The dated leucogabbro is characterized by a flat profile with strong Nb depletion on a N-MORB normalized trace element plot (Fig. 5a), characteristic of arc-related tholeiitic magmas. The sample plots in the volcanic arc tholeiite field (VAT) on tectonic discrimination diagrams (e.g. Fig. 5b). Positive Eu anomaly suggests plagioclase accumulation and is consistent with gabbroic nature of the host and pegmatitic nature of the sample. Altered ultramafic rocks yield harzburgite ( $\text{Al}_2\text{O}_3$  0.28 wt%) and websterite ( $\text{Al}_2\text{O}_3$  1.78 wt%) normative compositions (Fig. 5d), consistent with poorly preserved serpentine pseudomorphs after olivine and orthopyroxene. Trace element concentrations in harzburgite are near or below the analytical detection limit; however, the sample shows slight LREE enrichment relative to HREE (Gd and Dy) on a primitive mantle-normalized plot (Fig. 5c). Websterite shows a consistent negative slope on a

primitive mantle normalized diagram and a flat slope on N-MORB normalized diagram (Figs. 5a, c).

### *Midnight Dome complex*

The Midnight Dome ultramafic-mafic complex (Mortensen, 1990) occurs near the town of Dawson City (Fig. 1) roughly on strike with the Clinton Creek complex, which it closely resembles lithologically and in style of deformation and alteration. As in Clinton Creek, an intrusive leucogabbro (Fig. 4c) dike in the ultramafic rocks was sampled for geochronology.

### Geochronology

The sampled leucogabbro (VL10-09) has coarse pegmatitic pods and is locally weakly foliated (Fig. 4c). The leucogabbro cuts the altered and serpentinized peridotite, but itself generally displays good preservation of primary textures and little alteration (Fig. 4c). The sample yielded a small population of elongate crystals that display coarse oscillatory zoning in CL images (Fig. 3b). Zircons display well developed Eu anomalies ( $\text{Eu}/\text{Eu}^* = 0.3\text{-}0.6$ ) and steep HREE patterns ( $\text{Yb}/\text{Gd} = 10\text{-}26$ ; (Fig. 3b). U/Pb analyses range from 241 to 268 Ma. Assuming the youngest analysis reflects Pb-loss, nine of ten analyses define a  $^{206}\text{Pb}/^{238}\text{U}$  weighted mean age of  $264 \pm 4$  Ma (MSWD = 1.3; Fig. 3b). This age is interpreted as the crystallization age of the gabbro and the age of mafic magmatism in the Midnight Dome complex. This age is also interpreted to provide a minimum time constraint on the exhumation and alteration of the host harzburgite.

### Geochemical characteristics

Dated leucogabbro is characterized by a flat N-MORB normalized trace element profile with strong positive Eu anomaly indicative of plagioclase accumulation (Fig. 5a). Th and Nb are

below the detection limit. Other mafic samples (2 gabbro and 1 diabase) from the same complex have similarly flat REE profiles on an N-MORB normalized diagram. Gabbro and diabase have strong Nb depletion characteristic of arc-related tholeiitic magmas (Fig. 5a). These two samples plot in the volcanic arc tholeiite field (VAT) on tectonic discrimination diagrams (e.g. Fig. 5b). Altered ultramafic rocks yield harzburgite normative compositions (Fig. 5d), consistent with poorly preserved textural characteristics, as in the Clinton Creek complex. On primitive-mantle normalized trace element diagrams (Fig. 5c), these samples show prominent LREE enrichment and Ti depletion. On major element diagrams (not shown), these samples plot in depleted harzburgite fields ( $\text{Al}_2\text{O}_3$  0.46 to 0.98). Harzburgite contains unaltered Cr-spinel crystals, which were analyzed using a scanning electron microprobe. Cr-spinel is compositionally homogeneous with high Cr# and Mg #, and very low  $\text{TiO}_2$  concentration (Table 3). These analyses plot in the SSZ forearc peridotite fields on spinel tectonic discrimination diagrams (Fig. 6).

#### *St. Cyr klippe ultramafic-mafic rocks*

The St. Cyr klippe lies northeast of Quiet Lake (Fig.1.) and contains several structural slices including ultramafic and mafic rocks and YTT Snowcap assemblage rocks (Fallas et al., 1998, 1999; Petrie et al., 2015; Gilotti et al., 2017). MORB or BABB-like amphibolite correlated with the SMT is intruded by a hornblende tonalite which yielded a  $373 \pm 1$  Ma U-Pb zircon age (Fallas et al., 1998). The presence of several structural slices displaying a wide range of metamorphic grade within the St. Cyr klippe (Petrie et al., 2015; Gilotti et al., 2017) and the presumed tectonic contact with the ultramafic rocks leaves the age of the ultramafic and entrained mafic rocks poorly constrained. We sampled an intrusive trondhjemite to leucotonalite body (VL10-04) that cuts both the chromite bearing serpentinized ultramafic rocks and small

entrained pyroxenite and gabbro intrusive bodies (Fig. 4d) for geochronology. Chromite in the serpentinite locally preserves a shape fabric parallel to the foliation (Fig. 4e).

### Geochronology

The sample (VL10-04) yielded a population of subhedral zircon with complex internal zoning. Most grains contain oscillatory zoned cores that are overgrown by at least three rim domains. A discontinuous, 1- to 10- $\mu\text{m}$ -thick, CL-light inner rim typically truncates zoning in the cores (A in Fig. 3c). The inner rim is overgrown by a 5- to 50- $\mu\text{m}$ -thick, CL-dark mantle that is in turn overgrown by a 1- to 20- $\mu\text{m}$ -thick, CL-light outer rim (B and C in Fig. 3c, respectively). The cores give ages between  $387 \pm 3$  Ma and  $2656 \pm 10$  Ma with Th/U ratios of 0.3-0.7 that are characteristic of magmatic zircon. The CL-dark mantle domain, which appears to reflect the bulk of new zircon growth, yielded  $^{206}\text{Pb}/^{238}\text{U}$  ages of between  $335 \pm 1$  Ma and  $272 \pm 1$  Ma with Th/U ratios of 0.003-0.014. A single spot in the outermost low U (65 ppm) rim domain gave an age of  $348 \pm 9$  Ma but the age is compromised by relatively high common Pb and large uncertainty. The mantle domain is inferred to represent zircon growth at the time of trondhjemite-leucotonalite crystallization. The older ( $>300$  Ma) CL-dark mantle analyses likely reflect mixtures of core and rim domains and younger CL-dark ( $>275$  Ma) rim analyses likely reflect Pb-loss and/or metamorphism. The remaining subset of CL-dark mantle analyses defines a  $^{206}\text{Pb}/^{238}\text{U}$  age of  $309 \pm 5$  Ma ( $n=4/11$ , MSWD = 1.3) that is interpreted as the best approximation for the trondhjemite-leucotonalite crystallization age (Fig. 3c) and provides a minimum age of the pyroxenite and gabbroic magmatism associated with the ultramafic rocks.



### Geochemical characteristics

The serpentinized ultramafic rocks show no obvious compositional layering and are chromite-bearing peridotites with harzburgite normative compositions (Fig. 5d). On primitive-mantle normalized trace element diagrams (Fig. 5c), these samples show prominent Ti depletion, LREE enrichment and slight U-shaped trace element and rare earth patterns.

### *Discussion*

The Midnight Dome and Clinton Creek complexes are dominated by highly altered and serpentinized, depleted harzburgite intruded by small bodies of leucogabbro and rare diabase. Complete Penrose-type ophiolitic crustal sections characterised by a pseudo-stratigraphy of mantle tectonite, cumulate ultramafic-mafic rocks, isotropic gabbro, sheeted dikes, pillow basalt and pelagic-hemipelagic sediment (Anonymous, 1972) have not been recognised here or elsewhere in the SMT by us or previous workers (e.g. Piercey et al., 2012; Parsons et al., in pressa). Notably, sheeted dikes are poorly developed or missing altogether, ultramafic rocks are abundant, and the volume of crustal mafic igneous rocks is commonly subordinate to the associated ultramafic rocks. This suggests that these oceanic rocks formed in a ridge environment where spreading was predominantly accommodated by tectonic extension, either due to localization of strain and/or lower magma productivity than typical Penrose-type ophiolites (e.g., Robinson et al., 2008). That is, spreading in these complexes was likely slow and largely accommodated by exhumation of lower-crustal and/or upper-mantle rocks to shallow crustal levels and locally onto the seafloor along large-scale, shallowly dipping detachment faults, forming ocean core complex(s) (e.g., Schroeder and John, 2004; MacLeod et al., 2009; Miranda and Dilek, 2010; Tani et al., 2011). This setting is typically characterized by emplacement of gabbro into exhumed mantle sections, limited basaltic magmatism and

formation of active fault scarps exposing mantle rocks to mass wasting during eruption of the overlying basalts. Permian conglomerates and ophiolites containing serpentinite and gabbro have been identified in correlative SMT ophiolites in the Sylvester allochthon in British Columbia (Nelson, 1993; Roback et al., 1994; Ryan et al., 2015) and are consistent with this scenario.

Ocean core complexes are now recognized to be common in continent to ocean rifts (e.g., Manatschal et al., 2011), slow to oblique spreading mid-oceanic ridges (e.g., MacLeod et al., 2009) and backarc spreading centres (e.g., Ohara et al., 2003; Tani et al., 2011), and they form a major component of several suprasubduction zone ophiolite belts (e.g., Tremblay et al., 2009; Miranda and Dilek, 2010). Limited analyses of tholeiitic mafic plutonic rocks of the Midnight Dome and Clinton Creek complexes (Fig. 5, Table 2) are consistent with formation in a supra-subduction zone setting as indicated by strong Nb depletion (e.g., Cabanis and Lecolle, 1989; Pearce, 2014). Similarly, major element chemistry and Cr-spinel composition from the ultramafic rocks suggests a high degree of depletion typical of peridotites in arc settings (Fig. 6). LREE enrichment in harzburgite may indicate post-melt extraction enrichment, likely due to late stage melt percolation through exhumed and cooled peridotite at shallower depth; however, as similar enrichment has been observed in both forearc (Bedard and Escayola, 2010) and abyssal peridotites (e.g., Niu et al., 2004), this is not diagnostic of tectonic setting.

Gabbroic rocks from the Clinton Creek and Midnight Dome complexes yielded overlapping within-error middle Permian U-Pb zircon ages ( $264 \pm 4$  Ma and  $265 \pm 3$  respectively) indicating broadly coeval formation (Fig. 3) in a similar tectonic setting based on the overall geochemical characteristics. Gabbroic rocks intimately associated with ultramafic bodies elsewhere in the SMT also yielded similar radiometric ages, which mainly range between

275 and 260 Ma (Fig. 1; Gabrielse et al., 1993a; Nelson and Bradford, 1993; Colpron et al., 2006a; Murphy et al., 2006; Parsons et al., in pressa). Based on these age constraints we infer that spreading and mantle exhumation occurred throughout the SMO at ca. 265 Ma.

The felsic leucotonalite-trondhjemite intrusive bodies in the ultramafic rocks of the St. Cyr klippe yielded an age of  $309 \pm 5$  Ma (Fig. 3) and provides a minimum age of mafic magmatism, since no evidence of a consanguineous relationship between the felsic and mafic igneous rocks exists at present. The age of the intrusive felsic magmatism, suggest a relationship to the juvenile Klinkit arc cycle, provided that the tuffaceous rocks of the Klinkit Group are as old as Pennsylvanian as is generally inferred (Roots et al., 2006; Simard et al., 2003; Piercey et al., 2006). The age of the Klinkit Group tuffaceous rocks, the principal representative of the Klinkit arc cycle, is solely constrained by a U-Pb age of ca. 281 Ma from an andesitic tuff of the upper part of the Butsi Formation (Roots et al., 2002, 2006). The ultramafic-mafic complex of the St. Cyr klippe is thus older than those present in the Midnight Dome, Clinton Creek, Dunite Peak, Campbell Range Formation and the Sylvester allochthon and represents an earlier rifting event in the SMO. Considering its association with Late Devonian (ca. 373 Ma) or older oceanic-like mafic rocks (Fallas et al., 1998), it may be a correlative of the ophiolitic ultramafic-mafic body in the Klatsa metamorphic complex (Devine et al., 2006) and represent another slice of Late Devonian transitional oceanic lithosphere.

#### *Origin of middle Permian mafic-ultramafic complexes*

Previous geochemical studies of SMT mafic rocks in the Finlayson area lacked the resolution of trace elements to effectively differentiate IAT from MORB lavas (e.g., Plint and Gordon, 1997). On the basis of their Ti-V data, SMT in the Finlayson area are predominantly ocean floor basalts similar to some SSZ ophiolites (Pearce, 2014). Correlative rocks include a

mixture of MORB and IAT (Colpron et al., 2005; Parsons et al., in pressa). Marine basalts from the Sylvester allochthon in British Columbia also comprise a mixture of MORB and IAT. The IAT chemistry of the mafic rocks and highly depleted nature of the ultramafic rocks suggests a subduction zone-modified mantle for the SMT mafic-ultramafic complexes.

Subduction zone-modified mantle source can be either due to subduction coeval with emplacement of magmas or, less commonly, it can be inherited from a previous period of subduction-related melting and metasomatism. For example, Cretaceous hyperextension of the Newfoundland margin of the Atlantic Ocean resulted in exhumation of highly depleted spinel harzburgite subcontinental mantle lithosphere and emplacement of backarc-like magmas; however, the suprasubduction zone signature is most likely related to the closure of pre-Mesozoic oceans (Robertson, 2007). Similarly, the Woodlark basin in the southwest Pacific is characterized by both MORB and arc-like magmas, suggesting inheritance from earlier subduction (Perfit et al., 1987). The mixture of MORB and IAT magmas in the Permian ophiolite complexes thus presents a challenge regarding interpretation of their tectonic setting solely based on geochemistry. The regional distribution of arc signatures in the SMT, their dominantly Permian age, as well as their structural emplacement above the YTT and the Laurentian margin (e.g., Plint and Gordon, 1997; Canil and Johnston, 2003; Petrie et al., 2015; Parsons et al., in pressa) suggest that these ophiolite complexes did not form part of the subducting SMO floor or any other oceanic basin they may have formed in. Thus, these ophiolites did not form during rifting of YTT from Laurentia and subsequent spreading related to opening of the SMO. Rather we interpret them to have been part of an arc-backarc system formed during the oceanic basin's closure, which subsequently was obducted onto YTT. The Permian SMT arc-backarc rocks were referred to by Parsons et al. (in pressa) as the Dunite Peak oceanic arc.

# *Permian setting of the YTT*

The new and existing ages of mafic-ultramafic complexes in the SMT tightly constrain an important middle Permian event generating SSZ magmatism adjacent to the YTT. This event was broadly coeval with Permian deformation, metamorphism, exhumation and magmatism in the YTT, where the early Permian part of the juvenile Klinkit Arc phase of magmatism ( $281 \pm 2$  Ma, Roots et al., 2002, 2006; Colpron et al., 2006b) was followed by ca. 275-260 Ma blueschist to eclogite facies metamorphism of the YTT (Creaser et al., 1997b; Fallas et al., 1998; Petrie et al., 2015, 2016; Gilotti et al., 2017). The locus of the eclogite metamorphism approximately coincides with the SMT-YTT boundary (Fig. 1; Gilotti et al., 2017). Development of eclogite within the YTT basement was closely followed by structural emplacement of small orogenic peridotite bodies at ca. 262 Ma into the YTT basement (Buffalo Pitts peridotite: Canil et al., 2003; Johnston et al., 2007). The exhumation of orogenic peridotite was interpreted to have occurred as a result of relatively magma-poor hyperextension of continental crust located in a backarc setting of the east-facing middle Permian YTT Klondike arc (Canil et al., 2000; Johnston et al., 2007). The associated gabbroic rocks were interpreted to provide a minimum age for the structural emplacement of the mantle rocks in the crust and/or onto the seafloor (Reston and Manatschal, 2011), because they represent small batches of mafic melt generated during or shortly after exhumation (e.g., Jagoutz et al., 2007). Hyperextension was accompanied and followed by calc-alkaline felsic magmatism that involved crustal anatexis of YTT basement (ca. 265 to 257 Ma: Ruks et al., 2006), sparse peraluminous magmatism (ca. 252 Ma: Beranek and Mortensen, 2011) and high-grade metamorphism (ca. 239 Ma: Berman et al., 2007). The chronology of these middle to late Permian events suggests a period of major tectonic reorganization in the YTT and adjacent terranes.

## **Evaluation of tectonic models**

Any tectonic model that is proposed for the setting of the Clinton Creek and Midnight Dome complexes needs to address Permian subduction in the SMO, suprasubduction zone chemistry of the Clinton Creek and Midnight Dome complexes, obduction rather than subduction of Clinton Creek, Midnight Dome and related SMT ophiolite complexes, the spatially nearly coincident location of Permian and Mississippian eclogite-facies metamorphism, and broadly coeval exhumation of orogenic peridotites. Existing tectonic models (e.g. Piercey et al., 2006; Berman et al., 2007) do not adequately address all of these nearly coeval Permian events in a single tectonic framework. Hence, in the following sections we evaluate existing models and explore alternative tectonic scenarios based on modern and recent analogues in the southwest Pacific. We utilize the Taiwan collision zone, where part of the Luzon arc is presently colliding with the South China Sea continental margin (e.g., McIntosh et al., 2005), as a geometrical analogue for the oldest and most speculative parts of our models (Figs. 7, 8). The use of this analogue allows our framework to start with a tectonically reasonable configuration. From this initial configuration we explore possible tectonic scenarios that could, in principle, explain the observed relationships. We discuss multiple tectonic scenarios in order to demonstrate that existing tectonic models which treat YTT as a singular terrane are difficult to reconcile with the existing constraints (Fig. 7). We then explore the possibility that YTT is a composite terrane that formed by amalgamation of juvenile oceanic and continental fragments in the Permian (Figs. 8, 9). The various plate tectonic configurations that can create an YTT composite terrane are guided by the relationships in the Australia – Pacific boundary zone in Papua New Guinea (Fig. 10).

584 *YTT as a singular terrane*

585       Most recent models (Mortensen, 1992; Nelson, 1993; Piercey et al., 2006; Pecha et al.,  
586 2016 and references therein) assume that the present distribution of terranes is indicative of their  
587 original relative position and polarity of juxtaposition in the Late Paleozoic and Early Mesozoic,  
588 despite the complex structural overprint related to Jurassic to Cretaceous shortening and  
589 exhumation (e.g., Staples et al., 2016, Joyce et al., 2015) and Cretaceous strike-slip translation  
590 (e.g., Gabrielse et al., 2005). In these models the YTT arc-backarc terrane formed above an east-  
591 dipping subduction zone and separated from Laurentia during the Famennian-Early  
592 Mississippian, opening the SMO. Subsequently a subduction polarity flip initiated Permian  
593 subduction in the SMO (e.g. Devine et al., 2006; Piercey et al., 2006; Berman et al., 2007),  
594 although the cause of the cessation of east-directed subduction and the reversal of subduction  
595 polarity was not identified (see Fig. 2).

596       Subduction polarity flips generally require a collision (see above), hence the postulated  
597 east-dipping subduction should have been terminated by accretion of an as yet unidentified  
598 plateau, arc or microcontinent (Fig. 7a). Evidence for such a collider is not preserved, but  
599 Famennian-Mississippian deformation, metamorphism and an unconformity in YTT (Gabrielse  
600 et al., 1993; Colpron et al., 2006 a,b; Mihalynuk et al., 2006; Murphy et al., 2006; Roots et al.,  
601 2006; Devine et al., 2006; Berman et al., 2007; Ryan et al., 2015) may be related to such a  
602 collision. The strong Mesozoic tectonic and metamorphic overprint, including large tangential  
603 translations could have removed or masked a collider. Such a collision could be responsible for  
604 the Mississippian eclogite-facies metamorphism of parts of the downgoing lower plate (Erdmer et  
605 al., 1998; Devine et al., 2006). Rocks of the upper plate could also reach eclogite-facies  
606 conditions if rocks of the arc-trench gap are subjected to subduction erosion and/or partially

subducted and underplated during collision (Fig. 7a; e.g., McIntosh et al., 2005). Partial subduction of the forearc during collision is consistent with the arc-like geochemical characteristics of the Mississippian eclogite (Creaser et al., 1999). Previous models exhumed and then transported the Mississippian eclogite and associated Klatsa complex rocks over the associated arc towards the Permian foreland to finally emplace it along the eastern margin of YTT near its tectonic contact with the Laurentian margin (Fig. 2; Devine et al., 2006; Berman et al., 2007). This is a tectonically complicated and unlikely scenario (Fig. 2) because it involves exhumation of the Mississippian eclogite and associated rocks in the forearc, the cause of which is unclear, followed by retro-arc-directed thrusting prior to the initiation of west-directed subduction in the SMO (Devine et al., 2006). Hence, this would cause significant burial of a still hot and possibly still magmatically active arc segment without causing a magmatic and/or high-temperature metamorphic overprint in the overthrust eclogite-bearing allochthon.

The Taiwan collision zone, where the Luzon arc has overthrust its own forearc (e.g., McIntosh et al., 2005), shows a less complicated, albeit speculative, alternative. In this setting eclogite generated in forearc rocks can be transferred beneath the arc instead by underthrusting at depth into the backarc region (Fig. 7a, b). The Luzon arc is only ~25 km across in the collision zone (see Fig. 12, Line 23 in McIntosh et al., 2005), and any post-collisional rebound and/or tectonic exhumation could result in emplacement of parts of the partially subducted forearc block into the former backarc region. Ultimately, the continued convergence across the collision zone within YTT would induce subduction in the backarc region (Fig. 7a; e.g., Pubellier et al., 1999; Taira et al., 2004), thus initiating west-dipping subduction of the SMO inboard of YTT and exhuming the eclogites in the new subduction channel.



During west-directed subduction of the SMO, the YTT became the site of an early-middle Permian arc built upon the Snowcap siliciclastic substrate in the existing tectonic models (Colpron et al., 2006b; Piercey et al., 2006). By middle Permian, parts of the YTT were subjected to eclogite and blueschist facies metamorphism (275-260 Ma; Fallas et al., 1998; Erdmer et al., 1998; Creaser et al., 1999; Petrie et al., 2015; Petrie et al., 2016; Gilotti et al., 2017; Colpron et al., 2017). Since all phases of the early-middle Permian arc are interpreted to be built upon the YTT (Colpron et al., 2006b; Piercey et al., 2006; Gilotti et al., 2017), this requires that the upper plate was partly subducted, possibly for a second time. Mississippian tonalite and granite within YTT associated with the Permian eclogites were subjected to coeval high-pressure metamorphism (Petrie et al., 2015; Gilotti et al., 2017; Colpron et al., 2017), which suggests that these arc-like rocks and their Snowcap substrate were subducted together. Potential causes for this can include (i) YTT rocks were dragged into the subduction channel during subduction initiation in the SMO, forearc block underthrusting and/or during subduction erosion (Gilotti et al., 2017) that led to high pressure metamorphism by middle Permian (Fig. 7a); or (ii) a buoyant microcontinent calved off of YTT was partly subducted and underplated (Figs. 2, 7b; e.g., Devine et al., 2006). Continued subduction of the SMO and slab-rollback subsequently must have induced extension of the YTT and resulted in broadly coeval exhumation of eclogite in the forearc and exhumation of orogenic peridotite in the backarc (Fig. 7c; Johnston et al., 2007).

The large number of age constraints indicate that the change from eclogite formation/exhumation, exhumation of orogenic peridotites to formation of the Clinton Creek and Midnight Dome ophiolite complexes was very rapid, possibly as short as 2 my. The Clinton Creek and Midnight Dome and correlative SSZ ophiolite complexes in the SMT must have occupied an upper plate setting (see previous) and did not form part of the subducting SMO

floor. These relationships require a complex tectonic configuration between ca. 275 and 260 Ma. There are several types of configurations that could in principle explain these relationships, including (i) ocean-continent transition within the arc (Fig. 7d), (ii) propagating backarc rift in a continental arc (Fig. 7e), and (iii) discrete continental backarc rift, oceanic backarc and arc (Fig. 7f). Presence of an ocean-continent transition within the YTT (e.g., Mortensen, 1992) could have resulted from an original promontory – re-entrant configuration inherited from its rifting from the Laurentian margin. This configuration could explain exhumation of orogenic peridotite in continental basement on-strike with formation of an oceanic spreading centre (Fig. 7d; e.g., Davey et al., 2016). A similar along-strike relationship can be achieved by a propagating rift model, where oceanic crust is formed in areas with the greatest degree of extension on-strike with continental rifting (Fig. 7e; e.g., Taylor et al., 1999). Alternatively, orogenic peridotites may have been exhumed along a separate rift segment further in the backarc or along the margins of the rift (Fig. 7f; e.g., Canil et al., 2003; Johnston et al., 2007). This complex arc-backarc system would continue to develop above the subducting SMO until collision with and emplacement of YTT onto the Laurentian margin.

Modifying the existing models by introducing a Mississippian collision, emplacing Mississippian eclogite under the arc (Fig. 7a) and placing the suprasubduction zone Permian ophiolites into the upper arc plate (Figs. 7d-f) does improve the viability of the tectonic models as there are modern examples where such processes occur. However, this modification still requires several unusual tectonic circumstances such as lack of preservation of an obvious Late Devonian-Early Mississippian collider, coincident exhumation and emplacement of Mississippian and Permian eclogites, which allegedly formed on opposite sides of a continental arc system and partial subduction of parts of the upper plate arc terrane to eclogite facies at two

separate times. Although all of these processes are plausible on their own in principle, their juxtaposition in one terrane is rather improbable. In addition, these models still require subduction in the Permian backarc oceanic basin (SMO), represented by Clinton Creek, Midnight Dome and correlative ophiolites, and thus do not resolve the problem of obducting ophiolites from the subducting plate. Other tectonic models should therefore be considered (e.g. Parsons et al., in pressa), which are discussed below.

#### *YTT as a composite terrane*

As discussed above, the YTT is generally viewed as a single terrane characterised by multiple superposed magmatic cycles interpreted as arcs (see Colpron et al., 2006b; Piercey et al., 2006; Nelson et al., 2006 and references therein). One of the major weaknesses of this model is that it requires formation of alternating juvenile oceanic-like arc and continental magmatic suites above the same YTT continental basement. This continental basement must have undergone significant degrees of extension throughout its history as indicated by an abundance of tholeiitic and alkalic igneous rocks and close spatial links with ophiolitic rocks of various ages (e.g., Piercey et al., 2001, 2006, 2012; Simard et al., 2003; Murphy et al., 2006; Petrie et al., 2015, this paper). Specifically formation of ophiolites and juvenile arc magmatism (e.g. 314-269 Ma Klinkit cycle) suggest that the YTT continental crust had fully rifted, precluding preservation of significant continental basement inferred to be present beneath all of YTT's Snowcap assemblage (Piercey et al., 2006; Piercey and Colpron, 2009). Hence, formation of a subsequent continental arc cycle (e.g. 269-253 Ma Klondike cycle) above Snowcap Assemblage rocks either requires that the Klondike cycle magmatism formed in an unrelated tectonic setting and/or different plate, or that juvenile and continental domains were tectonically juxtaposed prior to the Klondike cycle magmatism. The latter is in our opinion a more viable hypothesis. That is, YTT

698 formed by amalgamation of a microcontinent and an intraoceanic arc-backarc terrane and then  
 699 subsequently evolved as a composite terrane (Parsons et al., in pressa). The dated, 309 Ma  
 700 leucotonalite-trondhjemite in the St. Cyr klippe is consistent with this hypothesis, because it may  
 701 correspond in age with the juvenile Klinkit arc cycle (Simard et al., 2003; Piercey et al., 2006),  
 702 yet intrudes into an oceanic assemblage represented by serpentinitized harzburgite, pyroxenite  
 703 and gabbro. We emphasize that the association and/or interaction of arc magmatic cycles with  
 704 Snowcap Assemblage rocks does not exclude formation of the arc rocks in an intra-oceanic  
 705 setting in the SMO (cf. Colpron et al., 2006a). The youngest component of the Snowcap  
 706 assemblage rocks could have been deposited in this basin during the early stages of SMO  
 707 development. Extensional allochthons with a Snowcap assemblage cover, isolated within a  
 708 progressively widening SMO (cf. Manatschal et al., 2006; Mohn et al., 2010) locally could have  
 709 become basement to subsequent arc volcanism (see Roots et al., 2006) following subduction  
 710 initiation in SMO and thereby cause zircon inheritance in otherwise intra-oceanic rocks.  
 711 Continental sources have been detected, for example, in the oceanic Solomon arc based on  
 712 inherited continental-derived zircons as old as Archean (Tapster et al., 2014).

713         The bulk of the continental YTT, which comprise the Snowcap Assemblage (e.g.,  
 714 Piercey and Colpron, 2009), Devonian to Early Carboniferous continentally contaminated  
 715 magmatic rocks and Permian K-feldspar megacrystic (Klondike) intrusions and related volcanic  
 716 rocks (Piercey et al., 2003, 2006; Ruks et al., 2006), are generally located to the west (outboard)  
 717 of the juvenile arc volcanic rocks and ophiolites (Fig. 1; Colpron et al., 2016). For the following  
 718 tectonic analysis, the continental part of composite YTT (YTTc), which is generally situated  
 719 farthest to the west, will refer to continental rocks, including any accreted outboard blocks, while  
 720 the ‘oceanic’ components of YTT (YTTj), which is generally situated more easterly will denote

the juvenile arc-backarc volcanic rocks and associated SSZ ophiolitic rocks emplaced onto YTTc (Fig. 1). YTTj corresponds with the Dunite Peak oceanic arc terrane of Parsons et al. (in pressa) and includes correlative SSZ ophiolitic rocks in the adjacent SMT such as the Clinton Creek and Midnight Dome complexes. The remnants of YTTj are now mainly preserved as relatively small klippe of oceanic crust and mantle above YTTc. Exhumation (e.g. Knight et al., 2013; Staples et al., 2016; Parsons et al., in pressa) has removed most of YTTj following its middle Permian to early Triassic obduction and subsequent Mesozoic thrusting and folding events (Figs. 8 b,c and 9c; Berman et al., 2007). In this tectonic model, the YTT of Colpron et al. (2006a) is thus a composite terrane comprising at least two separate blocks (YTTc and YTTj) before their middle Permian-early Triassic amalgamation (Fig. 8a) and the present distribution of the YTT components is representative of their relative Permian paleogeographic position.

The juvenile, oceanic constituents preserved in the YTT of Yukon and northern British Columbia (YTTj) range in age from the Carboniferous to Permian (Murphy et al., 2006; Piercey et al., 2006), although some (e.g. ultramafic-gabbro complex of St. Cyr) may be as old as Late Devonian. However, many age constraints are based on regional correlations and presumed stitching relationships into assemblages of multiple rock units. For example, presence of unrecognised low-angle faults within the assemblages is suggested by juxtaposition of boninite with continental-rift related magmatic rocks (Piercey et al., 2012; Ryan et al., 2017) and structural emplacement of mantle rocks previously mapped as intrusions (Murphy et al., 2006; Piercey et al., 2006) into supracrustal sequences of the Finlayson district. Lack of recognition of such low angle faults makes several lithological correlations and stratigraphic interpretations suspect. We hypothesize that juvenile arc volcanic rocks, such as those present in the Klinkit Group (Simard et al., 2003; Piercey et al., 2006) represent the product of an extensional oceanic

arc complex, which either initiated in the SMO, inboard of the composite continental YTTc block (Fig. 8a), along strike of YTTc or outboard of the YTTc (Fig. 9a). A Permian collision between YTTc and YTTj formed the YTT composite terrane and resulted in partial obduction of the oceanic YTTj, juxtaposition of Early Mississippian and Permian eclogite belts and initiation of west-dipping subduction east of the composite YTT by a Permian subduction polarity flip (Fig. 8b) as proposed by Parsons et al., (in pressa). The arc-backarc rocks of YTTj do not necessarily comprise all of the preserved SMT. Early Permian and older occurrences of SMT, such as chert and associated mafic volcanic rocks (Nelson, 1993), may represent accreted remnants of ocean floor rocks from the oceanic basin in which YTTj originally formed.

Slab rollback following the subduction flip led to extension and exhumation of orogenic Alpine-type peridotite in the composite YTT and isolation of klippen of oceanic YTTj above continental YTTc (Fig. 8c). This composite arc system subsequently continued to develop above the west-dipping subduction zone progressively consuming the remaining vestige of the SMO until composite YTT's collision with and obduction onto the trailing eastern passive margin of the SMO, which started sometime after the Middle Triassic (Parsons et al., in pressa), possibly during the Early Jurassic (Evenchick et al., 2007).

The coeval exhumation of orogenic peridotites and emplacement of the Clinton Creek and Midnight Dome ophiolite complexes onto YTTc can be explained by the same along or across strike tectonic settings discussed above (Figs. 7d-f). However, the composite nature of the YTT in this model allows several additional tectonic scenarios capable of explaining formation of the Clinton Creek and Midnight Dome ophiolite complexes within the oceanic YTTj (Figs. 8d, e). A diachronous collision of the continental YTTc and oceanic YTTj blocks could result in extensional arc or backarc magmatism in the overriding oceanic YTTj, where the collision has

not yet occurred, such that it is coeval with partial subduction of the continental YTTc to eclogite facies along strike where the collision already had started, and post-collisional extension along strike where the subduction polarity flip had occurred (Fig. 8d). The diachroneity of the collision may be due to oblique convergence or a marked promontory-re-entrant configuration of the margin of YTTc. The ongoing Luzon arc – China collision in central Taiwan, where a subduction polarity flip and collision are migrating diachronously from northeast to southwest in a geologically very short time frame is an example of such diachroneity (Huang et al., 2006).

The Clinton Creek and Midnight Dome ophiolite complexes form part of the overriding juvenile oceanic arc complex (YTTj) and do not represent normal oceanic lithosphere. In contrast to the singular YTT terrane model, this model is better at explaining the cause of the subduction flip, juxtaposition of continental and intraoceanic domains, isolation of ophiolites as klippen above YTT (e.g. St. Cyr klippe, Petrie et al., 2015; Dunite Peak, Parsons et al., in pressa; Harzburgite Peak complex, Canil and Johnston, 2003), juxtaposition of different ages of eclogite along the same boundary (Fig. 7b), and distribution of Carboniferous and Permian magmatism in distinct domains. Specifically, the Carboniferous-Permian oceanic arc complex (YTTj) is tectonically juxtaposed with a separate continental tectonic block (YTTc) (Fig. 8). As such, Carboniferous to Middle Permian arc magmatism is restricted to the overriding oceanic arc block (YTTj), whereas the Permian high grade metamorphism, crustal anatexis and post-collisional extension are generally restricted to the underthrust continental YTTc block (e.g., Ruks et al., 2006; Berman et al., 2007). This is consistent with previous suggestions that Carboniferous arc rocks form a separate nappe within the composite YTT (e.g., Tempelman-Kluit and Wanless, 1980; Ryan et al., 2013a, b; Ryan et al., 2014). The basal shear zone of this

nappe, the Yukon River shear zone, could be a remnant of the original thrust along which YTTj was emplaced over YTTc during the late Permian-early Triassic (Parsons et al., in press b).

In the composite YTT model, Permian eclogites could have formed by subduction of the leading edge of continental YTTc (Fig. 8b; Parsons et al., in pressa), including its entrained Mississippian tonalities and granite (Petrie et al., 2015; Colpron et al., 2017), partial subduction of a buoyant microcontinent calved off of YTTc (Fig. 2), or by subduction erosion of the YTTj forearc, which may have included some Snowcap Assemblage sediments and entrained intrusive rocks (Gilotti et al., 2017). However, the composite YTT model (Fig. 8) has a number of major drawbacks. Primarily it requires that subduction initiation in SMO (inboard of YTTc) had occurred during the Mississippian or earlier to account for eclogite formation at ca. 353 Ma (Erdmer et al., 1998; Devine et al., 2006) and its subsequent juxtaposition with the Permian eclogites (Fig. 8b, c). This implies that in the existing models subduction should have started immediately after the inferred Fammenian-earliest Mississippian rifting of YTTc from Laurentia, which in turn is mainly based on the occurrence of rift-related magmatism of this age in both terranes. Thus in the composite YTT model a separation of YTTc from Laurentia had to occur significantly earlier than the Famennian- earliest Mississippian, otherwise spreading in SMO could not be expected to generate enough oceanic lithosphere to sustain subduction for over 90 my. In addition, this model also requires that there was a significant volume of Laurentian derived sediment beneath the YTTj arc during the Mississippian phase of arc magmatism to explain the evidence for crustal contamination in its rocks (Piercey et al., 2006). As such, we further explore the Permian aspects of this model in more detail on the basis of a comparison with the tectonic evolution of the Australia – Pacific plate boundary zone (e.g. Hall, 2002; Baldwin et al., 2012).



## 812 *Comparison to modern tectonic configurations*

813         Below we briefly discuss aspects of the tectonics of the Solomon Islands – Papua New  
814 Guinea region of the southwest Pacific (Fig. 10a), which we consider a viable modern analogue.  
815 Arc-collision, suprasubduction zone backarc spreading, rift-related magmatism and exhumation  
816 of eclogite recently took place coevally or nearly so and/or is still ongoing. The model that  
817 invokes two separate YTT building blocks (Fig. 8) and their Permian amalgamation has many  
818 analogies with the tectonic relationships observed here, although the Australian - Pacific plate  
819 boundary zone displays very complex relationships between continental slivers, arcs, ocean  
820 basins and arc-collisions in time and space. Potential configurations of the Laurentian margin,  
821 SMO, YTTj and YTTc could broadly correspond to the Australian margin, Solomon Sea, New  
822 Britain-Solomon-New Hebrides arc system and micro continental slivers such as the Lord Howe  
823 rise respectively. This area also provides a cautionary note on correlations of deformation,  
824 magmatism and metamorphism in older orogens based on age alone (cf. van Staal et al., 1998).  
825 For the purpose of discussion, we will concentrate on the relationships across the New Britain-  
826 Solomon-New Hebrides arc system (Fig. 10a). From east to west, the north-east facing phase of  
827 the Solomon arc was involved in a Miocene collision with the outboard oceanic Ontong Java  
828 Plateau in the now inactive North Solomon-Kilinailu subduction zone, leading to a subduction  
829 reversal in the Neogene (Mann and Taira, 2004; Taira et al., 2004). Although the Solomon island  
830 arc is considered intra-oceanic, it does contain Cretaceous to Archaean zircon xenocrysts, which  
831 suggest derivation from a continental source such as Australia (Tapster et al., 2014). This has  
832 implications for the interpretation of the oceanic YTTj block in that the presence of sparse  
833 inheritance continentally derived zircons in volcanic and plutonic rocks does not necessarily  
834 indicate an autochthonous stratigraphic relationship with the inferred continental YTTc substrate.

No remnants of an Ontong Java-like oceanic plateau have been recognised in the composite YTT, although a collision between two buoyant blocks is a realistic mechanism to generate a subduction polarity reversal and induce subduction in a formerly opening oceanic basin.

Along-strike, the south-facing New Britain arc (Fig. 10a) is associated with normal subduction, whereas its westernmost segment has already collided with the Australian margin in the Finistere Range of the Huon Peninsula (Abers and McCaffrey, 1994). Further west along the Australian margin, arc polarity has switched to south dipping subduction along the west New Guinea trench. The collision between the Australian margin and the New Britain-Solomon arc system is diachronous, is propagating to the east, and will eventually lead to closure of the Solomon Sea. The Bismarck Sea, located in the backarc region of the New Britain Arc segment (Fig. 10a), is undergoing active spreading east of the collision zone near the Huon Peninsula. Hence, this zone is a realistic analogue for subduction polarity reversal overlapping with suprasubduction zone spreading and coeval arc-collision in the same tectonic system (Fig. 8d). We ignore the very slow, south-directed subduction along the Trobriand Trough along the south margin of the Solomon Sea as it only adds unnecessary complexity to this discussion. From west to east, the setting of the Australian continental margin changes from collision zone (with the western segment of the New Britain arc, Abers and McCaffrey, 1994), to a region of active continental rifting as a result of the westerly-propagating Woodlark rift along the eastern Papuan Peninsula (Fig. 10a). The latter rifting led to late Miocene exhumation of eclogite (Little et al., 2011; Baldwin et al., 2012; Webb et al., 2014). Further east, continental rifting has become fully oceanic in the Woodlark Basin (Taylor et al., 1999). The wedge-shaped spreading Woodlark Basin expands to the east and is here subducted under the Solomon Arc (Fig. 10a). Hence,

backarc spreading, arc-continent collision and extension-induced magmatism and exhumation (Fig. 8d, e) can coevally occur in different segments of one tectonic system.

The Solomon Islands – Papua New Guinea region of the southwest Pacific has undergone two separate subduction reversals related to the collisions with the Ontong Java Plateau (Mann and Taira, 2004; Taira et al., 2004) and the Australian margin (Abers and McCaffrey, 1994). These are two subduction reversals that are analogous to elements of both the singular and composite terrane model where YTTc could have collided with an outboard tectonic fragment leading to a Mississippian subduction reversal (Fig. 7a). Clinton Creek and Midnight Dome ophiolite complexes, along with other middle Permian ophiolites (e.g. Parsons et al., in pressa) formed in the upper plate and may be analogous to ophiolites that are forming in the Bismarck Sea coeval with the ongoing collision of the New Britain Arc with the Australian margin in the Finisterre Range of the Huon Peninsula. The Australian margin is partly subducted under the New Britain Arc during the collision and provides another potential mechanism for juxtaposition of two distinct, nonsynchronous eclogite belts in the YTT, an early Mississippian eclogite (Erdmer et al., 1998; Devine et al., 2006) that could have formed in the arc-trench gap of the oceanic YTTj and middle Permian eclogite (e.g. Petrie et al., 2015) that formed part of the subducting continental YTTc (Fig. 8b).

The Australian margin is subducted beneath the New Britain Arc and is likely subjected to eclogite-facies metamorphism at the same time as it is extending in the Woodlark Basin further to the east. The geological relationships provide two distinctly different analogues for emplacement of orogenic peridotites and eclogite facies metamorphism in the same plate. This is a conservative scenario to explain the complicated relationships in the composite YTT, but requires that continental YTTc is on the subducting plate (Figs. 8a, 9). However, this region also

serves as another cautionary note for two reasons: (i) calc-alkaline magmatism in the Woodlark rift is not related to subduction even though it is coeval with the active segments of the New Britain-Solomon Islands arc system (Fig. 10 a, b). Rather this magmatism is related to continental rifting and melting of previously subduction-modified mantle (Stolz et al., 1993). (ii) Eclogite is exhumed in the D'Entrecasteaux region, close to the western tip of the Woodlark Basin, but this eclogite is not associated with any active subduction zone. Rather it is related to exhumation of the deeper parts of a Miocene orogen, which formed between the rifted Australian margin and an outboard island arc terrane (Webb et al., 2014). If the Papuan Peninsula and Woodlark Basin area are indeed a viable analogue to the continental YTTc, it would imply that the continental Klondike "Arc" magmatism might actually represent a continental extensional province (e.g. Parsons et al, in press) that is coeval with orogenic peridotite exhumation on the same plate that was subducted along strike beneath the oceanic YTTj. In this scenario, Permian eclogites provide a constraint on the age of the collision (Fig. 8b) only if they formed in the position similar to the subducted Australian margin in the Finistere Range.

#### *Pre-Permian postulations*

The composite YTT hypothesis presented above (Fig. 8) improves the singular terrane based tectonic models (Fig. 7) and has a modern analogue in oceanic arc-continent collisions (e.g. Fig. 10a). However, this hypothesis (Parsons et al., in pressa) has difficulties providing a viable tectonic model for the pre-Permian evolution in the current tectonic framework. Specifically, this model is inconsistent with the inferred Late Devonian-early Mississippian opening of the SMO in previous models (e.g Colpron et al., 2007) and the required onset of east-directed subduction in SMO to generate the early Mississippian eclogite (Fig. 8 a,b). It is highly

unlikely that enough oceanic lithosphere was formed in the SMO by spreading within these time constraints to sustain subduction for over 90 my.

The composite YTT hypothesis and the modern analogues in the Australian and Pacific plate boundary zone discussed above provide an alternative model with respect to the polarity of subduction, formation of an oceanic arc-backarc terrane and opening the SMO. Most models (e.g. Nelson, 1993) assume that the present distribution of terranes is more or less indicative of their original paleogeographic position relative to each other and to the Laurentian margin (SMT mainly situated immediately east of YTT, hence formed between it and Laurentia). These models focus on the accretionary history, but they commonly ignore post-collisional extension in their ‘palinspastic’ reconstructions. Specifically, large portions of the YTTc are now known to have undergone exhumation in the Early Jurassic and later (e.g., Currie and Parrish, 1993; Berman et al., 2007; Knight et al., 2013; Staples et al., 2016; Morneau, 2017; Shirmohammad et al., 2011; Joyce et al., 2015). Jurassic and later exhumation of the YTTc indicates that the present distribution of terranes is not necessarily indicative of their relative paleogeographic position, but rather is a configuration that was established long after the closure of the SMO. Hence, the present distribution of terranes, with YTTc exhumed predominantly to the west of the YTTj, is an artefact of Mesozoic structural evolution and erosion and not necessarily indicative of the Paleozoic subduction polarity.

The simplest way of explaining the apparent longevity of Paleozoic subduction is by considering that YTTj originated outboard in Panthalassa above a west-dipping subduction zone (Fig. 9a). In this model, YTTj did not originate in a narrow SMO backarc seaway to the east of YTTc, but represents a part of a suprasubduction zone oceanic terrane situated west of YTTc in Panthalassa. The Late Devonian – earliest Mississippian rift-related magmatism in Laurentia and

YTTc would be akin to magmatism along the eastern Australian margin (Fig. 10b), which culminated in the Mesozoic to Tertiary separation of Lord Howe Rise and Norfolk Ridge (Schellart et al., 2006). The processes discussed in Fig. 8 to explain the nearly coeval obduction of the YTTj and exhumation of orogenic peridotite apply to this model as well, because both models create a similar geometry with YTTj structurally lying structurally above YTTc, followed by west-directed subduction in SMO (Fig. 9b, c). This model implies that a large part of the SMT rocks did not originate in the SMO as proposed by Nelson (1993) and Colpron and Nelson (2009), but outboard in the Panthalassa Ocean. To avoid confusion, we kept the SMO in figures 7, 8 and 9 as the ocean basin that was opening behind YTTc while it was moving westwards after rifting from Laurentia. However, we propose that the term SMO should be abandoned to avoid confusion with the proposed location where a large portion of the SMT (YTTj) was formed and instead replaced by Angayucham Ocean (cf. Colpron and Nelson, 2009; Sigloch and Mihalynuk, 2017). Nevertheless, it is possible that some ocean floor rocks of the oceanic seaway (SMO/Angayucham Ocean) that separated composite YTT from Laurentia were incorporated into the SMT during its terminal Mesozoic closure (Parsons et al., in pressa).

Formation of YTTj outboard in Panthalassa is attractive, because it could also explain the spatial association of continental rifting-related volcanic rocks (Fire Lake Formation) with boninites in the Finlayson district (Murphy et al., 2006, fig. 6; Ryan et al., 2017). Rift-related volcanic rocks may have formed in a setting similar to the northern Norfolk Ridge (Fig. 10a, b), whereas the boninites originated in a setting such as the southern New Hebrides island arc (Monzier et al., 1993). Norfolk Ridge and New Hebrides island arc are going to collide in the near future (Fig. 10a), coeval with the ongoing collision between the on-strike New Britain island arc and the Australian margin. In addition, slab-pull of the segment of Panthalassa Ocean

attached to YTTc subducting westwards beneath YTTj potentially could have moved YTTc a large distance from Laurentia after it had separated from it, opening a significantly wide oceanic basin behind it by spreading. This oceanic basin equates with the SMO and the along strike Angayucham Ocean further to the north of Nelson (1993) and Colpron and Nelson (2009). Following the middle Permian-early Triassic Klondike collision between the oceanic arc-backarc terrane (YTTj or the Dunite Peak oceanic arc of Parsons et al., (in pressa) and YTTc, subduction would have stepped back in the trailing Slide Mountain/Angayucham Ocean, the closure of which is probably preserved in the vertical slab wall imaged by tomography in the mantle beneath North America (Sigloch and Mihalynuk, 2013, 2017; Hildebrand, 2014). The time span of accretion of composite YTT to Laurentia and its possible complex interactions with other Mesozoic terranes (e.g. Stikinia-Quesnellia) forming an even larger composite terrane (Johnston, 2008; Hildebrand, 2013), prior to its Jurassic-Cretaceous arrival at the Laurentian margin (e.g. Evenchick et al., 2007; Pană and van der Pluijm, 2015; Sigloch and Mihalynuk, 2017), is still a matter of debate and outside the scope of this paper.

## **Conclusions**

Investigation of the Clinton Creek and Midnight Dome ophiolite complexes revealed that they formed in a suprasubduction zone spreading centre at ca. 265 Ma and were subsequently rapidly tectonically emplaced onto the YTTc during the Klondike orogeny as proposed by Parsons et al. (in pressa) for other Permian ophiolite complexes obducted onto YTTc and correlative SSZ volcanic rocks in the SMT. The Permian age of the SSZ setting and tectonic position above the YTTc indicate that these ophiolites did not form part of the subducting SMO floor during the Permian and that parts of the SMT have been erroneously assigned to the subducting plate in previous tectonic models. Formation of middle Permian SSZ ophiolite

complexes, obduction rather than subduction of ophiolite complexes, juxtaposition of Mississippian and Permian eclogites along the suture between YTT and Laurentia (e.g., Erdmer et al., 1998; Devine et al., 2006), and broadly coeval exhumation of orogenic peridotites (e.g., Canil et al., 2003; Johnston et al., 2007) are difficult to reconcile with existing tectonic models. These relationships require YTT to be composite and composed of an oceanic arc-backarc terrane (YTTj) obducted onto a continental fragment (YTTc) outboard of Laurentia. This composite terrane was subsequently emplaced onto Laurentia during the Jurassic-Cretaceous.

Although the Sea of Japan has been used to explain the evolution of the SMO (e.g., Creaser et al., 1997a, 1999), comparison of the observed relationships to modern analogues in the Australia-Pacific boundary zone combined with the time constraints on rifting and opening of the SMO, provides a viable alternative. In this alternative, the SMO (Angayucham Ocean) formed during rifting of YTTc from the Laurentian margin but did not host Permian subduction (Fig. 9). The Laurentian margin and YTTc are represented by Australia and outboard continental ribbon(s) (Lord Howe and Norfolk ridges), respectively, whereas YTTj is represented by parts of the New Britain-Solomon-New Hebrides arc (Fig. 10b) and respective back-arc spreading centres, including production of boninite (Monzier et al., 1993). In this alternative model, YTTj originated outboard in the Panthalassa Ocean rather than in the probably narrow SMO seaway. In addition, several diachronous collisions, arc and rifting episodes that are ongoing in the Australia-Pacific boundary region (e.g., Hall, 2002; Baldwin et al., 2012; Webb et al., 2014) could explain the disparate Carboniferous-Permian tectonic, metamorphic and magmatic events and unconformities recognised in the YTT (Colpron et al., 2006a, 2007; Berman et al., 2007). The tectonic mechanisms responsible for YTTc's rifting and drifting away from Laurentia as well the subsequent Mississippian initiation of west-directed subduction outboard in Panthalassa



are not well understood, but Late Devonian deformation, metamorphism and coeval magmatism in YTTc (see section of YTT as a singular terrane) hints at an important tectonic event that may be related to these processes.

## **Acknowledgements**

The authors are grateful to members of the British Columbia (JoAnne Nelson, Mitch Mihalynuk) and Yukon geological surveys (Maurice Colpron and Don Murphy) for their introduction into the complex Paleozoic and Mesozoic geology of the Intermontane Belt of the Canadian Cordillera, sharing data as well logistical support. The first (CvS) and third author (WMcL) would like to acknowledge close cooperation with Jane Gilotti and Meredith Petrie on the geology of the St. Cyr klippe. Detailed and careful journal reviews by Tekla Harms and Dan Gibson were very useful and improved the paper. The first author (CvS) would also like to thank Brendan, Alex, Shoufa and Dave for organizing this special volume. This is NRCAN contribution # 20180125.

## **References**

- Abbott, G., 1983, Origin of the Clinton Creek asbestos deposit: in Yukon Exploration and Geology 1982: Exploration and Geological Services Division, Yukon, Indian and Northern Affairs Canada, p. 18-25.
- Abbott, L. D., Silver, E. A., and Galewsky, J., 1994, Structural evolution of a modern arc-continent collision in Papua New Guinea: *Tectonics*, v. 13, no. 5, p. 1007-1034.
- Abers, G. A., and McCaffrey, R., 1994, Active arc-continent collision; earthquakes, gravity anomalies, and fault kinematics in the Huon-Finisterre collision zone, Papua New Guinea: *Tectonics*, v. 13, no. 2, p. 227-245.
- Anders, E., and Grevesse, N., 1989, Abundances of the elements; meteoritic and solar: *Geochimica et Cosmochimica Acta*, v. 53, no. 1, p. 197-214.

- 1017 Anonymous, 1972, Penrose field conference on ophiolites: *Geotimes*, v. 17, no. 12, p. 22-24.
- 1018 Baldwin, S. L., Fitzgerald, P. G., and Webb, L. E., 2012, Tectonics of the New Guinea region:  
1019 *Annual Review of Earth and Planetary Sciences*, v. 40, p. 495-520.
- 1020 Barth, A. P., and Wooden, J. L., 2006, Timing of magmatism following initial convergence at a  
1021 passive margin, Southwestern U.S. Cordillera, and ages of lower crustal magma sources:  
1022 *Journal of Geology*, v. 114, no. 2, p. 231-245.
- 1023 Barth, A. P., and Wooden, J. L., 2010, Coupled elemental and isotopic analyses of polygenetic  
1024 zircons from granitic rocks by ion microprobe, with implications for melt evolution and  
1025 the sources of granitic magmas: *Chemical Geology*, v. 277, no. 1-2, p. 149-159.
- 1026 Bedard, J. H., and Escayola, M., 2010, The Advocate Ophiolite mantle, Baie Verte,  
1027 Newfoundland; regional correlations and evidence for metasomatism: *Canadian Journal*  
1028 *of Earth Sciences*, v. 47, no. 3, p. 17.
- 1029 Belasky, P., Haggart, J. W., Stevens, C. H., Enkin, R. J., and Monger, J. W. H., 2006, Permian  
1030 faunas of westernmost North America; paleobiogeographic constraints on Permian  
1031 positions of Cordilleran terranes: *In* Haggart, J. W., Enkin, R. J., and Monger, J. W.  
1032 h.(eds), *Paleogeography of the North American Cordillera: evidence for and against*  
1033 *large-scale displacements*. Geological Association of Canada, v. 46, p. 71-80.
- 1034 Belasky, P., Stevens, C. H., and Hanger, R. A., 2002, Early Permian location of western North  
1035 American terranes based on brachiopod, fusulinid, and coral biogeography:  
1036 *Palaeogeography, Palaeoclimatology, Palaeoecology*, v. 179, no. 3-4, p. 245-266.
- 1037 Beranek, L. P., and Mortensen, J. K., 2011, The timing and provenance record of the Late  
1038 Permian Klondike Orogeny in northwestern Canada and arc-continent collision along  
1039 western North America: *Tectonics*, v. 30, p. 5.

- 1040 Berman, R. G., Ryan, J. J., Gordey, S. P., and Villeneuve, M., 2007, Permian to Cretaceous  
1041 polymetamorphic evolution of the Stewart River region, Yukon-Tanana Terrane, Yukon,  
1042 Canada; P-T evolution linked with in situ SHRIMP monazite geochronology: *Journal of*  
1043 *Metamorphic Geology*, v. 25, no. 7, p. 803-827.
- 1044 Black, L. P., Kamo, S. L., Allen, C. M., Davis, D. W., Aleinikoff, J. N., Valley, J. W., Mundil,  
1045 R., Campbell, I. H., Korsch, R. J., Williams, I. S., and Foudoulis, C., 2004, Improved  
1046 (super 206) Pb/ (super 238) U microprobe geochronology by the monitoring of a trace-  
1047 element-related matrix effect; SHRIMP, ID-TIMS, ELA-ICP-MS and oxygen isotope  
1048 documentation for a series of zircon standards: *Chemical Geology*, v. 205, no. 1-2, p.  
1049 115-140.
- 1050 Breitsprecher, K., Mortensen, J.K. (2004). Yukon Age 2004 - A database of isotopic age  
1051 determinations for rock units in Yukon Territory. Yukon Geological Survey, CD-ROM.
- 1052 Brown, D., Ryan, P.D., Afonso, J.C., Boutelier, D., Burg, J.P., Byrne, T., Calvert, A., Cook, F.,  
1053 Debari, S., Dewey, J.F., Gerya, T.V., Harris, R., Herrington, R., Konstantinovskaya, E.,  
1054 Reston, T. & Zagorevski, A. 2011. Arc–Continent Collision: The Making of an Orogen.  
1055 *In: Brown, D. & Ryan, P.D. (eds.) Arc-Continent Collision*. Berlin, Heidelberg: Springer  
1056 Berlin Heidelberg, p. 477-493.
- 1057 Cabanis, B., and Lecolle, M., 1989, Le diagramme La/10-Y/15-Nb/8; un outil pour la  
1058 discrimination des series volcaniques et la mise en evidence des processus de melange  
1059 et/ou de contamination crustale. The La/10-Y/15-Nb/8 diagram; a tool for distinguishing  
1060 volcanic series and discovering crustal mixing and/or contamination: *Comptes Rendus de*  
1061 *l'Academie des Sciences, Serie 2, Mecanique, Physique, Chimie, Sciences de l'Univers,*  
1062 *Sciences de la Terre*, v. 309, no. 20, p. 2023-2029.

- 1063 Calvert, A. J., 1996, Seismic reflection constraints on imbrication and underplating of the  
1064 northern Cascadia convergent margin: Canadian Journal of Earth Sciences, v. 33, no. 9,  
1065 p. 1294-1307.
- 1066 Canil, D., and Johnston, S. T., 2003, Harzburgite Peak: A large mantle tectonite massif in  
1067 ophiolite from southwest Yukon, *in* Emond, D. S., and Lewis, L. L., eds., 2002 Yukon  
1068 Exploration and Geology Exploration and Geological Services Division, Yukon Region,  
1069 Indian and Northern Affairs Canada, p. 77- 84.
- 1070 Canil, D., Johnston, S. T., Evers, K., Shellnutt, J. G., and Creaser, R. A., 2003, Mantle  
1071 exhumation in an early Paleozoic passive margin, northern Cordillera, Yukon: Journal of  
1072 Geology, v. 111, no. 3, p. 313-327.
- 1073 Cloos, M., 1993, Lithospheric buoyancy and collisional orogenesis; subduction of oceanic  
1074 plateaus, continental margins, island arcs, spreading ridges, and seamounts: Geological  
1075 Society of America Bulletin, v. 105, no. 6, p. 715-737.
- 1076 Colpron, M., and Nelson, J. L., 2009. A Paleozoic Northwest Passage: incursion of Caledonian,  
1077 Baltican and Siberian terranes into eastern Panthalassa and the early evolution of the  
1078 North American Cordillera. *In* Cawood, P. A., and Kroner, A., (eds.) Earth Accretionary  
1079 systems in Space and Time. The Geological Society, London, Special Publications, 318,  
1080 p. 273-307.
- 1081 Colpron, M., Gladwin, K., Johnston, S. T., Mortensen, J. K., and Gehrels, G. E., 2005, Geology  
1082 and juxtaposition history of the Yukon-Tanana, Slide Mountain, and Cassiar Terranes in  
1083 the Glenlyon area of central Yukon: Canadian Journal of Earth Sciences, v. 42, no. 8, p.  
1084 1431-1448.

- 1085 Colpron, M., Mortensen, J. K., Gehrels, G. E., and Villeneuve, M., 2006a, Basement complex,  
 1086 Carboniferous magmatism and Paleozoic deformation in Yukon-Tanana Terrane of  
 1087 central Yukon; field, geochemical and geochronological constraints from Glenlyon map  
 1088 area: . *In*: Colpron, M., Nelson, J.L. (eds.) Paleozoic evolution and metallogeny of  
 1089 pericratonic terranes at the ancient Pacific margin of North America, Canadian and  
 1090 Alaskan Cordillera. Geological Association of Canada, v. 45, p. 131-151.
- 1091 Colpron, M., Nelson, J. L., and Murphy, D. C., 2006b, A tectonostratigraphic framework for the  
 1092 pericratonic terranes of the northern Canadian Cordillera. *In*: Colpron, M., Nelson, J.L.  
 1093 (eds.) Paleozoic evolution and metallogeny of pericratonic terranes at the ancient Pacific  
 1094 margin of North America, Canadian and Alaskan Cordillera. Geological Association of  
 1095 Canada, v. 45, p. 1-23.
- 1096 Colpron, M., Nelson, J. L., and Murphy, D. C., 2007, Northern Cordilleran terranes and their  
 1097 interactions through time: GSA Today, v. 17, no. 4-5, p. 4-10.
- 1098 Colpron, M., Israel, S., Murphy, D., Pigage, L., and Moynihan, D., 2016, Yukon bedrock  
 1099 geology map, Yukon Geological Survey, Open File 2016-1, scale 1:1 000 000, map and  
 1100 legend.
- 1101 Colpron, M., Carr, S., Hildes, D., Piercey, S. (2017). Geophysical, geochemical and  
 1102 geochronological constraints on the geology and mineral potential of the Livingstone  
 1103 Creek area, south-central Yukon (NTS 105E/8). *In*: MacFarlane, K.E., Weston, L.H.  
 1104 (eds.) Yukon Exploration and Geology Overview 2016. Yukon Geological Survey, 47-  
 1105 86.
- 1106 Creaser, R. A., Goodwin-Bell, J.-A. S., and Erdmer, P., 1999, Geochemical and Nd isotopic  
 1107 constraints for the origin of eclogite protoliths, northern Cordillera; implications for the

- 1108 Paleozoic tectonic evolution of the Yukon-Tanana Terrane: Canadian Journal of Earth  
1109 Sciences, v. 36, no. 10, p. 1697-1709.
- 1110 Creaser, R. A., Erdmer, P., Stevens, R. A., and Grant, S. L., 1997a. Tectonic affinity of Nisutlin  
1111 and Anvil assemblage strat from the Teslin tectonic zone, northern Canadian Cordillera:  
1112 Constraints from neodymium isotope and geochemical evidence. *Tectonics* 16, 107-  
1113 121.
- 1114 Creaser, R.A., Heaman, L.M., Erdmer, P., 1997b. Timing of high-pressure metamorphism in the  
1115 Yukon – Tanana terrane, Canadian Cordillera: constraints from U – Pb zircon dating of  
1116 eclogite from the Teslin tectonic zone. *Canadian Journal of Earth Sciences*. 34, 709-715.
- 1117 Creaser, R.A., Goodwin-Bell, J.-a.S. & Erdmer, P. 1999. Geochemical and Nd isotopic  
1118 constraints for the origin of eclogite protoliths, northern Cordillera: implications for the  
1119 Paleozoic tectonic evolution of the Yukon-Tanana terrane. *Canadian Journal of Earth*  
1120 *Sciences*, 36, 1697-1709.
- 1121 Currie and Parrish, 1993, Jurassic accretion of Nisling terrane along the western margin of  
1122 stikinia, coast mountains, northwestern British Columbia. *Geology*, v. 21, 235-238
- 1123 Davey, F. J., Granot, R., Cande, S. C., Stock, J. M., Selvens, M., and Ferraccioli, F., 2016,  
1124 Synchronous oceanic spreading and continental rifting in West Antarctica: Geophysical  
1125 Research Letters, v. 43, no. 12, p. 6162-6169.
- 1126 De Keijzer, M., Williams, P.F., Carr, S.D. (2000). Reflections on Lithoprobe SNORCLE Line 31  
1127 in light of the structure of the Teslin zone in the Last Peak area (NTS map 105 E/9),  
1128 southern Yukon Territory. *In: Cook, F., Erdmer, P. (eds.) Slave – North American*  
1129 *Cordillera Lithospheric Evolution (SNORCLE) Transect and Cordilleran Tectonics*  
1130 *Workshop Meeting*. Calgary, Alberta. Lithoprobe Report 72: 114–118.

- 1131 Devine, F., Colpron, M., Carr, S. D., Murphy, D. C., Davis, W. J., Smith, S., Villeneuve, M., and  
 1132 Nelson, J. L., 2006, Geochronological and geochemical constraints on the origin of the  
 1133 Klatsa metamorphic complex; implications for early Mississippian high-pressure  
 1134 metamorphism within Yukon-Tanana Terrane: . *In*: Colpron, M., Nelson, J.L. (eds.)  
 1135 *Paleozoic evolution and metallogeny of pericratonic terranes at the ancient Pacific*  
 1136 *margin of North America, Canadian and Alaskan Cordillera*. Geological Association of  
 1137 Canada, v. 45, p. 107-130.
- 1138 Dick, H.J.B. and Bullen, T., 1984, Chromian spinel as a petrogenetic indicator in abyssal and  
 1139 alpine-type peridotites and spatially associated lavas. *Contributions to Mineralogy and*  
 1140 *Petrology*, 86(1): 54-76. Dickinson, W. R., 2004, Evolution of the North American  
 1141 Cordillera: *Annual Review of Earth and Planetary Sciences*, v. 32, p. 13-45.
- 1142 Dusel-Bacon, C., Colpron, M., Hopkins, M. J., Mortensen, J. K., Dashevsky, S. S., Bressler, J.  
 1143 R., Day, W. C., and Nelson, J. L., 2006, Paleozoic tectonic and metallogenic evolution of  
 1144 the pericratonic rocks of east-central Alaska and adjacent Yukon: . *In*: Colpron, M.,  
 1145 Nelson, J.L. (eds.) *Paleozoic evolution and metallogeny of pericratonic terranes at the*  
 1146 *ancient Pacific margin of North America, Canadian and Alaskan Cordillera*. Geological  
 1147 Association of Canada, v. 45, p. 25-74.
- 1148 Dusel-Bacon, C., Day, W. C., and Aleinikoff, J. N., 2013, Geochemistry, petrography, and  
 1149 zircon U-Pb geochronology of Paleozoic metaigneous rocks in the Mount Veta area of  
 1150 east-central Alaska; implications for the evolution of the westernmost part of the Yukon-  
 1151 Tanana Terrane: *Canadian Journal of Earth Sciences*, v. 50, no. 8, p. 826-846.

- 1152 Erdmer, P., and Helmstaedt, H., 1983, Eclogite from central Yukon; a record of subduction at the  
 1153 western margin of ancient North America: *Canadian Journal of Earth Sciences*, v. 20, no.  
 1154 9, p. 1389-1408.
- 1155 Erdmer, P., Armstrong, R.L. (1988). Permo-Triassic Isotopic Dates for Blueschist, Ross River  
 1156 Area, Yukon. *In*: Abbott, J.G. (ed.) Yukon Geology Volume 2. Exploration & Geological  
 1157 Services Division, Yukon, Indian & Northern Affairs Canada, p 33-36.
- 1158 Erdmer, P., Ghent, E.D., Archibald, D.A., Stout, M.Z. (1998). Paleozoic and Mesozoic high-  
 1159 pressure metamorphism at the margin of ancestral North America in central Yukon. *GSA*  
 1160 *Bulletin*. 110, 615-629.
- 1161 Evenchick, C. A., McMechan, M. E., McNicoll, V. J., and Carr, S. D., 2007. A synthesis of the  
 1162 Jurassic-Cretaceous tectonic evolution of the central and southwestern Canadian  
 1163 cordillera: Exploring links across the orogen. *In* Sears, J. W., Harms, T. A., and  
 1164 Evenchick, C. A., eds., *Whence the mountains? Inquiries into the evolution of orogenic*  
 1165 *systems: A volume in honor of Raymond A. Price*. Geological Society of America  
 1166 Special Paper 433, 117-145.
- 1167 Fallas, K. M., Cook, F., Erdmer, P., Archibald, D. A., Heaman, L. M., Creaser, R. A., and  
 1168 Erdmer, P., 1998, The St. Cyr Klippe, south-central Yukon; an outlier of the Teslin  
 1169 tectonic zone?: *Lithoprobe Report*, 131-138.
- 1170 Foster, H. L., and Keith, T. E. C., 1974, Ultramafic rocks of the Eagle Quadrangle, east-central  
 1171 Alaska: *Journal of Research of the U. S. Geological Survey*, v. 2, no. 6, p. 657-669.
- 1172 Foster, H.L., Keith, T.E.C., Menzie, W.D. (1994). Geology of the Yukon-Tanana area of east-  
 1173 central Alaska. *In*: Plafker, G., Berg, H.C. (eds.) *The Geology of Alaska*. Geological  
 1174 Society of America, 205–240.



- 1175 Gabrielse, H., Mortensen, J. K., Parrish, R. R., Harms, T. A., Nelson, J. L., and van der Heyden,  
 1176 P., 1993a, Late Paleozoic plutons in the Sylvester allochthon, north-central British  
 1177 Columbia: Radiogenic Age and Isotopic Studies: Report 7; Geological Survey of Canada,  
 1178 v. Paper 93-2, p. 107-118.
- 1179 Gabrielse, H., Murphy, D.C., Mortensen, J.K., (2006). Cretaceous and Cenozoic dextral orogen-  
 1180 parallel displacements, magmatism and paleogeography, north-central Canadian  
 1181 Cordillera. *In*: Haggart, J.W., Enkin, R.J., Monger, J.W.H., (eds.) Paleogeography of the  
 1182 North American Cordillera: Evidence for and against large-scale displacements.  
 1183 Geological Association of Canada, Special Paper 46, 255-276.
- 1184 Galewsky, J., Silver, E. A., Gallup, C. D., Edwards, R. L., and Potts, D. C., 1996, Foredeep  
 1185 tectonics and carbonate platform dynamics in the Huon Gulf, Papua New Guinea:  
 1186 *Geology* (Boulder), v. 24, no. 9, p. 819-822.
- 1187 Gehrels, G.E., McClelland, W.C., Samson, S.D., Patchett, P.J., and Orchard, M.J., 1992,  
 1188 *Geology of the western flank of the Coast Mountains between Cape Fanshaw and Taku*  
 1189 *Inlet, southeastern Alaska: Tectonics*, v. 11, no. 3, p. 567–585, doi: 10.1029/92TC00482
- 1190 Gilotti, J. A., McClelland, W. C., van Staal, C. R., Petrie, M. B., 2017 detrital zircon evidence  
 1191 for eclogite formation by basal subduction erosion – An example from the Yukon-Tanana  
 1192 composite arc, Canadian Cordillera. *Geological Society of America Special Paper* , v.  
 1193 526, 17 p.
- 1194 Goodwin-Bell, J.-A. (1998). A geochemical and Sm-Nd isotopic study of Cordilleran eclogites  
 1195 from the Yukon-Tanana terrane. [*MSc Thesis*] University of Alberta, Edmonton, AB,  
 1196 pp145

- 1197 Gordey, S.P. 2002. Is Yukon-Tanana Terrane North America? *In*: Cook, F. & Erdmer, P. (eds.)  
 1198 *SNORCLE Transect and Cordilleran Tectonics Workshop Meeting*. Pacific Geoscience  
 1199 Centre.  
 1200 Lithoprobe Reort no. 82, p. 39-42
- 1201 Gordey, S. P., Geldsetzer, H.H. J.,Morrow, D.W., Bamber, E. W., Henderson, C. W., Richards,  
 1202 B. C. 1991.Upper Devonian to Middle Jurassic assemblages. Part A, Ancestral North  
 1203 America. In *Geology of the Cordilleran orogen in Canada*. Edited by H. Gabrielse and C.  
 1204 Yorath. Geological Society of America Decade of North American Geology G2, p. 221-  
 1205 328.
- 1206 Hall, R., 2002, Cenozoic geological and plate tectonic evolution of SE Asia and the SW Pacific:  
 1207 computer-based reconstructions, model and animations: *Journal of Asian Earth Sciences*,  
 1208 v. 20, no. 4, p. 353-431.
- 1209 Harms, T. A., and Murchey, B. L., 1992, Setting and occurrence of late Paleozoic radiolarians in  
 1210 the Sylvester Allochthon, part of a proto-Pacific ocean floor terrane in the Canadian  
 1211 Cordillera: *Palaeogeography, Palaeoclimatology, Palaeoecology*, v. 96, no. 1-2, p. 127-  
 1212 139.
- 1213 Hildebrand, R. S., 2013.Mesozoic Assembly of the North American Cordillera.GSA Special  
 1214 Paper 495, 169p.
- 1215 Hildebrand, R. S., 2014, Geology, Mantle tomography, and inclination corrected  
 1216 paleogeographic trajectories support westward subduction during Cretaceous orogenesis  
 1217 in the north american Cordillera. *In*:Hibbard, J. P., Pollock, J. C., Murphy, J. B., van  
 1218 Staal, C. R. and Greenough, J. D. (eds.)*Reeltime Geological Syntheses -Remembering*  
 1219 *Harold 'Hank' Williams*. Geoscience Canada Reprint Series 10, p.439-456.

- 1220 Huang, C., Yuan, P., and Tsao, S., 2006. Temporal and spatial record of active arc-continent  
1221 collision in Taiwan: A synthesis. *Geol. Soc. Am. Bull.* 118, 274-288.
- 1222 Htoon, M. (1981), Isotopic age determinations of some metamorphic and igneous rocks from  
1223 Clinton Creek area, Yukon. *In: Tempelman-Kluit, D.J. (ed.) Yukon Geology and*  
1224 *Exploration 1979-80. Indian and Northern Affairs Canada, Exploration & Geological*  
1225 *Services Division, 65-67.*
- 1226 Jagoutz, O., Müntener, O., Manatschal, G., Rubatto, D., Péron-Pinvidic, G., Turrin, B.D., and Villa, I.M.,  
1227 2007, The rift-to-drift transition in the North Atlantic: A stuttering start of the MORB machine?:  
1228 *Geology*, v. 35, p. 1087–1090.
- 1229 Johnston, S.T., 2008. The cordilleran ribbon continent of North America. *Annual Review of*  
1230 *Earth and Planetary Sciences*, 36, p. 495-530.
- 1231 Johnston, S. T., Canil, D., and Heaman, L. H., 2007, Permian exhumation of the Buffalo Pitts  
1232 orogenic peridotite massif, northern Cordillera, Yukon: *Canadian Journal of Earth*  
1233 *Sciences*, v. 44, no. 3, p. 275-286.
- 1234 Joyce, N.L., Ryan, J.J., Colpron, M., Hart, C.J.R., Murphy, D.C. (2015). A compilation of  
1235  $^{40}\text{Ar}/^{39}\text{Ar}$  age determinations for igneous and metamorphic rocks, and mineral  
1236 occurrences from central and southeast Yukon. *Geological Survey of Canada, Open File*  
1237 *7924*, pp229.
- 1238 Kimura, G., and Ludden, J., 1995, Peeling oceanic crust in subduction zones: *Geology (Boulder)*,  
1239 v. 23, no. 3, p. 217-220.
- 1240 Knight, E., Schneider, D.A. & Ryan, J.J. 2013. Thermochronology of the Yukon-Tanana  
1241 Terrane, West-Central Yukon: Evidence for Jurassic Extension and Exhumation in the  
1242 Northern Canadian Cordillera. *The Journal of Geology* v. 121, pp. 371-400.

- 1243 Korotev, R. L., 1996, On the relationship between the Apollo 16 ancient regolith breccias and  
 1244 feldspathic fragmental breccias, and the composition of the prebasin crust in the Central  
 1245 Highlands of the Moon: *Meteoritics*, v. 31, no. 3, p. 403-412.
- 1246 Lallemand, S., Heuret, A., and Boutelier, D., 2005, On the relationships between slab dip, back-  
 1247 arc stress, upper plate absolute motion, and crustal nature in subduction zones:  
 1248 *Geochemistry, Geophysics, Geosystems* - G [super 3], p. 18.
- 1249 Little, T. A., Hacker, B. R., Gordon, S. M., Baldwin, S. L., Fitzgerald, P. G., Ellis, S., and  
 1250 Korchinski, M., 2011, Diapiric exhumation of Earth's youngest (UHP) eclogites in the  
 1251 gneiss domes of the D'Entrecasteaux Islands, Papua New Guinea: *Tectonophysics*, v.  
 1252 510, no. 1-2, p. 39-68.
- 1253 Ludwig, K. R., 2003, User's manual for Isoplot/Ex rev. 3.00: a Geochronological Toolkit for  
 1254 Microsoft Excel, Berkeley Geochronology Center, Berkeley, Special Publication 4, 70 p.:
- 1255 MacLeod, C. J., Searle, R. C., Murton, B. J., Casey, J. F., Mallows, C., Unsworth, S. C.,  
 1256 Achenbach, K. L., and Harris, M., 2009, Life cycle of oceanic core complexes: Earth and  
 1257 Planetary Science Letters, v. 287, no. 3-4, p. 333-344.
- 1258 Manatschal, G., 2004, New models for evolution of magma-poor rifted margins based on a review  
 1259 of data and concepts from West Iberia and the Alps: *International Journal of Earth*  
 1260 *Sciences*, v. 93, p. 432-466,
- 1261 Manatschal, G., Engstrom, A., Desmurs, L., Schaltegger, U., Cosca, M., Muntener, O., Bernoulli,  
 1262 D., 2006, What is the tectono-metamorphic evolution of continental break-up: The  
 1263 example of the Tasna Ocean-Continent transition: *Journal of Structural Geology*, v. 28,  
 1264 p. 1849-1869

- 1265 Manatschal, G., Montanini, A., Sauter, D., Karpoff, A. M., Masini, E., Mohn, G., Lagabriele,  
1266 Y., Piccardo, G. B., Tribuzio, R., and Dick, H. J. B., 2011, The Chenaillet Ophiolite in  
1267 the French/Italian Alps; an ancient analogue for an oceanic core complex?: *Lithos* [Oslo],  
1268 v. 124, no. 3-4, p. 169-184.
- 1269 Mann, P., and Taira, A., 2004, Global tectonic significance of the Solomon Islands and Ontong  
1270 Java Plateau convergent zone: *Tectonophysics*, v. 389, no. 3-4, p. 137-190.
- 1271 Mattinson, J. M., 2010, Analysis of the relative decay constants of (super 235) U and (super 238)  
1272 U by multi-step CA-TIMS measurements of closed system natural zircon samples:  
1273 *Chemical Geology*, v. 275, no. 3-4, p. 186-198.
- 1274 Mazdab, F. K., 2009, Characterization of flux-grown trace-element-doped titanite using the high-  
1275 mass-resolution ion microprobe (SHRIMP-RG): *Canadian Mineralogist*, v. 47, no. 4, p.  
1276 813-831.
- 1277 Mazdab, F. K., and Wooden, J. L., 2006, Trace element analysis in zircon by ion microprobe  
1278 (SHRIMP-RG); technique and applications: *Geochimica et Cosmochimica Acta*, v. 70,  
1279 no. 18S, p. A405.
- 1280 McIntosh, K., Nakamura, Y., Wang, T. K., Shih, R. C., Chen, A., and Liu, C. S., 2005, Crustal-  
1281 scale seismic profiles across Taiwan and the western Philippine Sea: *Tectonophysics*, v.  
1282 401, no. 1-2, p. 23-54.
- 1283 Miranda, E. A., and Dilek, Y., 2010, Oceanic core complex development in modern and ancient  
1284 oceanic lithosphere; gabbro-localized versus peridotite-localized detachment models:  
1285 *Journal of Geology*, v. 118, no. 1, p. 95-109.

- 1286 Mohn, G., Manatschal, G., Müntener, O., Beltrando, M., and Masini, E., 2010, Unravelling the  
1287 interaction between tectonic and sedimentary processes during lithospheric thinning in  
1288 the Alpine Tethys margins: *International Journal of Earth Sciences*, v. 99, p. 75–101.
- 1289 Monzier, M., Danyushevsky, L. V., Crawford, A. J., Bellon, H., and Cotten, J., 1993, High-Mg  
1290 andesites from the southern termination of the New Hebrides island arc (SW Pacific):  
1291 *Journal of Volcanology and Geothermal Research*, v. 57, no. 3-4, p. 193-217.
- 1292 Moores, E. M., 1982, Origin and emplacement of ophiolites: *Reviews of Geophysics and Space*  
1293 *Physics*, v. 20, no. 4, p. 735-760.
- 1294 Morneau, Y.E. 2017. Tectono-Metamorphic Evolution of the Snowcap Assemblage, Yukon-  
1295 Tanana Terrane, West-Central Yukon. [MSc Thesis], pp. 199. Carleton University,  
1296 Ottawa, ON., Canada.
- 1297 Mortensen, J.K., 1990. Geology and U–Pb geochronology of the Klondike District, west-central  
1298 Yukon Territory. *Canadian Journal of Earth Sciences*, 27, 903-914.
- 1299 Mortensen, J. K., 1992, Pre-mid-Mesozoic tectonic evolution of the Yukon-Tanana Terrane,  
1300 Yukon and Alaska: *Tectonics*, v. 11, no. 4, p. 18.
- 1301 Murphy, D. C., Colpron, M., Mortensen, J. K., Piercey, S. J., Orchard, M. J., Gehrels, G. E., and  
1302 Nelson, J. L., 2006, Mid-Paleozoic to early Mesozoic tectonostratigraphic evolution of  
1303 Yukon-Tanana and Slide Mountain terranes and affiliated overlap assemblages,  
1304 Finlayson Lake massive sulphide district, southeastern Yukon: . *In*: Colpron, M., Nelson,  
1305 J.L. (eds.) *Paleozoic evolution and metallogeny of pericratonic terranes at the ancient*  
1306 *Pacific margin of North America, Canadian and Alaskan Cordillera*. Geological  
1307 Association of Canada, v. 45, p. 75-105.

- 1308 Nelson, J. L., 1993, The Sylvester Allochthon; upper Paleozoic marginal-basin and island-arc  
 1309 terranes in northern British Columbia: Canadian Journal of Earth Sciences, v. 30, no. 3, p.  
 1310 631-643.
- 1311 Nelson, J. L., and Bradford, J. A., 1993, Geology of the Midway-Cassiar area, northern British  
 1312 Columbia (104O, 104P): Ministry of Energy, Mines and Petroleum Resources. Bulletin  
 1313 83, p. 94
- 1314 Nelson, J. L., Colpron, M., Israel, S., 2013, The Cordillera of British Columbia, Yukon, and  
 1315 Alaska; tectonics and metallogeny: *In* Bissig, T., Rusk, B. G., and Thompson, J. F. H.  
 1316 (eds.) Special Publication [Society of Economic Geologists [U. S.]], v. 17, p. 53-109.
- 1317 Nelson, J. L., Colpron, M., Piercey, S. J., Dusel-Bacon, C., Murphy, D. C., Roots, C. F., and  
 1318 Nelson, J. L., 2006, Paleozoic tectonic and metallogenetic evolution of pericratonic  
 1319 terranes in Yukon, northern British Columbia and eastern Alaska: . *In*: Colpron, M.,  
 1320 Nelson, J.L. (eds.) Paleozoic evolution and metallogeny of pericratonic terranes at the  
 1321 ancient Pacific margin of North America, Canadian and Alaskan Cordillera. Geological  
 1322 Association of Canada, v. 45, p. 323-360.
- 1323 Niu, Y., Herzberg, C., and Wilson, M., 2004, Bulk-rock major and trace element compositions of  
 1324 abyssal peridotites; implications for mantle melting, melt extraction and post-melting  
 1325 processes beneath mid-ocean ridges: Journal of Petrology, v. 45, no. 12, p. 2423-2458.
- 1326 Ohara, Y., Fujioka, K., Ishii, T., and Yurimoto, H., 2003, Peridotites and gabbros from the  
 1327 Parece Vela backarc basin; unique tectonic window in an extinct backarc spreading ridge:  
 1328 Geochemistry, Geophysics, Geosystems - G super 3, v. 4, no. 7, p. 8611.
- 1329 Orchard, M.J. (2006). Late Paleozoic and Triassic conodont faunas of Yukon and northern  
 1330 British Columbia and implications for the evolution of the Yukon-Tanana terrane. *In*:

- 1331 Colpron, M., Nelson, J.L. (*eds.*) Paleozoic evolution and metallogeny of pericratonic  
 1332 terranes at the ancient Pacific margin of North America, Canadian and Alaskan  
 1333 Cordillera. Geological Association of Canada, Special Paper 45, 229-260.
- 1334 Pană, D. I., and van der Pluijm, B. A., 2015. Orogenic pulses in the Alberta rocky mountains:  
 1335 radiometric dating of major faults and comparison with the regional tectono-stratigraphic  
 1336 record. GSA Bulletin, v. 127, p. 480-502.
- 1337 Parsons, A.J., Ryan, J.J., Coleman, M., van Staal, C.R. (2017). The Slide Mountain ophiolite,  
 1338 Big Salmon Range, south-central Yukon: Preliminary results from fieldwork. *In*:  
 1339 MacFarlane, K.E., Weston, L.H. (*eds.*) Yukon Exploration and Geology Overview 2016.  
 1340 Yukon Geological Survey, 181-196.
- 1341 Parsons, A. J., Zagorevski, A., Ryan, J. J, McClelland, W. C., van Staal, C. R., Coleman, M. C.,  
 1342 Golding, M. L., 2018. Petrogenesis of the dunite Peak ophiolite, south-central yukon: a  
 1343 new hypothesis for the late Paleozoic-early mesozoic tectonic evolution of the northern  
 1344 cordillera. GSA Bulletin, in pressa
- 1345 Parsons, A.J., Coleman, M.J., Ryan, J.J., Joyce, N.L., Gibson, H.D., and Larson, K.P. 2018, The Yukon  
 1346 River Shear Zone: A complex record of mid- to upper-crustal deformation of the Yukon-Tanana  
 1347 terrane, NW Cordillera; Lithosphere, in pressb
- 1348 Pearce, J. A., 1996, A user's guide to basalt discrimination diagrams, *in* Wyman, D. A., ed.,  
 1349 Trace element geochemistry of volcanic rocks: Applications for massive sulphide  
 1350 exploration, Volume 12, Geological Association of Canada, Short Course, p. 79-113.
- 1351 Pearce, J. A., 2014, Immobile element fingerprinting of ophiolites: Elements, v. 10, no. 2, p.  
 1352 101-108.
- 1353 Pecha, M. E., Gehrels, G. E., McClelland, W. C., Giesler, D., White, C., Yokelson, I., 2016,



- 1354 detrital Zircon U-Pb geochronology and Hf- isotope geochemistry of the Yukon-Tanana  
1355 terrane, Coast Mountains, southeast Alaska. *Geosphere*, v. 12, no 5, p., 19p. doi: 10  
1356 .1130 /GES01303 .1 .
- 1357 Perfit, M. R., Taylor, B., Langmuir, C. H., Baekisapa, M., Chappell, B. W., Johnson, R. W.,  
1358 Staudigel, H., Taylor, S. R., and Exon, N. F., 1987, Geochemistry and petrology of  
1359 volcanic rocks from the Woodlark Basin; addressing questions of ridge subduction: *Earth*  
1360 *Science Series*, v. 7, p. 113-154.
- 1361 Petrie, M. B., 2014, Evolution of eclogite facies metamorphism in the St. Cyr Klippe, Yukon-  
1362 Tanana Terrane, Yukon, Canada [Ph.D.: University of Iowa, 185 p.
- 1363 Petrie, M. B., Gilotti, J. A., McClelland, W. C., van Staal, C. R., and Isard, S. J., 2015, Geologic  
1364 setting of Eclogite-facies assemblages in the St. Cyr klippe, Yukon-Tanana terrane,  
1365 Yukon, Canada: *Geoscience Canada*, v. 42, p. 327-350.
- 1366 Petrie, M. B., Massonne, H.-J., Gilotti, J. A., McClelland, W. C., and Van Staal, C., 2016, The P-  
1367 T path of eclogites in the St. Cyr Klippe, Yukon, Canada; Permian metamorphism of a  
1368 coherent high-pressure unit in an accreted terrane of the North American Cordillera:  
1369 *European Journal of Mineralogy*, v. **28**, p. 1111-1130
- 1370 Philippot, P., Blichert-Toft, J., Perchuk, A., Costa, S., Gerasimov, V. (2001). Lu-Hf and Ar-Ar  
1371 chronometry supports extreme rate of subduction zone metamorphism deduced from  
1372 geospeedometry. *Tectonophysics*. 342, 23-38.
- 1373 Pidgeon, R. T., Lanphere, M. A., Furfaro, D., Kennedy, A. K., Nemchin, A. A., van Bronswijk,  
1374 W., Dalrymple, G. B., and Turrin, B. D., 1994, Calibration of zircon standards for the  
1375 Curtin SHRIMP II: Geological Survey Circular, 251.

- 1376 Piercey, S. J., and Colpron, M., 2009, Composition and provenance of the Snowcap assemblage,  
 1377 basement to the Yukon-Tanana Terrane, northern Cordillera; implications for Cordilleran  
 1378 crustal growth: *Geosphere*, v. 5, no. 5, p. 439-464.
- 1379 Piercey, S. J., Colpron, M., Nelson, J. L., Colpron, M., Dusel-Bacon, C., Simard, R.-L., Roots, C.  
 1380 F., and Nelson, J. L., 2006, Paleozoic magmatism and crustal recycling along the ancient  
 1381 Pacific margin of North America, northern Cordillera: . *In*: Colpron, M., Nelson, J.L.  
 1382 (eds.) *Paleozoic evolution and metallogeny of pericratonic terranes at the ancient Pacific*  
 1383 *margin of North America, Canadian and Alaskan Cordillera*. Geological Association of  
 1384 Canada, v. 45, p. 281-322.
- 1385 Piercey, S. J., Mortensen, J. K., and Creaser, R. A., 2003, Neodymium isotope geochemistry of  
 1386 felsic volcanic and intrusive rocks from the Yukon-Tanana Terrane in the Finlayson Lake  
 1387 region, Yukon, Canada: *Canadian Journal of Earth Sciences*, v. 40, no. 1, p. 77-97.
- 1388 Piercey, S. J., Murphy, D. C., and Creaser, R. A., 2012, Lithosphere-asthenosphere mixing in a  
 1389 transform-dominated late Paleozoic backarc basin: Implications for northern Cordilleran  
 1390 crustal growth and assembly *Geosphere*, v. 8, p. 716-739.
- 1391 Piercey, S. J., Murphy, D. C., Mortensen, J. K., and Creaser, R. A., 2004, Mid-Paleozoic  
 1392 initiation of the northern Cordilleran marginal backarc basin; geologic, geochemical, and  
 1393 neodymium isotope evidence from the oldest mafic magmatic rocks in the Yukon-Tanana  
 1394 Terrane, Finlayson Lake District, southeast Yukon, C: *Geological Society of America*  
 1395 *Bulletin*, v. 116, no. 9-10, p. 1087-1106.
- 1396 Piercey, S. J., Murphy, D. C., Mortensen, J. K., and Paradis, S., 2001, Boninitic magmatism in a  
 1397 continental margin setting, Yukon-Tanana Terrane, southeastern Yukon, Canada:  
 1398 *Geology [Boulder]*, v. 29, no. 8, p. 731-734.

- 1399 Plint, H. E., and Gordon, T. M., 1997, The Slide Mountain Terrane and the structural evolution  
1400 of the Finlayson Lake fault zone, southeastern Yukon: *Canadian Journal of Earth*  
1401 *Sciences*, v. 34, no. 2, p. 105-126.
- 1402 Pubellier, M., Bader, A. G., Rangin, C., Deffontaines, B., and Quebral, R., 1999, Upper plate  
1403 deformation induced by subduction of a volcanic arc; the Snellius Plateau (Molucca Sea,  
1404 Indonesia and Mindanao, Philippines): *Tectonophysics*, v. 304, no. 4, p. 345-368.
- 1405 Reston, T. Manatschal, G., 2011. Rifted margins: Building blocks of later collisions. Chapter 1,  
1406 in Brown, D., and Ryan, P. D., eds. *Arc-continent collision, frontiers in Earth Sciences*
- 1407 Richards, D.R., Butler, R.F., Harms, T.A. (1993). Paleomagnetism of the late Paleozoic Slide  
1408 Mountain terrane, northern and central British Columbia. *Canadian Journal of Earth*  
1409 *Sciences*, 30, 898-1913.
- 1410 Roback, R. C., Sevigny, J. H., and Walker, N. W., 1994, Tectonic setting of the Slide Mountain  
1411 Terrane, southern British Columbia: *Tectonics*, v. 13, no. 5, p. 1242-1258.
- 1412 Robinson, P. T., Malpas, J., Dilek, Y., and Zhou, M., 2008, The significance of sheeted dike  
1413 complexes in ophiolites: *GSA Today*, v. 18, no. 11, p. 4-11.
- 1414 Roots, C.F., Harms, T.A., Simard, R.-L., Orchard, M.J., Heaman, L. (2002). Constraints on the  
1415 age of the Klinkit assemblage east of Teslin Lake, northern British Columbia. *Geological*  
1416 *Survey of Canada, Current Research 2002-A7*, pp 11
- 1417 Roots, C. F., Nelson, J. L., Simard, R. L., and Harms, T. A., 2006. Continental fragments, mid-  
1418 Paleozoic arcs and overlapping late Paleozoic arc and Triassic sedimentation in the  
1419 Yukon-Tanana terrane of northern British Columbia and southern Yukon. *In: Colpron,*  
1420 *M., Nelson, J.L. (eds.) Paleozoic evolution and metallogeny of pericratonic terranes at*

- 1421 *the ancient Pacific margin of North America, Canadian and Alaskan Cordillera.*  
 1422 Geological Association of Canada, v. 45, p. 153-178.
- 1423 Ross, 1969C. a., 1969. Upper Paleozoic Fusulinacea Eowaeringella and Wedekindelina from  
 1424 Yukon territory and giant Parafusulina from British Columbia. contributions to to  
 1425 Canadian Paleontology, Geological Survey of Canada Bulletin182.
- 1426 Ryan, J. J., Nelson, J., van Staal, C. R., 2015. Fieldwork in Sylvester Allochthon, Cassiar  
 1427 mountains, British Caledonides : investigations of the Rapid River tectonite and the Slide  
 1428 Mountain terrane. In: Geological Fieldwork 2014, British Columbia Ministry of Energy  
 1429 and Mines, British Columbia Geological Survey Paper 2015-1, pp. 113-128.
- 1430 Ryan, J.J., Zagorevski, A., Williams, S.P., Roots, C., Ciolkiewicz, W., Hayward, N. and  
 1431 Chapman, J.B., 2013a. Geology, Stevenson Ridge (northeast part), Yukon; Geological  
 1432 Survey of Canada, Canadian Geoscience Map 116 (2nd edition, preliminary), scale 1:100  
 1433 000. doi:10.4095/292407
- 1434 Ryan, J.J., Zagorevski, A., Williams, S.P., Roots, C., Ciolkiewicz, W., Hayward, N. and  
 1435 Chapman, J.B., 2013b. Geology, Stevenson Ridge (northwest part), Yukon; Geological  
 1436 Survey of Canada, Canadian Geoscience Map 117 (2nd edition, preliminary), scale 1:100  
 1437 000. doi:10.4095/292408
- 1438 Ryan, J.J., Zagorevski, A., Roots, C.F., and Joyce, N., 2014. Paleozoic tectonostratigraphy of the  
 1439 northern Stevenson Ridge area, Yukon; Geological Survey of Canada, Current Research  
 1440 2014-4, 13 p. doi:10.4095/293924
- 1441 Ryan, J.J., Zagorevski, A., Joyce, N.L., Staples, R.D.3, Jones, J.V., Gibson, H.D. 2017. Mid-  
 1442 Cretaceous core complexes in the Northern Cordillera: exposing the parautochthon

- 1443 through a thin flap of allochthonous Yukon-Tanana terrane in western Yukon. GSA  
 1444 Annual Meeting, Washington, USA
- 1445 Ruks, T. W., Piercey, S. J., Ryan, J. J., Villeneuve, M. E., and Creaser, R. A., 2006, Mid- to late  
 1446 Paleozoic K-feldspar augen granitoids of the Yukon-Tanana Terrane, Yukon, Canada;  
 1447 implications for crustal growth and tectonic evolution of the northern Cordillera:  
 1448 Geological Society of America Bulletin, v. 118, no. 9-10, p. 1212-1231.
- 1449 Sajona, F. G., Maury, R. C., Pubellier, M., Leterrier, J., Bellon, H., and Cotten, J., 2000,  
 1450 Magmatic source enrichment by slab-derived melts in a young post-collision setting,  
 1451 central Mindanao (Philippines): Lithos, v. 54, no. 3-4, p. 173-206.
- 1452 Schellart, W. P., Lister, G. S., and Toy, V. G., 2006. A late Cretaceous and Cenozoic  
 1453 reconstruction of the Southwest Pacific region: Tectonics controlled by subduction and  
 1454 slab rollback processes. Earth-Science Reviews, 76, p. 191-233.
- 1455 Scholl, D. W., and von Huene, R., 2007, Crustal recycling at modern subduction zones applied to  
 1456 the past issues of growth and preservation of continental basement crust, mantle  
 1457 geochemistry, and supercontinent reconstruction: Memoir - Geological Society of  
 1458 America, v. 200, p. 9-32.
- 1459 Schroeder, T., and John, B. E., 2004, Strain localization on an oceanic detachment fault system,  
 1460 Atlantis Massif, 30 degrees N, Mid-Atlantic Ridge: Geochemistry, Geophysics,  
 1461 Geosystems - G super 3, v. 5, no. 11, p. 30.
- 1462 Shirmohammad, F., Wierzbowski, A., Smith, P. L., Anderson, R. G., McNicoll, V. J.,  
 1463 Pienkowski, G., Sha, J., and Wang, Y., 2011, The Jurassic succession at Lisadele Lake  
 1464 (Tulsequah map area, British Columbia, Canada) and its bearing on the tectonic evolution  
 1465 of the Stikine Terrane: Volumina Jurassica, v. 9, p. 43-60.

- 1466 Sigloch, K., and Mihalynuk, M.G. 2013, Intraoceanic subduction shaped the assembly of  
1467 cordilleran North America. *Nature*, v. 496, p.50-56.
- 1468 Sigloch, K., and Mihalynuk, M.G. 2017. Mantle and geological evidence for a Late Jurassic–  
1469 Cretaceous suture spanning North America. *GSA Bulletin*, 129, 1489-1520.
- 1470 Simard, R.-L., Dostal, J., Roots, C.F. (2003). Development of late Paleozoic volcanic arcs in the  
1471 Canadian Cordillera: an example from the Klinkit Group, northern British Columbia and  
1472 southern Yukon. *Canadian Journal of Earth Sciences*. v. 40, p. 907-924.
- 1473 Staples, R.D., Murphy, D.C., Gibson, H.D., Colpron, M., Berman, R.G., Ryan, J.J. (2014).  
1474 Middle Jurassic to earliest Cretaceous mid-crustal tectono-metamorphism in the northern  
1475 Canadian Cordillera: Recording foreland-directed migration of an orogenic front. *GSA*  
1476 *Bulletin*. v.126, p. 1511-1530.
- 1477 Staples, R.D., Gibson, H.D., Colpron, M. & Ryan, J.J. 2016. An orogenic wedge model for  
1478 diachronous deformation, metamorphism, and exhumation in the hinterland of the  
1479 northern Canadian Cordillera. *Lithosphere*, v. 8, p. 165-184.
- 1480 Stern, C. R., 2011, Subduction erosion; rates, mechanisms, and its role in arc magmatism and the  
1481 evolution of the continental crust and mantle: *Gondwana Research*, v. 20, no. 2-3, p. 284-  
1482 308.
- 1483 Stevens, R. A., Erdmer, P., Creaser, R. A., and Grant, S. L., 1996, Mississippian assembly of the  
1484 Nisutlin assemblage; evidence from primary contact relationships and Mississippian  
1485 magmatism in the Teslin tectonic zone, part of the Yukon-Tanana Terrane of south-  
1486 central Yukon: *Canadian Journal of Earth Sciences = Revue Canadienne des Sciences de*  
1487 *la Terre*, v. 33, no. 1, p. 103-116.

- 1488 Stolz, A. J., Davies, G. R., Crawford, A. J., and Smith, I. E. M., 1993, Sr, Nd and Pb isotopic  
1489 compositions of calc-alkaline and peralkaline silicic volcanics from the D'Entrecasteaux  
1490 Islands, Papua New Guinea, and their tectonic significance: *Mineralogy and Petrology*, v.  
1491 47, no. 2-4, p. 103-126.
- 1492 Taira, A., Mann, P., and Rahardiawan, R., 2004, Incipient subduction of the Ontong Java Plateau  
1493 along the North Solomon Trench: *Tectonophysics*, v. 389, no. 3-4, p. 247-266.
- 1494 Tani, K., Dunkley, D. J., and Ohara, Y., 2011, Termination of backarc spreading; zircon dating  
1495 of a giant oceanic core complex: *Geology [Boulder]*, v. 39, no. 1, p. 47-50.
- 1496 Tapster, S., Roberts, N. M. W., Petterson, M. G., Saunders, A. D., and Naden, J., 2014, From  
1497 continent to intra-oceanic arc: Zircon xenocrysts record the crustal evolution of the  
1498 Solomon island arc: *Geology*, v. 42, no. 12, p. 1087-1090.
- 1499 Taylor, B., Goodliffe, A. M., and Martinez, F., 1999, How continents break up; insights from  
1500 Papua New Guinea: *Journal of Geophysical Research*, v. 104, no. B4, p. 7497-7512.
- 1501 Tempelman-Kluit, D. J., 1979. Transported cataclasite, ophiolite, and granodiorite in Yukon:  
1502 Evidence of arc-continent collision. *Geological Survey of Canada, Paper 79-14*, 27 p.
- 1503 Tempelman-Kluit, D. J., and Wanless, R. K., 1980, Zircon ages for the Pelly gneiss and  
1504 Klotassin granodiorite in western Yukon. *Canadian journal of Earth Sciences*, v. 17, p.  
1505 297-306.
- 1506 Tremblay, A., Robertson, A. H. F., Meshi, A., Bedard, J. H., Parlak, O., and Koller, F., 2009,  
1507 Oceanic core complexes and ancient oceanic lithosphere; insights from Iapetan and  
1508 Tethyan ophiolites (Canada and Albania): *Tectonophysics*, v. 473, no. 1-2, p. 36-52.
- 1509 van Staal, C. R., Dewey, J. F., MacNiocaill, C. and McKerrow, S., 1998. The Cambrian-Silurian  
1510 tectonic evolution of the northern Appalachians: history of a complex, southwest Pacific-

- 1511 type segment of Iapetus. *In* Blundell, D. J. and Scott, A. C., eds., *Lyell: the Past is the*  
 1512 *Key to the Present*. Geological Society Special Publication v. 143, p. 199-242
- 1513 van Staal, C. R., Chew, D. M., Zagorevski, A., McNicoll, V., Hibbard, J., Skulski, T.,  
 1514 Castonguay, S., Escayola, M. P., and Sylvester, P. J., 2013, Evidence of Late Ediacaran  
 1515 Hyperextension of the Laurentian Iapetan Margin in the Birchy Complex, Baie Verte  
 1516 Peninsula, Northwest Newfoundland: Implications for the Opening of Iapetus, Formation  
 1517 of Peri-Laurentian Microcontinents and Taconic – Grampian Orogenesis: *Geoscience*  
 1518 *Canada*, v. 40, p. 94-117.
- 1519 von Huene, R., and Scholl, D. W., 1991, Observations at convergent margins concerning  
 1520 sediment subduction, subduction erosion, and the growth of continental crust: *Reviews of*  
 1521 *Geophysics*, v. 29, no. 3, p. 279-316.
- 1522 Webb, L. E., Baldwin, S. L., and Fitzgerald, P. g., 2014. the Early-Middle Miocene subduction  
 1523 complex of the Louisiade Archipelago, southern margin of the Woodlark Rift.  
 1524 *Geochemistry, Geophysics, Geosystems*, 15, doi:10.1002/2014GC005500

1525

## 1526 **Figure Captions**

- 1527 Figure 1. Distribution of the Slide Mountain and Yukon-Tanana terranes in the northern  
 1528 Cordillera (after Colpron and Nelson, 2011; Colpron et al., 2016; Pecha et al., 2016 and Parsons  
 1529 et al., in pressa). Ages from Htoon, 1981; Erdmer and Armstrong (1988); Mortensen (1992);  
 1530 Gabrielse et al. (1993); Oliver (1996); Creaser et al. (1997); Erdmer et al., (1998); Fallas et al.  
 1531 (1998); Godwin-Bell (1998); de Keijzer et al. (2000); Philippot et al. (2001); Breitsprecher and  
 1532 Mortensen (2004); Colpron et al. (2005, 2006); Murphy et al., (2006); Berman et al. (2007);



1533 Staples (2014); Joyce et al. (2015); Petrie et al (2015, 2016); Gilotti et al. (2017); Parsons et al.  
 1534 (in pressa) and this paper.

1535 Figure 2. Schematic late Paleozoic tectonic evolution of the Yukon-Tanana (YTT) and Slide  
 1536 Mountain (SMT) terranes (modified from Devine et al., (2006); Berman et al., (2007)). The  
 1537 principle differences between the Devine et al. (2006) and Berman et al. (2007) models is the  
 1538 degree of fragmentation of YTT and timing of intra-arc shortening. These models imply that  
 1539 SMT ophiolitic rocks form part of the subducting Slide Mountain Ocean (SMO). A. East-  
 1540 directed Late Devonian-Mississippian subduction of Panthalassa Ocean under YTT producing  
 1541 eclogite and arc magmatism (orange plutons). Slab rollback causes arc rifting and opening of the  
 1542 SMO. Early Mississippian intra-arc shortening is generated when westward movement of YTT  
 1543 overtakes slab rollback although backarc opening continues. Dense eclogite produced in the  
 1544 downgoing Panthalassan slab is transferred into the subduction complex and exhumed to shallow  
 1545 levels, the cause of which is unspecified, during continuous eastward-directed subduction and  
 1546 backarc opening. East-directed subduction ceases for unknown reason in the early Permian,  
 1547 causing further intra-arc shortening, followed by a subduction polarity flip into the SMO. B.  
 1548 West-directed subduction of the SMO slab causes the Permian Klondike phase of arc magmatism  
 1549 (purple plutons) in YTT and eclogite facies metamorphism in the east-facing subduction  
 1550 complex. Intra-arc shortening reactivates earlier formed thrusts and transports Mississippian  
 1551 eclogites over the YTT and active? Klondike arc. The final location of the Mississippian  
 1552 eclogites eventually coincides with the YTT-SMT boundary nearly coincident with the location  
 1553 of most Permian eclogites (see Fig. 1). CLT – Cleaver Lake Thrust; FIT – Future Inconnu  
 1554 Thrust; MCT – Money Creek Thrust; L - Laurentia P – Panthalassa Ocean; SMO – Slide

1555 Mountain Ocean; YTT1/2 – Yukon Tanana terrane east and west; Devine et al., (2006) suggested  
 1556 that Yukon-Tanana terrane may have been fragmented into several microcontinents.

1557 Figure 3. Tera-Wasserburg plots, chondrite-normalized rare earth plots, and  
 1558 cathodoluminescence images of zircon from the Clinton Creek (VL10-12), Midnight Dome  
 1559 (VL10-09) and St. Cyr (VL10-04) complexes. . U/Pb data plotted as  $1\sigma$  error ellipses  
 1560 uncorrected for common Pb. Black ellipses and grains noted with \* in CL images are used in  
 1561 calculating weighted mean ages. Weighted mean age uncertainty is reported at the 95%  
 1562 confidence level. Letters in 3c show inner rims (A), CL-dark mantles that are interpreted to  
 1563 represent zircon growth during trondhjemite-leucotonalite crystallization (B) and outermost rims  
 1564 (C).

1565 Figure 4. A.Strongly serpentinized and listwanitized Clinton Creek ultramafic rocks; B. Close-  
 1566 up of altered pegmatitic leucogabbro that has intruded serpentinite of Clinton Creek complex.  
 1567 Gabbro itself also altered to chlorite and carbonate and cut by serpentine veins; C. Leucogabbro  
 1568 intrusion into the Midnight Dome serpentinized ultramafic complex. Gabbro displays a weak  
 1569 foliation. D. Leucotonalite cutting harzburgite of D and pyroxenite dike. The pyroxenite in turn  
 1570 cuts the serpentinized harzburgite. E. Foliated and lineated St. Cyr serpentinized harzburgite in  
 1571 part defined by a shape fabric of bastite pseudomorphs after orthopyroxene and chromite  
 1572 aggregates.

1573 Figure 5. Geochemical characteristics of the Clinton Creek, Midnight Dome and St. Cyr  
 1574 complexes. A. N-MORB normalized (Sun and McDonough, 1989) multi-element diagram of  
 1575 mafic rocks. Websterite plotted for reference. Composition of Cretaceous basalts (mainly sheet  
 1576 flows) erupted along the distal part of the hyperextended Newfoundland margin (ocean-continent

transition) are plotted in the grey band (Robertson, 2007) for reference. B. Tectonic setting discrimination plot of mafic rocks (Cabanis and Lecolle, 1989). C. Primitive mantle normalized (Sun and McDonough, 1989) multi-element diagram of ultramafic rocks and comparison to peridotites from known tectonic settings (1 – Savov et al., 2005; 2- Niu et al., 2004; 3 – Baie Verte Oceanic Tract (BVOT) – Bedard and Escayola, 2010). D. IUGS modal classification of ultramafic rocks.

Figure 6. Chromian spinel discrimination plots of peridotite in Midnight Dome complex (modified from Dick and Bullen, 1984)

Figure 7. Yukon-Tanana (YTT) as a singular late Paleozoic terrane. YTT is in the upper plate during both Late Devonian-early Permian subduction of the Panthalassa Ocean (PO) and early-late Permian subduction of the Slide Mountain Ocean (SMO) following a subduction polarity reversal. A. Collision of seamount or crustal ribbon terminates east-dipping subduction beneath YTT and induces subduction in the SMO. Mississippian eclogite formed during east-directed subduction and incorporated in a west-facing subduction complex. Following early Permian collision with an outboard terrane (not preserved?), the Mississippian eclogite and parts of the host subduction complex were progressively emplaced further to the east beneath the eastern (backarc) edge of the YTT arc as a result of forearc subduction (process based on Sajona et al., 2000; McIntosh et al., 2005). B. Tectonic capture of the Mississippian eclogite and incorporation in an east-facing Permian subduction complex following initiation of a west-dipping subduction zone in the SMO, which leads to its subsequent juxtaposition with Permian eclogite. The Permian eclogite formed by partial subduction of a small continental ribbon fragment (YTTf, see also Fig. 2) or as a result of subduction erosion (Gilotti et al., 2017). C. Subduction rollback drives asymmetrical extension and exhumation of orogenic peridotites (op) in YTT (upper plate)

immediately after underthrusting and formation of eclogite. D-F. Possible relationships between orogenic peridotite (op) and Clinton Creek (CC) and Midnight Dome (MD) complexes following the initiation of subduction in the SMO. D. Clinton Creek-Midnight Dome spreading centre is located in YTT re-entrant and propagates into YTT leading to continental rifting and exhumation of Buffalo Pitts orogenic peridotites (Johnston et al., 2007). Permian eclogite is exhumed in the subduction channel along the YTT promontory. E. Asymmetrical rifting leads to orogenic peridotite exhumation and ophiolite formation along strike. F. Orogenic peridotites are exhumed along a separate rift from the ophiolites.

Figure 8. YTT as a composite terrane. Late Paleozoic tectonic configurations of the Yukon-Tanana microcontinent (YTTc) and the converging oceanic arc-backarc terrane (YTTj) after initiation of east-directed subduction beneath YTTj during the Mississippian or earlier, modified and expanded from Parsons et al. (in pressa). A. Subduction initiation beneath YTTj leads to formation of Mississippian eclogite (see text). B. Middle-late Permian collision (Klondike orogeny) between YTTj and YTTc leads to partial subduction of the leading edge of the YTTc, formation of Permian eclogite and juxtaposition with the Mississippian eclogite near the suture following exhumation. The YTTj-microcontinent (YTTc) collision is followed by a subduction polarity flip and initiation of west-directed subduction in the remaining part (backarc region of YTTj) of the SMO. C. Post-collisional extension driven by slab rollback results in exhumation of orogenic peridotite (op) and post-collisional magmatism. D. The relationship between ophiolites and orogenic peridotites can be explained by diachronous collision, such that orogenic peridotite is exhumed in already collided part of the orogen whereas YTTj is rifting where the collision has not yet occurred. As a result the subduction polarity reversal is accordingly diachronous (van Staal et al., 1998, fig. 6). E. Similar to D but non-cylindrical, asymmetrical rifting in YTTc leads

1623 to ophiolite formation along strike of where orogenic peridotite is exhumed. The final  
 1624 configuration of the eclogites, YTTc and possible remnants of accreted of ocean floor rocks in  
 1625 SMT is mainly a result of Mesozoic shortening and extension (see Fig. 9c and text)

1626 Figure 9. A. Formation of an oceanic arc-backarc complex (YTTj) outboard in the Panthalassa  
 1627 Ocean as a result of west-directed subduction. B. Obduction of YTTj onto YTTc during the  
 1628 Klondike orogeny, followed by stepping-back of subduction in the SMO or Angayucham Ocean.  
 1629 The processes discussed in Fig. 8 to account for exhumation of orogenic peridotite and post-  
 1630 collisional magmatism are principally the same. C. Further east-directed translation of the YTTj  
 1631 and eclogites above YTTc and Laurentia took place during the Jurassic-Cretaceous. The final  
 1632 present day configuration with the SMT rocks outlining the contact between Laurentia and  
 1633 composite YTT is principally a product of Mesozoic and later thrusting and exhumation.

1634 Figure 10.A. Simplified geology of the Australia – Pacific plate boundary zone. Background  
 1635 image is generated from <http://www.geomapapp.org>. Collision between Australia and the New  
 1636 Britain arc (NBA) in Huon Peninsula (HP) propagates towards the east progressively closing the  
 1637 Solomon Sea. The Woodlark basin (WB) is actively spreading and propagating into Australian  
 1638 crust in eastern Papua New Guinea (PNG). Here exhumation of eclogite (ec) and calc alkaline  
 1639 magmatism (ca) has occurred recently in the d’Entrecasteaux Islands (d’E). The Woodlark Basin  
 1640 spreading centre is subducted beneath the Solomon Arc (SA) at its eastern edge. Stippled line is  
 1641 the now inactive North Solomon Trench (NST), which accommodated convergence between the  
 1642 Solomon arc and Ontong Java plateau (OJP) until the subduction polarity reversal and formation  
 1643 of the New Britain Trench (NBT) and its extension to the southeast (South Solomon Trench).  
 1644 New Caledonia (NC) and Norfolk Ridge are going to collide with the New Hebrides Arc (NHA)  
 1645 in the future, juxtaposing NHA boninites (bon) with rifted continental margin rocks. B. Elements

of Laurentia and Yukon Tanana composite terrane superimposed on the Australia – Pacific plate boundary zone. In this analogy, Australia is Laurentia, the New Britain-Solomon arc backarc system is YTTj, which is mainly characterised by IAT and BABB rocks; YTTc are the continental ribbons such as Lord Howe rise and Norfolk ridge. The intervening basin between the Lord Howe Rise and Australia could be analogous to the Selwyn basin. In this analogy, the diachronous collision, outlined in eastern New Guinea is not between Laurentia and the YTT, but between YTTc and YTTj. EC, OP and CA are exhumed eclogite, orogenic peridotite and calc-alkaline magmatism respectively generated as a result of rifting propagating into the Permian collision zone between YTTj and YTTc. MT, Manus Trench; TT, Trobriand Trough.

Table 1. SIMS zircon U-Pb geochronologic zircon data, apparent ages and trace element data.

Table 2. whole rock geochemical data (major elements at wt% oxides, trace and rare earth elements in ppm) for the St. Cyr, Clinton Creek (CC) and Midnight Dome (MD) ophiolite complexes. See text for methods used. B.D. = below detection

Table 3. Chemical composition of chromian spinel of Midnight Dome serpentinised peridotite

1666

1667

1668

Table 1. SIMS Zircon U-Pb Geochronologic Data, Apparent Ages and Trace Element Data

Spot <sup>a</sup>	U (ppm)	Th (ppm)	Th/U	<sup>206</sup> Pb/ <sup>b</sup> (ppm)	<sup>206</sup> Pb/ <sup>b</sup> f <sup>206</sup> Pb <sup>c</sup>	<sup>238</sup> U/ <sup>206</sup> Pb <sup>c</sup>	1σ (%)	<sup>207</sup> Pb/ <sup>206</sup> Pb (%)	1σ (Ma)	<sup>36</sup> Pb/ <sup>238</sup> U (Ma)	1σ (Ma)	<sup>37</sup> Pb/ <sup>206</sup> Pb (Ma)	1σ	Y (ppm)	La (ppm)	Ce (ppm)	Nd (ppm)	Sm (ppm)	Eu (ppm)	Gd (ppm)	Dy (ppm)	Er (ppm)	Yb (ppm)	Hf (ppm)	Ce/Ce* (ppm)	Eu/Eu* (ppm)	Yb/Gd (ppm)		
VL010-12: Clinton Creek complex, pegmatitic leucogabbro UTMX: 513855; UTMY: 7146707																													
11.1 r	2	0.04	0.03	0.03	12.23	45.381	13.8	.1457	29	123	19			207	0.541	1	0.0	0.0	0.02	1	9	63	288	9887		2	0.69	554.4	
12.1 r	1	0.01	0.03	0.01	2.72	48.856	19.8	.0702	48	127	26			2104	0.070	0	0.0	0.1	0.04	2	69	571	2195	8142		1	0.33	1191.9	
13.1 r	9	1	0.13	0.2	1.93	38.183	9.2	.06471	27	163	15			6753	0.431	1	0.1	0.4	0.28	22	382	1551	3707	13245		3	0.29	165.3	
3.1 c	164	122	0.77	5.4	<0.01	26.214	1.1	.05099	2.8	241	3			3872	0.188	26	8.8	13.2	9.35	97	353	631	1251	5873		19	0.79	12.8	
6.1 r	320	150	0.48	10.8	0.34	25.539	1.2	.05382	3.0	247	3			1442	1.905	7	0.8	0.8	1.25	22	121	294	679	14161		2	0.90	30.7	
10.1 c	99	42	0.44	3.5	<0.01	24.623	1.4	.04897	3.7	257	4			1401	0.033	8	1.1	2.4	2.19	22	99	234	549	6767		36	0.93	25.0	
8.1 c	127	41	0.33	4.5	0.07	24.153	2.1	.05204	3.5	261	5			1634	0.125	8	1.0	2.0	1.75	21	115	296	733	7130		16	0.83	35.7	
14.1 c	133	46	0.36	4.7	<0.01	24.024	1.2	.05146	3.1	263	3			1241	0.019	4	0.7	2.0	1.88	21	101	223	512	8009		27	0.88	24.2	
5.1 c	233	144	0.64	8.4	0.13	23.922	1.0	.05253	2.3	264	3			3635	0.122	23	5.3	9.2	6.81	78	311	605	1251	6508		26	0.77	16.1	
2.1 c	326	190	0.60	11.8	0.20	23.767	1.0	.05313	2.6	265	3			3780	0.059	20	4.1	8.5	6.44	81	342	649	1336	7236		40	0.75	16.6	
1.1 c	132	66	0.51	4.8	0.27	23.711	1.2	.05370	3.0	266	3			2301	0.124	13	3.3	5.8	4.26	46	199	400	897	7245		17	0.80	19.6	
4.1 c	73	24	0.35	2.7	0.39	23.334	1.5	.05476	4.1	269	4			1553	0.028	7	1.6	2.9	2.28	27	113	277	667	7025		30	0.79	24.7	
7.1 c	308	223	0.75	11.3	<0.01	23.381	1.0	.05033	2.2	270	3			4468	0.201	32	9.8	14.9	11.96	118	420	706	1370	9113		21	0.87	11.7	
9.1 c	162	107	0.68	6.1	<0.01	22.724	1.2	.05129	3.7	278	3			4500	0.131	27	9.8	15.2	10.74	109	421	761	1572	7000		24	0.80	14.4	
VL010-09: Midnight Dome complex, leucogabbro UTMX: 578726; UTMY: 7104571																													
1.1 c	24	12	0.50	0.8	0.00	26.149	2.6	.05101	8.3	242	6			2200	0.012	6	1.7	4.9	1.88	53	211	389	648	7922		42	0.35	12.1	
7.1 c	52	30	0.61	1.8	0.60	24.552	1.8	.05612	5.4	256	5			3350	0.040	10	2.4	7.2	3.02	82	342	599	991	8073		31	0.38	12.1	
6.1 c	42	20	0.50	1.5	0.96	24.233	1.9	.05911	5.7	258	5			2673	0.025	9	2.2	5.9	1.75	63	242	453	762	9211		37	0.28	12.1	
2.1 c	24	12	0.52	0.9	0.62	24.298	2.6	.05639	7.6	258	7			324	0.026	2	0.2	0.6	0.39	7	33	57	98	9277		14	0.57	13.7	
8.1 c	70	40	0.59	2.5	<0.01	24.234	1.5	.04657	4.9	262	4			2320	0.031	6	2.4	6.7	1.97	63	232	387	603	7646		24	0.29	9.5	
5.1 c	28	14	0.52	1.0	<0.01	23.745	2.3	.04909	7.5	267	6			2084	0.023	5	1.6	4.5	1.52	48	192	358	620	8318		26	0.31	12.9	
10.1 c	50	31	0.65	1.8	<0.01	23.615	1.8	.05076	5.6	268	5			4475	0.023	15	4.0	12.2	3.55	118	447	775	1224	8243		57	0.28	10.3	
4.1 c	47	28	0.61	1.7	<0.01	23.507	1.8	.05062	9.3	269	5			1335	0.043	3	1.1	2.3	0.91	21	103	252	467	8777		10	0.39	21.8	
3.1 c	16	7	0.45	0.6	0.47	23.170	3.1	.05545	9.3	271	9			1419	0.026	4	1.2	3.5	1.11	35	134	246	418	8075		23	0.31	12.1	
9.1 c	49	22	0.45	1.8	0.65	23.101	1.8	.05690	5.7	271	5			2483	0.024	11	0.7	2.4	1.07	33	203	460	846	8410		69	0.37	26.0	
VL010-04: St. Cyr klippe, trondhjemite-leucotonalite UTMX: 615398 ; UTMY: 6792127																													
8.1 m	2515	34	0.014	93.1	0.09	23.219	0.3	.05244	0.8	272	1			145	1.419	6	3.4	3.1	1.26	10	23	18	18	12270		2	0.68	1.8	
3.1 m	714	3	0.004	26.6	0.16	23.013	0.4	.05300	1.2	274	1			184	1.082	2	0.2	0.2	0.12	2	13	33	65	5666		2	0.51	28.7	
2.1 m	2216	6	0.003	87.6	<0.01	21.724	0.3	.05181	0.8	290	1			321	0.025	0	0.1	0.3	0.26	5	30	70	201	11977		5	0.65	42.8	
6.1 m	1531	14	0.010	61.4	0.30	21.426	0.3	.05460	1.3	293	1			496	0.167	1	0.7	0.8	0.30	5	39	114	339	11735		2	0.45	62.1	
12.1 m	1964	7	0.004	79.9	0.03	21.126	0.3	.05249	1.0	298	1			327	1.505	4	0.8	0.6	0.27	4	25	65	206	9896		1	0.50	47.4	
4.1 m	2096	8	0.004	87.2	<0.01	20.650	0.3	.05194	0.8	305	1			367	0.662	1	0.4	0.5	0.30	5	31	77	215	11068		1	0.59	41.4	
10.1 m	657	4	0.006	27.7	0.32	20.365	0.6	.05511	2.0	308	2			123	3.193	6	0.6	0.5	0.23	3	10	18	39	4686		2	0.56	12.1	
14.1 m	1708	7	0.004	72.5	0.04	20.231	0.2	.05293	0.7	311	1			452	0.072	1	0.3	0.4	0.19	5	40	83	144	11526		2	0.39	30.7	
15.1 m	1653	5	0.003	70.4	0.11	20.165	0.3	.05352	0.8	312	1			695	0.017	0	0.0	0.3	0.11	5	55	146	341	12106		6	0.28	68.7	
13.1 m	1201	5	0.004	55.1	0.11	18.721	0.3	.05404	1.0	335	1			621	0.053	0	0.1	0.3	0.11	4	49	131	307	11273		3	0.30	71.3	
11.1 r	65	1	0.012	3.1	1.47	17.788	2.6	.06531	6.9	348	9	1253	241	58	1.179	2	0.2	0.2	0.04	1	4	8	16	6318		2	0.35	24.9	
7.1 c	197	61	0.32	10.5	0.81	16.033	0.7	.06094	4.2	387	3			710	0.190	4	1.3	2.3	0.26	19	70	123	205	9655		5	0.12	11.0	
9.1 c	119	56	0.49	18.7	1.21	5.439	0.8	.08540	1.3	1076	9	1314	26	984	0.116	12	4.1	5.9	0.69	38	121	173	273	8089		15	0.14	7.2	
5.1 c	233	123	0.55	65.7	7.71	3.050	0.6	.17123	0.5	1704	11	2560	9	552	1.129	16	5.9	6.1	2.06	23	71	99	170	9137		4	0.52	7.3	
1.1 c	158	100	0.66	53.0	6.56	2.559	0.6	.18091	0.6	2006	13	2656	10	300	0.124	39	1.2	2.2	0.84	12	30	49	100	8213		70	0.49	8.3	

Note: All analyses were performed on the SHRIMP-RG ion microprobe at the United States Geological Survey-Stanford Microanalytic Center at Stanford University. The analytical routine followed Barth and Wooden (2006, 2010). Data reduction utilized the Squid 2.51 program of Ludwig (2009).

<sup>a</sup> Abbreviations and CL designations: c = core; m = CL-dark mantle; r = rim.

<sup>b</sup> Pb\* denotes radiogenic Pb; Pb<sub>c</sub> denotes common Pb; f<sup>206</sup>Pb<sub>c</sub> = 100\*(<sup>206</sup>Pb<sub>c</sub>/<sup>206</sup>Pb<sub>total</sub>).

<sup>c</sup> Calibration concentrations and isotopic compositions were based on replicate analyses of R33 (421 Ma, Black et al., 2004; Mattinson, 2010) and Madagascar Green (MADDER; 3435 ppm U, Barth and Wooden, 2010). Reported ratios are not corrected for common Pb. Errors are reported in parentheses as percent at the 1σ level.

<sup>d</sup> Ages were calculated from <sup>206</sup>Pb/<sup>238</sup>U ratios corrected for common Pb using the <sup>207</sup>Pb method (see Williams, 1998). Initial common Pb isotopic composition approximated from Stacey and Kramers (1975). Uncertainties in millions of years reported as 1σ. Ages in bold were used in age calculation



Table

Table 2																			
Sample	VL10-02	VL10-07	VL10-08	VL10-10	VL10-11	VL10-12	VL10-09	10VLE-A101-02	10VLE-A101-03	10VLE-A101-04	10VLE-A101-05	10VLE-A101-06	10VLE-A101-07	10VLE-A101-08	10VLE-A101-09	10VLE-A101-10	10VLE-A101-12	10VLE-A101-13	
Complex	St. Cyr	St. Cyr	St. Cyr	CC	CC	CC	MD	MD	MD	MD	MD	MD	MD	MD	MD	MD	MD	MD	
Lithology	peridotite	peridotite	peridotite	peridotite	websterite/gabbro	gabbro	gabbro	peridotite	peridotite	peridotite	peridotite	peridotite	peridotite	gabbro	gabbro	peridotite	peridotite	diabase	
UTMX	629509	615202	603281	513855	513855	514067	578811	578726	578726	578726	578726	578726	578726	578726	578726	578726	578726	578726	578726
UTMY	6785757	6791831	6799407	7146707	7146707	7146561	7704372	7104571	7104571	7104571	7104571	7104571	7104571	7104571	7104571	7104571	7104571	7104571	7104571
SiO2	41.23	39.66	35.98	38.7	55.19	40.95	50.3	39.41	41.94	39.78	40.4	39.8	40.91	51.86	47.84	40.72	40.42	53.16	
Al2O3	1.13	0.53	0.74	0.28	1.76	16.47	16.53	0.83	0.46	0.49	0.71	0.98	0.71	15.03	16.34	0.73	0.55	16.06	
Fe2O3	8.7	7.8	14	5.26	4.75	11.01	6.98	10.03	7.32	8.56	7.75	7.98	7.56	9.26	10.66	7.65	9.76	9.52	
MnO	0.13	0.056	0.116	0.095	0.089	0.16	0.138	0.058	0.088	0.077	0.072	0.069	0.074	0.185	0.159	0.075	0.056	0.137	
MgO	41.26	39.63	35.75	39.07	19.57	9.11	8.6	36.86	38.74	37.1	39.1	38.23	39.4	6.04	6.16	38.47	37.99	6.15	
CaO	1.15	0.02	0.27	1	16.37	14.86	7.99	0.14	0.1	0.04	0.03	0.02	0.02	9.81	9.82	0.04	0.02	5.53	
Na2O	0.02	B.D.	0.01	0.02	0.16	0.45	2.7	0.01	0.01	B.D.	B.D.	B.D.	0.01	3.38	3.33	0.01	0.01	3.93	
K2O	B.D.	B.D.	B.D.	B.D.	0.03	0.48	1.92	0.01	0.01	0.01	B.D.	B.D.	B.D.	0.2	0.06	B.D.	B.D.	0.02	
TiO2	0.053	0.007	0.01	0.005	0.121	1.405	0.275	0.009	0.005	0.004	0.01	0.013	0.009	1.185	1.344	0.012	0.011	0.482	
P2O5	B.D.	0.03	B.D.	0.02	0.03	0.13	B.D.	0.03	B.D.	B.D.	0.04	B.D.	B.D.	0.14	0.08	B.D.	B.D.	0.06	
LOI	6.43	12.47	12.01	15.9	2.74	4.79	3.88	12.17	12.09	11.96	11.84	11.79	11.87	3.07	4.71	11.64	11.58	3.58	
Total	100.1	100.2	98.91	100.4	100.8	99.81	99.32	99.57	100.8	98.04	99.96	98.9	100.6	100.2	100.5	99.36	100.4	98.64	
Ba	B.D.	9	B.D.	536	33	3282	1519	11	13	15	23	18	28	80	80	4	11	12	
Co	115	95	94	79	50	40	27	91	83	90	78	68	71	27	30	84	96	27	
Cr	2470	2770	2600	2420	1770	200	250	2550	2530	3150	2520	2570	2400	120	130	2700	2530	20	
Cs	B.D.	B.D.	B.D.	1.4	7.4	2.5	1.1	0.2	0.3	0.1	B.D.	B.D.	B.D.	0.1	0.4	B.D.	B.D.	B.D.	
Cu	10.3	2.1	17.3	2.8	2.7	8.8	1.6	15.3	27.9	6.7	9.5	8.3	8.8	64.8	96.4	12.5	9.1	81.7	
Hf	B.D.	B.D.	B.D.	B.D.	0.2	2.2	0.3	B.D.	B.D.	B.D.	B.D.	B.D.	B.D.	1.7	1.9	B.D.	B.D.	0.6	
Nb	B.D.	B.D.	B.D.	B.D.	B.D.	0.6	B.D.	B.D.	B.D.	B.D.	B.D.	B.D.	B.D.	0.7	1	B.D.	B.D.	B.D.	
Ni	2100	2190	2060	2120	451	87	133	1990	2040	2650	1890	1560	1520	60	69	2270	2300	49	
Pb	B.D.	B.D.	B.D.	B.D.	B.D.	B.D.	B.D.	2	B.D.	B.D.	B.D.	B.D.	B.D.	B.D.	B.D.	B.D.	B.D.	B.D.	
Rb	B.D.	B.D.	B.D.	B.D.	2	12	22	B.D.	B.D.	B.D.	B.D.	B.D.	B.D.	6	B.D.	B.D.	B.D.	B.D.	
Sr	B.D.	B.D.	B.D.	85	36	357	92	5	2	B.D.	B.D.	B.D.	B.D.	117	90	B.D.	B.D.	97	
Ta	B.D.	B.D.	B.D.	B.D.	B.D.	0.06	B.D.	B.D.	B.D.	B.D.	B.D.	B.D.	B.D.	0.04	0.08	B.D.	B.D.	0.02	
Th	B.D.	B.D.	B.D.	B.D.	B.D.	0.1	B.D.	0.13	0.05	B.D.	B.D.	B.D.	B.D.	0.15	0.17	B.D.	B.D.	0.12	
U	B.D.	0.02	B.D.	B.D.	0.28	0.07	0.02	0.23	0.15	0.15	0.02	0.03	0.02	0.12	0.08	0.01	0.02	0.14	
V	42	30	42	20	67	308	148	29	27	22	26	28	27	350	389	31	31	294	
Y	1.3	B.D.	1.1	B.D.	2.7	31	6.5	1.2	B.D.	B.D.	0.8	1.2	0.7	25.2	27.5	0.8	0.7	12.2	
Zr	2	B.D.	B.D.	B.D.	5	83	10	B.D.	B.D.	B.D.	B.D.	B.D.	B.D.	66	72	B.D.	B.D.	22	
La	0.38	0.22	0.25	0.13	0.27	3.48	0.68	2.39	0.48	0.45	0.61	0.33	0.64	3.5	3.55	0.19	0.3	1.24	
Ce	0.62	0.53	0.25	0.25	0.81	10.6	1.84	3.67	0.53	0.52	1.01	0.66	0.87	9.66	10.2	0.4	0.49	3.05	
Pr	0.08	0.06	0.07	0.03	0.14	1.85	0.32	0.37	0.1	0.08	0.11	0.07	0.07	1.59	1.68	0.05	0.07	0.5	
Nd	0.41	0.2	0.23	0.11	0.81	10.2	1.6	1.26	0.38	0.32	0.47	0.36	0.32	8.26	8.61	0.26	0.34	2.61	
Sm	0.1	0.03	0.07	0.03	0.27	3.52	0.58	0.17	0.05	0.04	0.07	0.13	0.1	2.84	2.86	0.04	0.08	0.93	
Eu	0.035	0.016	0.01	0.008	0.088	1.77	0.402	0.041	0.028	0.032	0.021	0.015	0.019	1.04	1.09	0.015	0.022	0.405	
Gd	0.18	0.03	0.16	0.03	0.41	4.93	1.02	0.18	0.07	0.07	0.12	0.17	0.12	3.78	4.15	0.11	0.08	1.52	
Tb	0.04	B.D.	0.03	B.D.	0.08	0.87	0.17	0.03	0.01	0.01	0.02	0.03	0.02	0.72	0.77	0.02	0.02	0.32	
Dy	0.23	0.03	0.21	0.03	0.55	5.76	1.2	0.19	0.08	0.09	0.14	0.19	0.14	4.49	4.81	0.15	0.12	2.05	
Ho	0.05	B.D.	0.03	B.D.	0.1	1.18	0.24	0.04	0.02	0.02	0.03	0.04	0.03	0.93	1.05	0.03	0.02	0.47	
Er	0.15	0.01	0.09	B.D.	0.3	3.56	0.74	0.1	0.04	0.05	0.09	0.14	0.08	2.73	3.09	0.1	0.08	1.44	
Tm	0.027	B.D.	0.018	B.D.	0.052	0.525	0.112	0.017	0.005	0.01	0.014	0.024	0.015	0.396	0.464	0.017	0.016	0.229	
Yb	0.17	0.02	0.14	B.D.	0.32	3.45	0.79	0.14	0.04	0.07	0.09	0.15	0.09	2.64	3.11	0.1	0.11	1.54	
Lu	0.025	0.004	0.022	B.D.	0.059	0.562	0.128	0.027	0.005	0.009	0.016	0.021	0.011	0.42	0.481	0.015	0.014	0.258	

Table

Table 3 - Microprobe analyses of chromian spinel in peridotite of Midnight Dome complex

Sample	10VLE-101-05															10VLE-101-10												
UTMX	582490															578294												
UTMY	7105755															7105301												
crystal	sp1-1	sp1-2	sp1-3	sp1-4	sp1-5	sp1-6	sp2-1	sp2-2	sp2-3	sp2-4	sp2-5	sp2-6	sp3-1	sp3-2	sp3-3	sp1-1	sp1-2	sp1-3	sp1-4	sp1-5	sp1-6	sp2-1	sp2-2	sp2-3	sp2-4	sp2-5	sp2-6	sp2-7
SiO2	0.09	0.12	0.08	0.12	0.04	0.05	0.09	0.09	0.12	0.49	0.05	0.09	0.1	0.08	0.04	0.11	0.09	0.08	0.06	0.11	0.08	0.06	0.07	0.15	0.08	0.04	0.11	0.08
TiO2	0.07	0.03	0.06	0.09	0.05	0.08	0.05	0.06	0.05	0.08	0.08	0.07	0.06	0.05	0.08	0.06	0.04	0.02	0.07	0.05	0.08	0.04	0.02	0.04	0.09	0.04	0.05	0.06
Al2O3	21.02	20.91	20.96	20.62	20.98	20.47	19.87	20.22	20.35	20.35	20.47	20.21	20.99	21.09	21.02	18.93	19.03	18.88	19.19	19.21	19.02	18.41	18.24	18.54	18.26	18.3	18.46	18.51
Cr2O3	47.81	47.84	48.54	48.59	48.25	48.89	48.8	49.17	49.13	48.49	48.89	49.06	48.12	48.33	48.48	47.73	47.26	47.52	47.21	47.28	47.11	49.29	49.28	49.27	48.89	48.8	49.45	49.27
Fe2O3	1.94	1.73	1.99	2.07	1.79	2.08	2.1	1.92	1.88	1.26	2.08	1.79	1.97	1.94	1.96	4.53	4.48	4.64	4.32	4.17	4.35	3.08	3.39	3.24	3.54	3.51	3.09	3.52
FeO	15.12	15.01	15.43	15.15	15.31	15.69	15.32	15.68	15.42	16.28	15.69	15.88	15.5	15.79	15.82	17.13	17.76	17.57	17.22	17.29	17.6	16.7	16.52	16.51	16.46	16.6	16.57	16.74
V2O3	0.22	0.18	0.21	0.19	0.22	0.18	0.21	0.19	0.15	0.23	0.18	0.13	0.33	0.25	0.2	0.3	0.27	0.27	0.32	0.28	0.26	0.24	0.37	0.23	0.25	0.29	0.23	0.25
MnO	0.28	0.25	0.19	0.3	0.29	0.19	0.22	0.2	0.29	0.28	0.31	0.18	0.4	0.24	0.25	0.26	0.26	0.25	0.26	0.33	0.22	0.28	0.23	0.27	0.17	0.28	0.25	0.3
MgO	13.02	12.99	12.77	12.97	13.14	12.95	12.77	12.73	12.86	12.67	12.72	12.59	12.9	12.82	12.73	11.73	11.24	11.36	11.54	11.5	11.25	11.69	11.92	12	11.94	11.7	11.95	11.87
ZnO	0.15	0.17	0.26	0.2	0.1	0.1	0.15	0.19	0.26	0.12	0.16	0.16	0.07	0.11	0.2	0.19	0.15	0.16	0.2	0.15	0.25	0.2	0.07	0.2	0.15	0.14	0.14	0.16
Total	99.73	99.24	100.26	100.75	100.35	99.87	99.57	100.45	100.51	100.25	100.63	100.17	100.43	100.69	100.78	100.96	100.59	100.74	100.38	100.37	100.21	99.99	100.11	100.45	99.82	99.7	100.31	100.75
Chromite composition																												
Si	0.003	0.004	0.002	0.003	0.004	0.001	0.003	0.003	0.004	0.015	0.001	0.003	0.003	0.002	0.001	0.003	0.003	0.002	0.002	0.003	0.003	0.002	0.002	0.005	0.003	0.001	0.004	0.003
Ti	0.002	0.001	0.002	0.001	0.002	0.001	0.001	0.001	0.001	0.002	0.002	0.002	0.001	0.001	0.002	0.002	0.001	0.001	0.002	0.001	0.002	0.001	0.001	0.001	0.002	0.001	0.001	0.001
Al	0.768	0.768	0.766	0.76	0.75	0.766	0.732	0.738	0.742	0.743	0.746	0.74	0.763	0.765	0.763	0.697	0.705	0.698	0.71	0.711	0.707	0.685	0.677	0.685	0.68	0.683	0.683	0.683
Cr	1.172	1.178	1.175	1.181	1.186	1.182	1.206	1.204	1.201	1.188	1.195	1.205	1.174	1.176	1.181	1.179	1.174	1.179	1.172	1.174	1.175	1.23	1.228	1.221	1.221	1.221	1.228	1.22
Fe3+	0.045	0.041	0.045	0.046	0.048	0.042	0.049	0.045	0.044	0.029	0.048	0.042	0.046	0.045	0.045	0.106	0.106	0.11	0.102	0.098	0.103	0.073	0.08	0.077	0.084	0.084	0.073	0.083
Fe2+	0.392	0.391	0.404	0.397	0.391	0.397	0.4	0.406	0.399	0.422	0.406	0.413	0.4	0.406	0.408	0.448	0.467	0.461	0.452	0.454	0.464	0.441	0.435	0.433	0.435	0.439	0.435	0.438
V	0.006	0.005	0.007	0.005	0.005	0.005	0.005	0.005	0.004	0.006	0.005	0.003	0.008	0.006	0.005	0.008	0.007	0.007	0.008	0.007	0.006	0.006	0.009	0.006	0.006	0.007	0.006	0.006
Mn	0.007	0.007	0.005	0.008	0.007	0.005	0.006	0.005	0.008	0.007	0.008	0.005	0.01	0.006	0.006	0.007	0.007	0.007	0.007	0.009	0.006	0.007	0.006	0.007	0.004	0.008	0.007	0.008
Mg	0.602	0.603	0.589	0.595	0.605	0.598	0.595	0.588	0.593	0.585	0.586	0.583	0.593	0.588	0.584	0.546	0.527	0.531	0.54	0.538	0.529	0.55	0.56	0.561	0.562	0.552	0.559	0.554
Zn	0.003	0.004	0.006	0.005	0.002	0.002	0.003	0.004	0.006	0.003	0.004	0.004	0.001	0.003	0.005	0.004	0.004	0.004	0.005	0.003	0.006	0.005	0.002	0.005	0.004	0.003	0.003	0.004

**Figure (with caption below and on the same page)**

**Ophiolite / eclogite occurrences**

- (a) Zus Mountain, Blue Dome (Sylvester allochthon)
- (b) Klatsa
- (c) Finlayson Lake
- (d) St Cyr / Quiet Lake
- (e) Dunite Peak
- (f) Last Peak
- (g) Faro / Ross River
- (h) Tummel fault zone
- (i) Ragged Lake klippe
- (j) Buffalo Pitts
- (k) Midnight Dome
- (l) Clinton Creek

**Cordilleran Terranes**

**Outboard**

- YA - Yakutat
- CG - Chugach

**Insular**

- WR - Wrangellia
- AX - Alexander
- KS - Kluane, Windy, Coast
- Taku terrane

**Intermontane**

- CC - Cache Creek
- ST - Stikinia
- QN - Quesnellia
- YT - Yukon-Tanana
- SM - Slide Mountain

**Klondike Assemblage / Sulphur Creek Suite (YT)**

- Endicott Arm & Port Houghton assemblages

**Ancestral N America**

- CA - Cassiar
- NAb - NA basal
- NAP - NA platform
- NAC - NA craton & cover

**Legend**

- Slide Mountain Terrane - U/Pb age
- YTT alpine-type peridotite - U/Pb age
- YTT Eclogite - U/Pb & Sm/Nd age

(a) Letters correspond to data location (see figure caption)

\* Asterisk denotes new data from this study

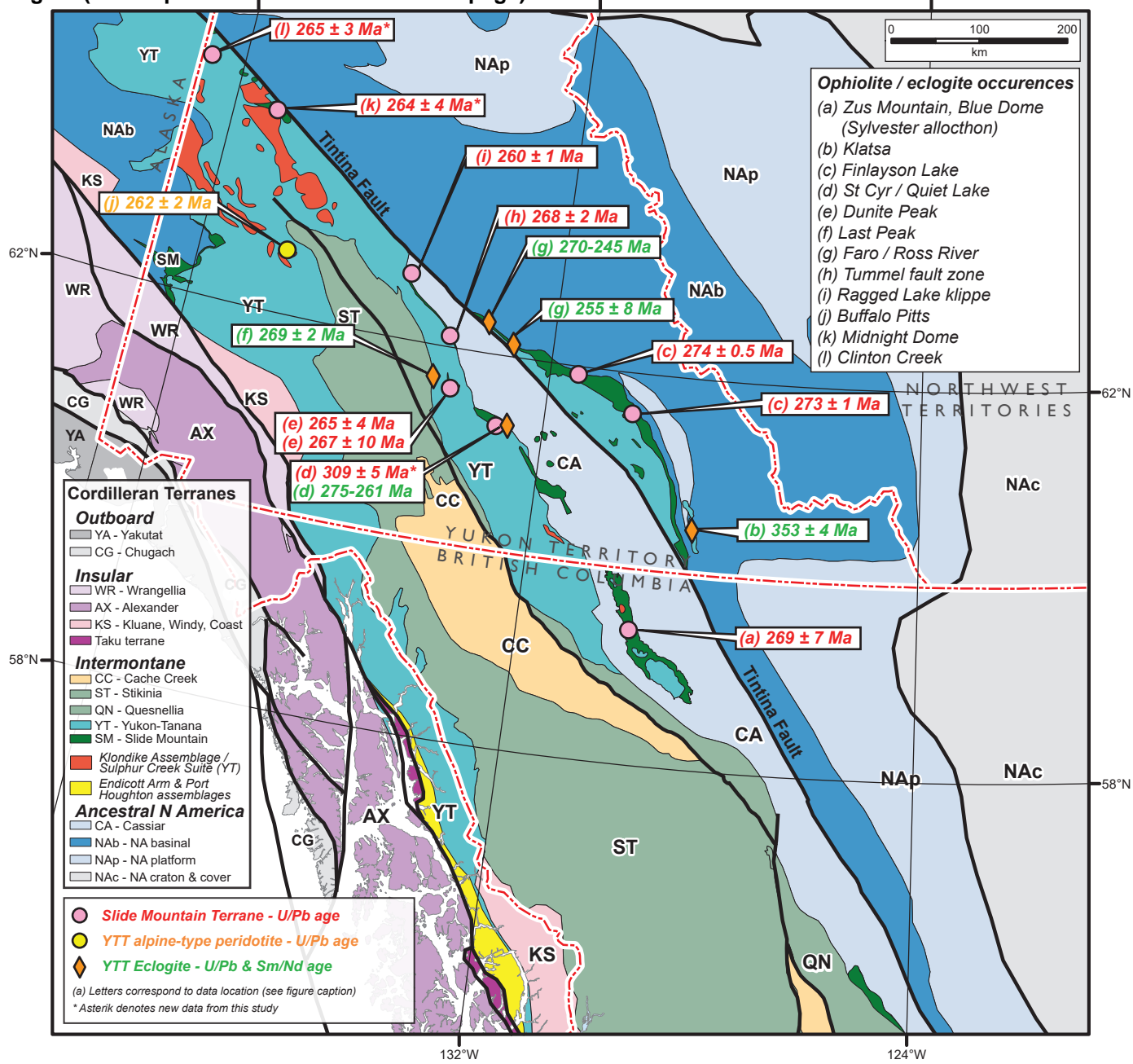
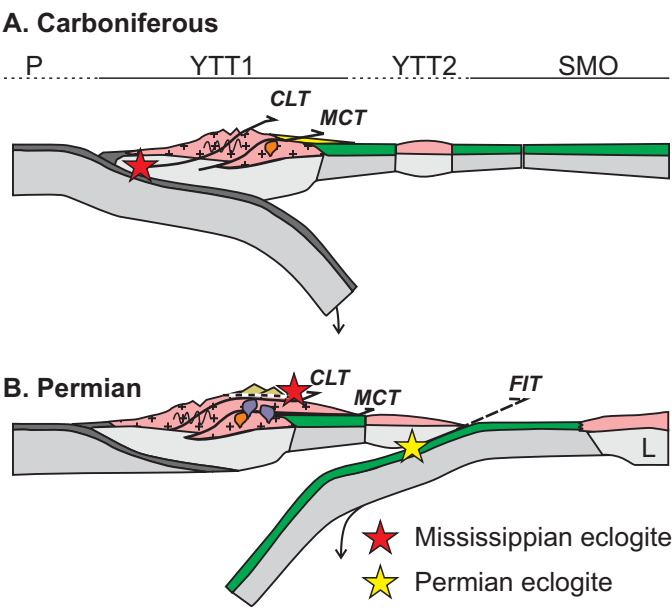
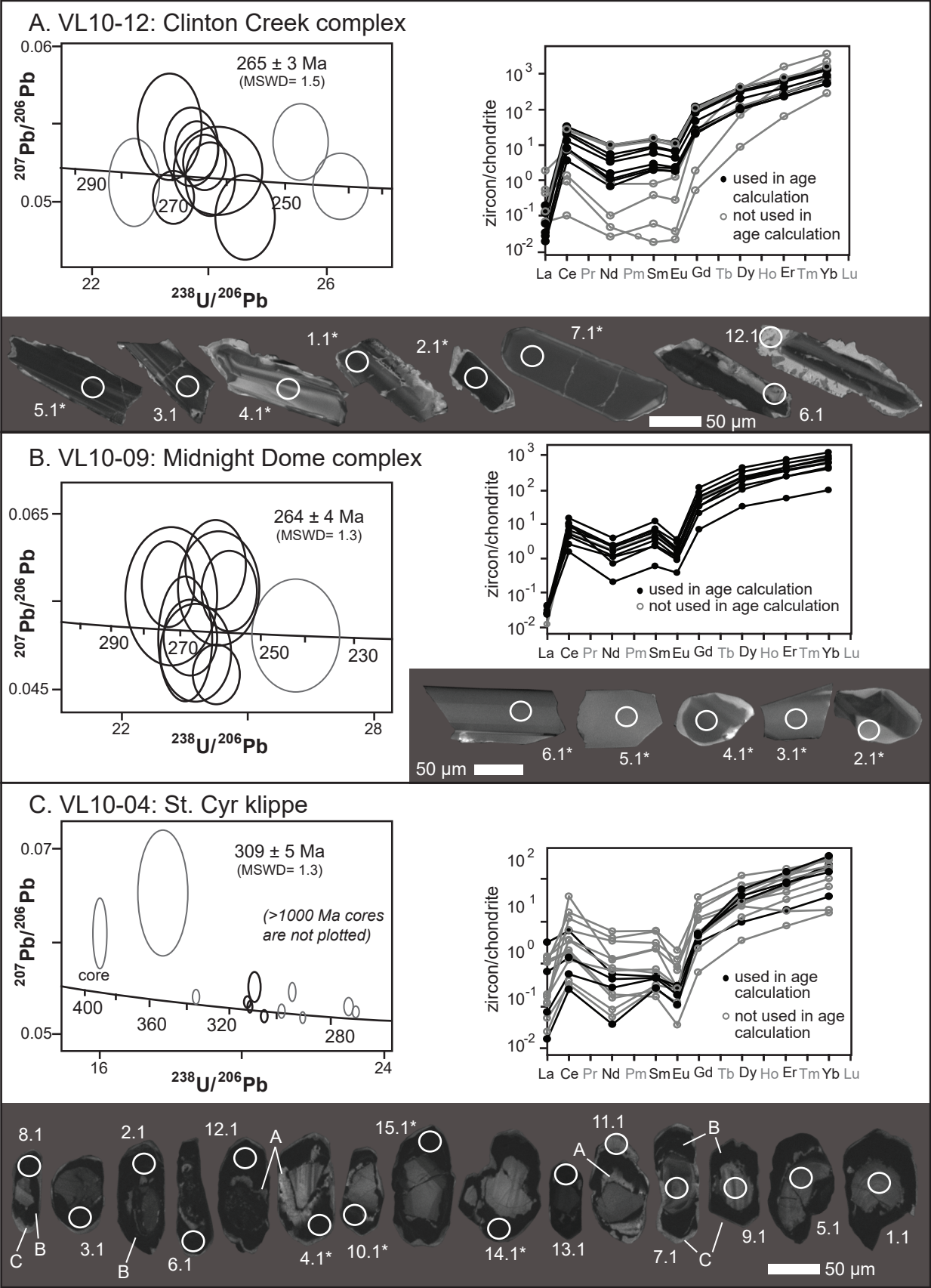


Figure (with caption below and on the same page)



van Staal et al., Figure 2

Figure (with caption below and on the same page)





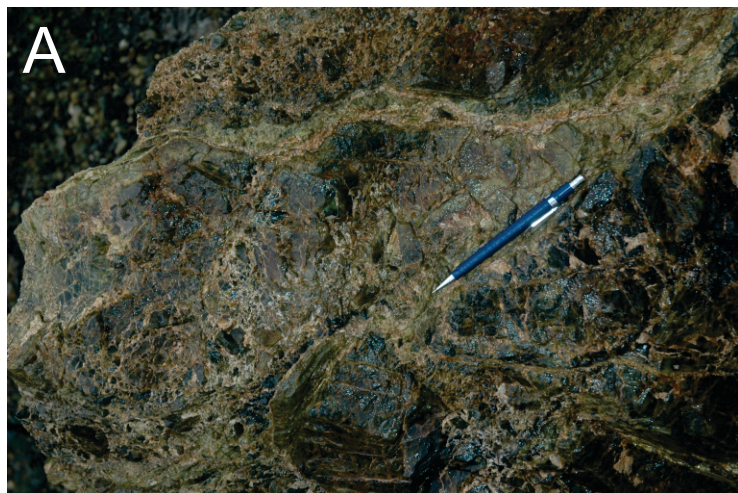
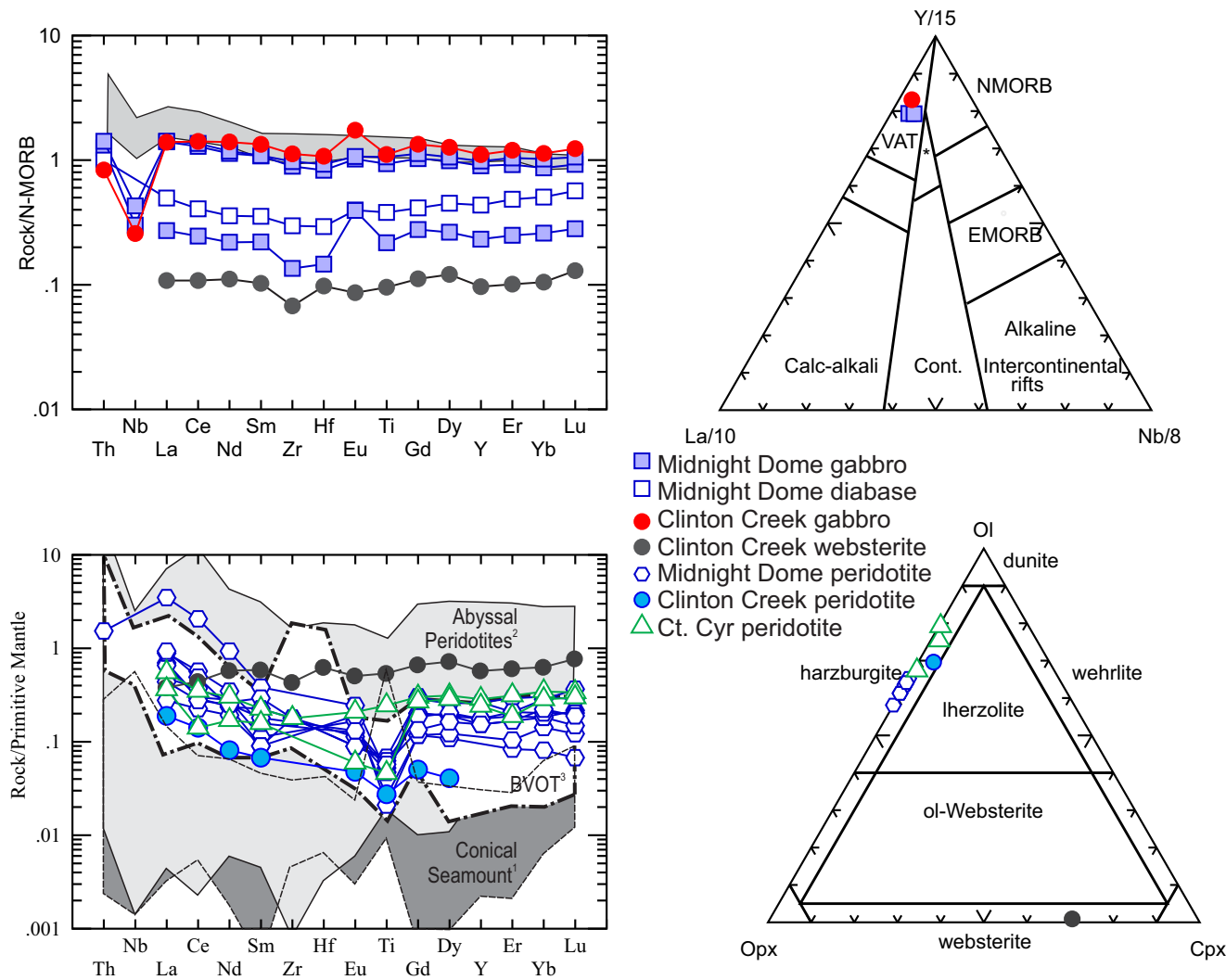


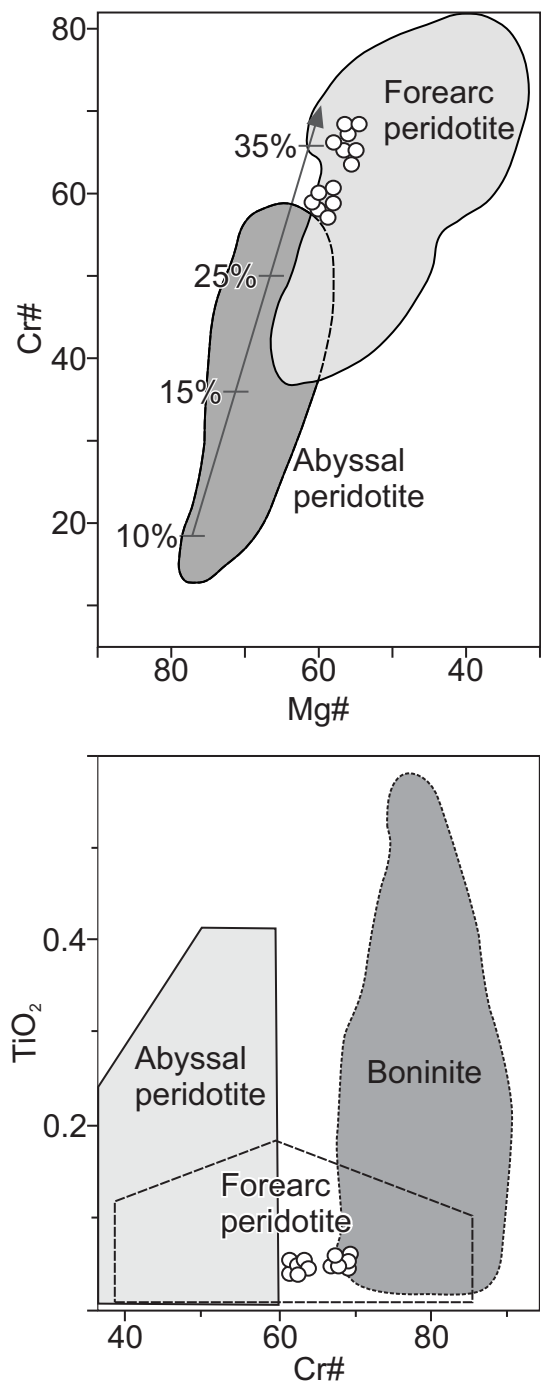


Figure (with caption below and on the same page)



van Staal et al. Figure 6

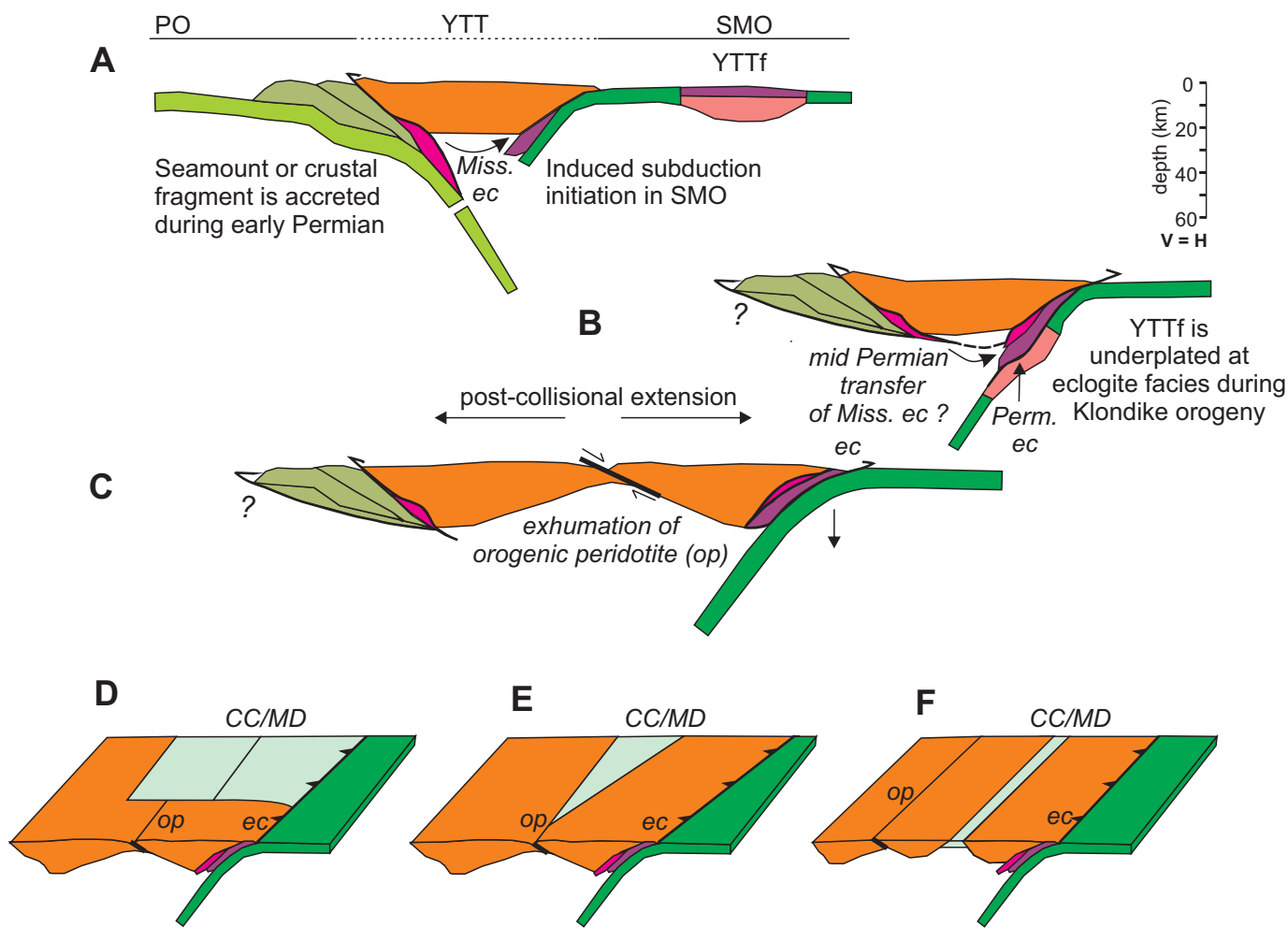
Figure (with caption below and on the same page)



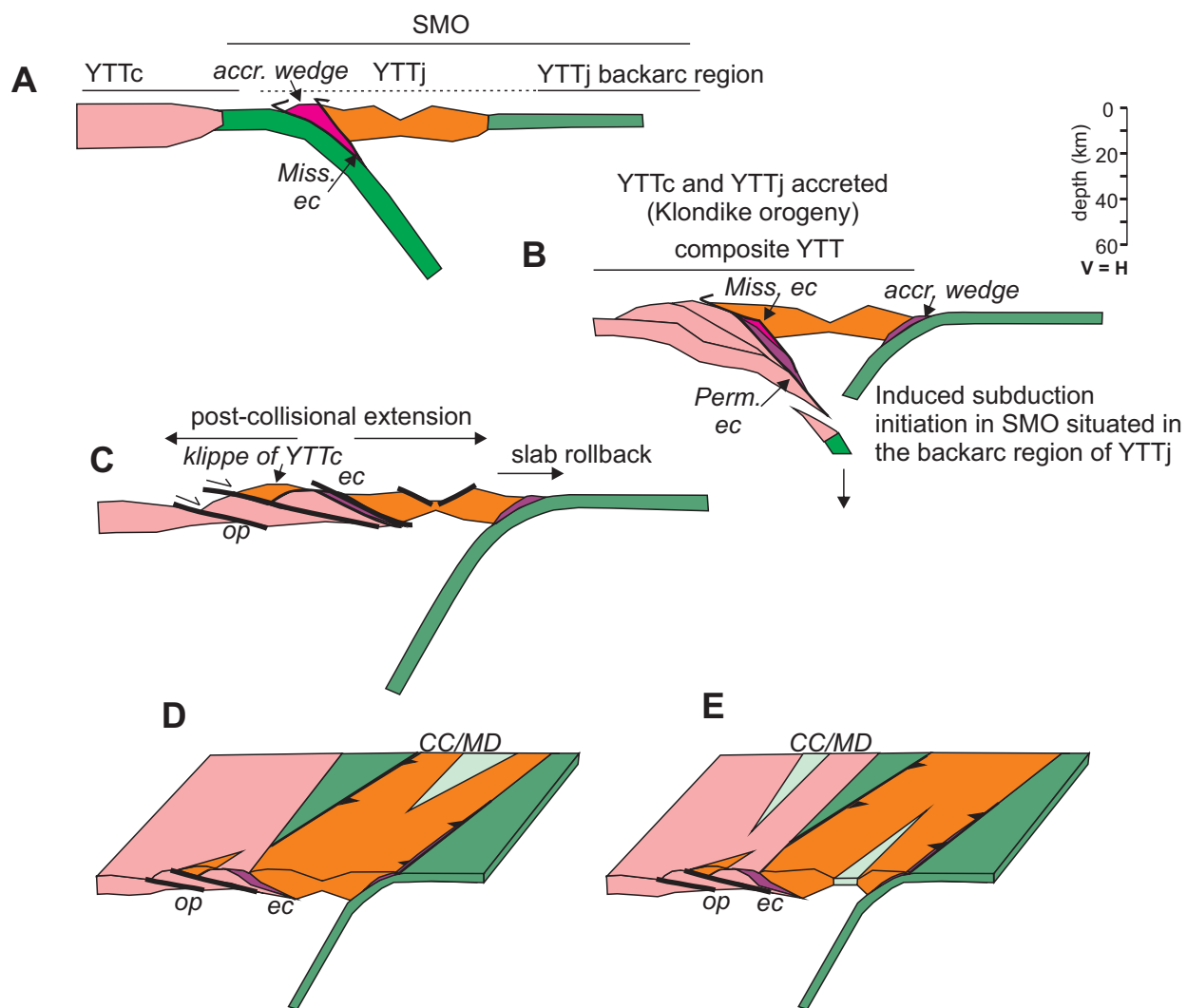
van Staal et al. Figure 6



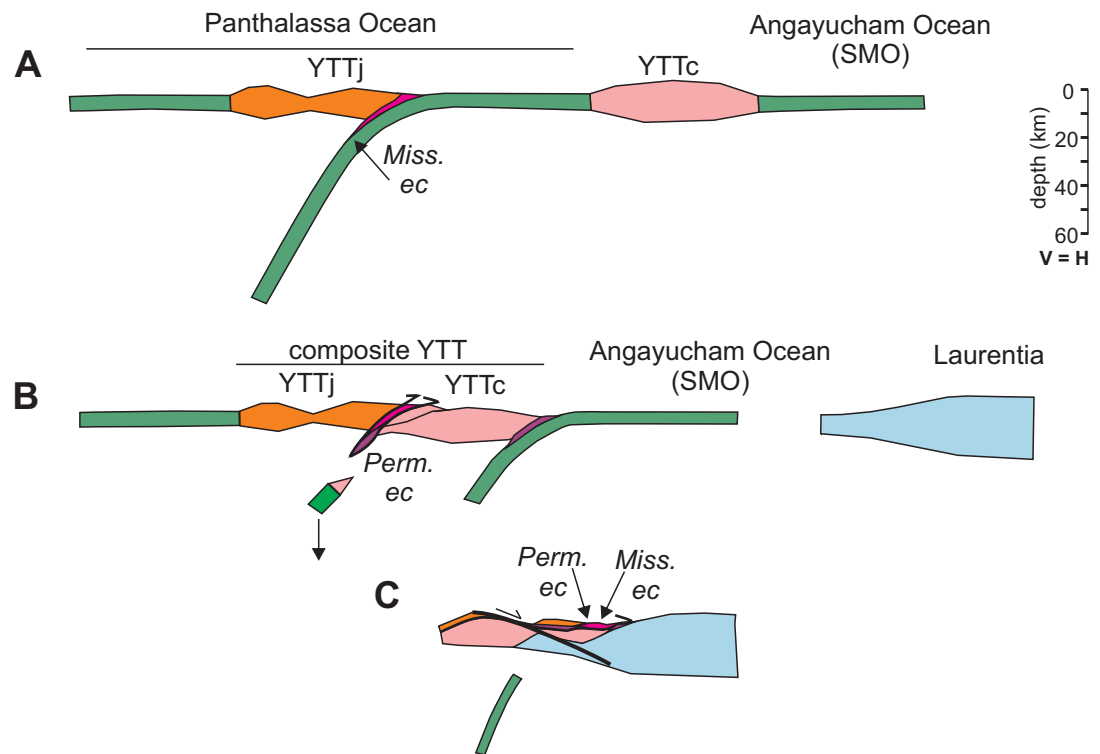
Figure (with caption below and on the same page)



van Staal et al. Figure 7

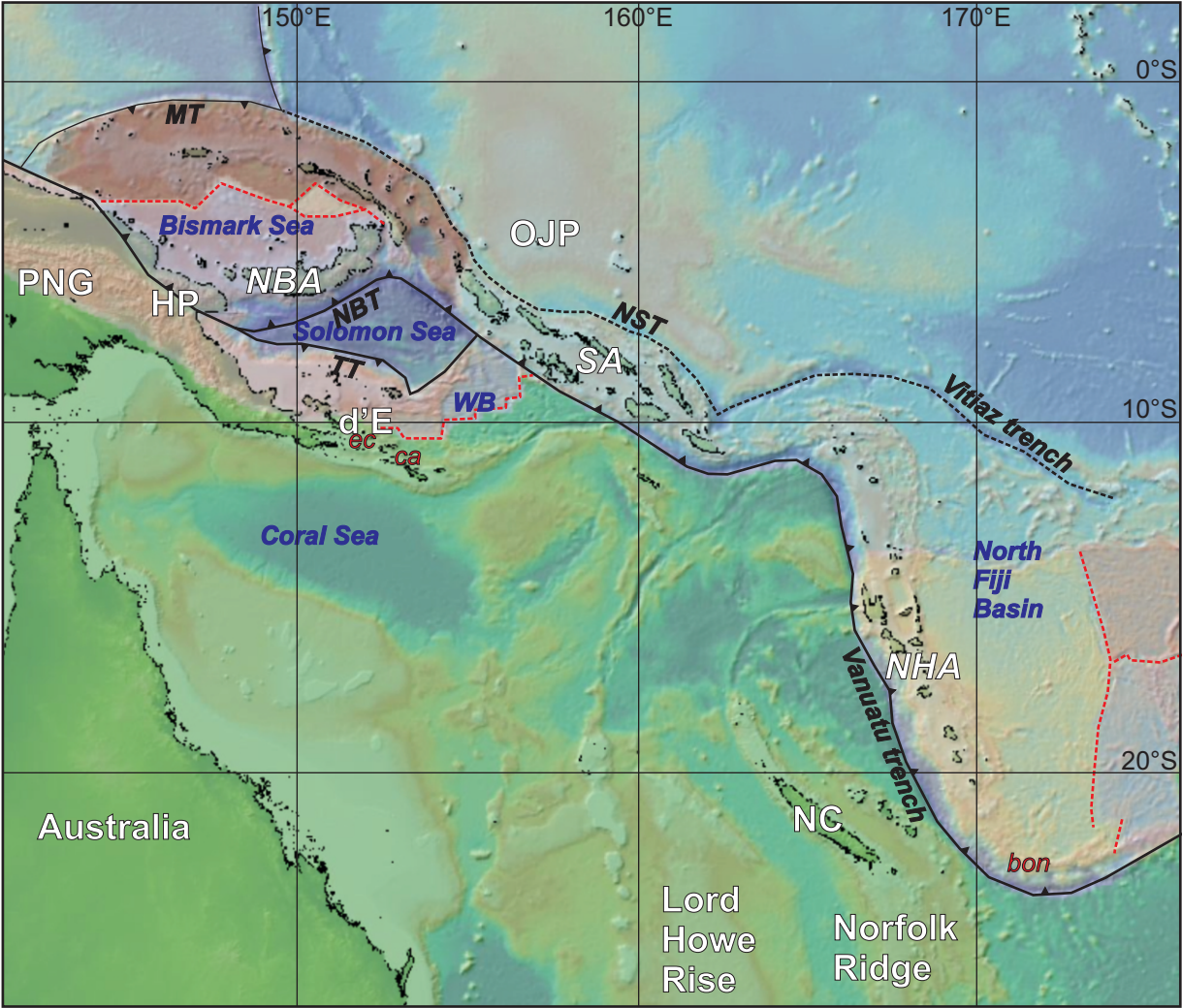


van Staal et al. Figure 8



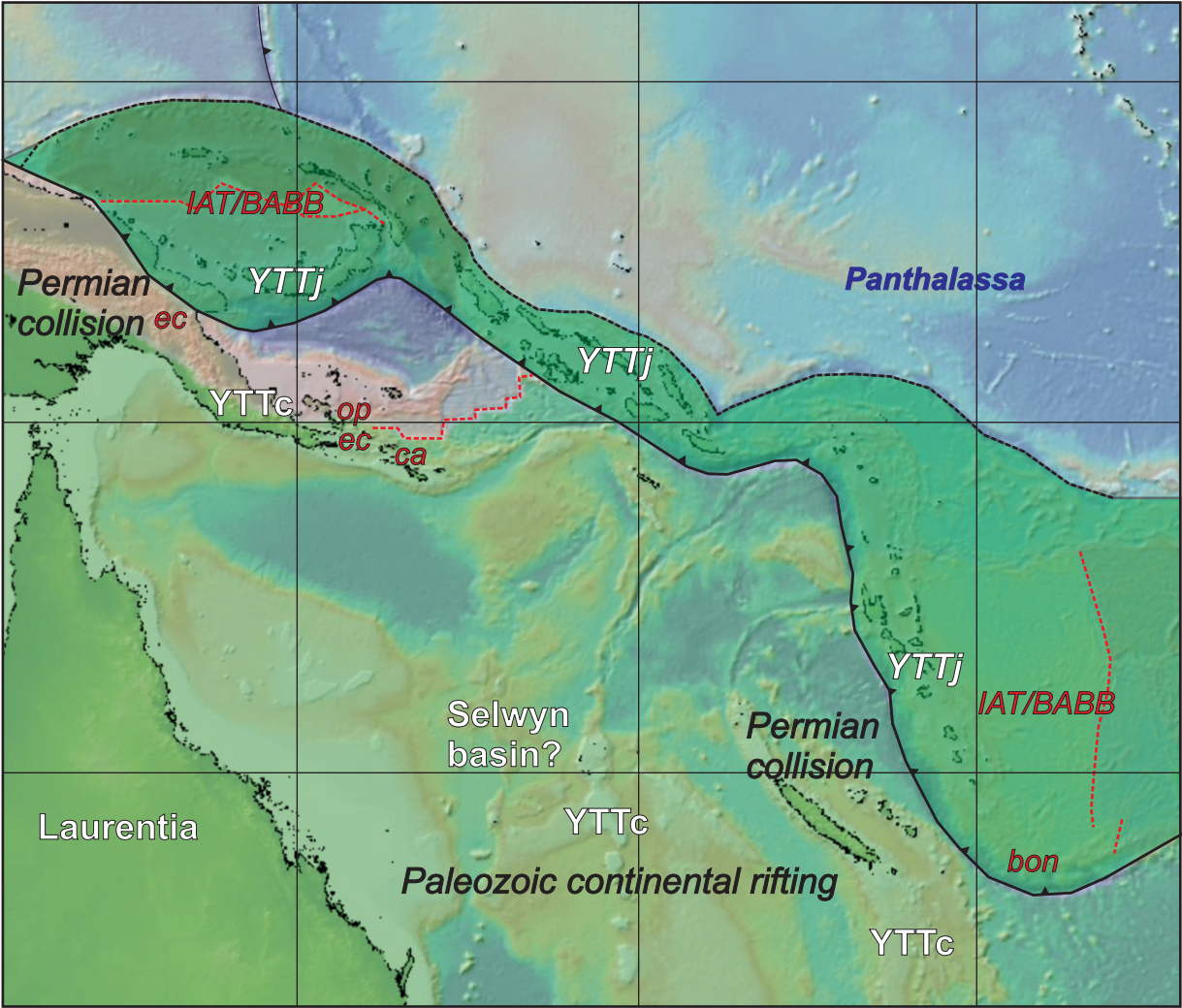
van Staal et al. Figure 9

Figure (with caption below and on the same page)



van Staal et al. Figure 10a

Figure (with caption below and on the same page)



van Staal et al. Figure 10b